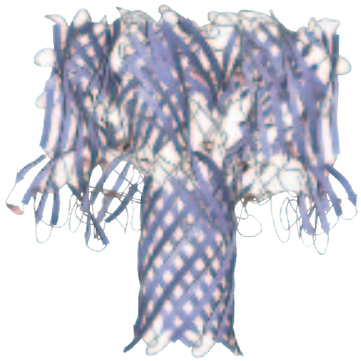

chapter 11

BIOLOGICAL MEMBRANES AND TRANSPORT

Good fences make good neighbors.

—Robert Frost, "Mending Wall," in North of Boston, *1914*

The first cell probably came into being when a membrane formed, enclosing a small volume of aqueous solution and separating it from the rest of the universe. Membranes define the external boundaries of cells and regulate the molecular traffic across that boundary (Fig. 11–1); in eukaryotic cells, they divide the internal space into discrete compartments to segregate processes and components. They organize complex reaction sequences and are central to both biological energy conservation and cell-to-cell communication. The biological activities of membranes flow from their remarkable physical properties. Membranes are flexible, self-sealing, and selectively permeable to polar solutes. Their flexibility permits the shape changes that accompany cell growth and movement (such as amoeboid movement). With their ability to break and reseal, two membranes can fuse, as in exocytosis, or a single membrane-enclosed compartment can undergo fission to yield two sealed compartments, as in endocytosis or cell division, without creating gross leaks through cellular surfaces. Because membranes are selectively permeable, they retain certain compounds and ions within cells and within specific cellular compartments, while excluding others.

Membranes are not merely passive barriers. They include an array of proteins specialized for promoting or catalyzing various cellular processes. At the cell surface, transporters move specific organic solutes and inorganic ions across the membrane; receptors sense extracellular signals and trigger molecular changes in the cell; adhesion molecules hold neighboring cells together. Within the cell, membranes organize cellular processes such as the synthesis of lipids and certain proteins, and the energy transductions in mitochondria and chloroplasts. Because membranes consist of just two layers of molecules, they are very thin—essentially two-dimensional. Intermolecular collisions are far more probable in this two-dimensional space than in three-dimensional space, so the efficiency of enzyme-catalyzed processes organized within membranes is vastly increased.

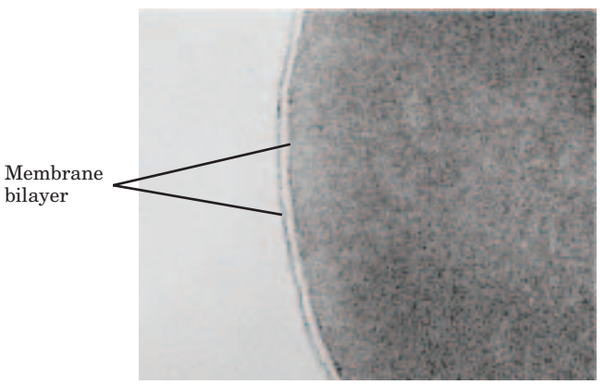

FIGURE 11–1 Biological membranes. Viewed in cross section, all cell membranes share a characteristic trilaminar appearance. When an erythrocyte is stained with osmium tetroxide and viewed with an electron microscope, the plasma membrane appears as a three-layer structure, 5 to 8 nm (50 to 80 Å) thick. The trilaminar image consists of two electron-dense layers (the osmium, bound to the inner and outer surfaces of the membrane) separated by a less dense central region.

In this chapter we first describe the composition of cellular membranes and their chemical architecture—the molecular structures that underlie their biological functions. Next, we consider the remarkable dynamic features of membranes, in which lipids and proteins move relative to each other. Cell adhesion, endocytosis, and the membrane fusion accompanying neurotransmitter secretion illustrate the dynamic role of membrane proteins. We then turn to the protein-mediated passage of solutes across membranes via transporters and ion channels. In later chapters we discuss the role of membranes in signal transduction (Chapters 12 and 23), energy transduction (Chapter 19), lipid synthesis (Chapter 21), and protein synthesis (Chapter 27).

11.1 The Composition and Architecture of Membranes

One approach to understanding membrane function is to study membrane composition—to determine, for example, which components are common to all membranes and which are unique to membranes with specific functions. So before describing membrane structure and function we consider the molecular components of membranes: proteins and polar lipids, which account for almost all the mass of biological membranes, and carbohydrates, present as part of glycoproteins and glycolipids.

Each Type of Membrane Has Characteristic Lipids and Proteins

The relative proportions of protein and lipid vary with the type of membrane (Table 11–1), reflecting the diversity of biological roles. For example, certain neurons have a myelin sheath, an extended plasma membrane that wraps around the cell many times and acts as a passive electrical insulator. The myelin sheath consists primarily of lipids, whereas the plasma membranes of bacteria and the membranes of mitochondria and chloroplasts, the sites of many enzyme-catalyzed processes, contain more protein than lipid (in mass per total mass).

For studies of membrane composition, the first task is to isolate a selected membrane. When eukaryotic cells are subjected to mechanical shear, their plasma membranes are torn and fragmented, releasing cytoplasmic components and membrane-bounded organelles such as mitochondria, chloroplasts, lysosomes, and nuclei. Plasma membrane fragments and intact organelles can be isolated by centrifugal techniques described in Chapter 1 (see Fig. 1–8).

Chemical analyses of membranes isolated from various sources reveal certain common properties. Each kingdom, each species, each tissue or cell type, and the organelles of each cell type have a characteristic set of membrane lipids. Plasma membranes, for example, are enriched in cholesterol and contain no detectable cardiolipin (Fig. 11–2); in the inner mitochondrial membrane of the hepatocyte, this distribution is reversed: very low cholesterol and high cardiolipin. Cardiolipin is essential to the function of certain proteins of the inner mitochondrial membrane. Cells clearly have mechanisms to control the kinds and amounts of membrane lipids they synthesize and to target specific lipids to particular organelles. In many cases, we can surmise the adaptive advantages of distinct combinations of membrane lipids; in other cases, the functional significance of these combinations is as yet unknown.

The protein composition of membranes from different sources varies even more widely than their lipid composition, reflecting functional specialization. In a rod cell of the vertebrate retina, one portion of the cell is highly specialized for the reception of light; more than 90% of the plasma membrane protein in this region is the light-absorbing glycoprotein rhodopsin. The less-specialized plasma membrane of the erythrocyte has about 20 prominent types of proteins as well as scores of minor ones; many of these are transporters, each moving a specific solute across the membrane. The plasma membrane of *Escherichia coli* contains hun-

TABLE 11–1 Major Components of Plasma Membranes in Various Organisms

	Components (% by weight)				
	Protein	*Phospholipid*	*Sterol*	*Sterol type*	*Other lipids*
Human myelin sheath	30	30	19	Cholesterol	Galactolipids, plasmalogens
Mouse liver	45	27	25	Cholesterol	—
Maize leaf	47	26	7	Sitosterol	Galactolipids
Yeast	52	7	4	Ergosterol	Triacylglycerols, steryl esters
Paramecium (ciliated protist)	56	40	4	Stigmasterol	—
E. coli	75	25	0	—	—

Note: Values do not add up to 100% in every case, because there are components other than protein, phospholipids, and sterol; plants, for example, have high levels of glycolipids.

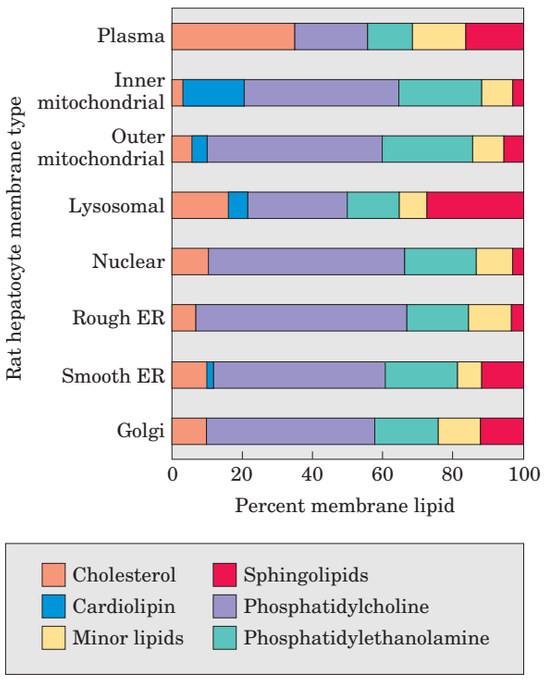

FIGURE 11–2 Lipid composition of the plasma membrane and organelle membranes of a rat hepatocyte. The functional specialization of each membrane type is reflected in its unique lipid composition. Cholesterol is prominent in plasma membranes but barely detectable in mitochondrial membranes. Cardiolipin is a major component of the inner mitochondrial membrane but not of the plasma membrane. Phosphatidylserine, phosphatidylinositol, and phosphatidylglycerol are relatively minor components (yellow) of most membranes but serve critical functions; phosphatidylinositol and its derivatives, for example, are important in signal transductions triggered by hormones. Sphingolipids, phosphatidylcholine, and phosphatidylethanolamine are present in most membranes, but in varying proportions. Glycolipids, which are major components of the chloroplast membranes of plants, are virtually absent from animal cells.

dreds of different proteins, including transporters and many enzymes involved in energy-conserving metabolism, lipid synthesis, protein export, and cell division. The outer membrane of *E. coli*, which encloses the plasma membrane, has a different function (protection) and a different set of proteins.

Some membrane proteins are covalently linked to complex arrays of carbohydrate. For example, in glycophorin, a glycoprotein of the erythrocyte plasma membrane, 60% of the mass consists of complex oligosaccharide units covalently attached to specific amino acid residues. Ser, Thr, and Asn residues are the most common points of attachment (see Fig. 7–31). At the other end of the scale is rhodopsin of the rod cell plasma membrane, which contains just one hexasaccharide. The sugar moieties of surface glycoproteins influence the folding of the proteins, as well as their stabilities and intracellular destinations, and they play a significant role in the specific binding of ligands to glycoprotein surface receptors (see Fig. 7–37).

Some membrane proteins are covalently attached to one or more lipids, which serve as hydrophobic anchors that hold the proteins to the membrane, as we shall see.

All Biological Membranes Share Some Fundamental Properties

Membranes are impermeable to most polar or charged solutes, but permeable to nonpolar compounds; they are 5 to 8 nm (50 to 80 Å) thick and appear trilaminar when viewed in cross section with the electron microscope (Fig. 11–1). The combined evidence from electron microscopy and studies of chemical composition, as well as physical studies of permeability and the motion of individual protein and lipid molecules within membranes, led to the development of the **fluid mosaic model** for the structure of biological membranes (Fig. 11–3). Phospholipids form a bilayer in which the nonpolar regions of the lipid molecules in each layer face the core of the bilayer and their polar head groups face outward, interacting with the aqueous phase on either side. Proteins are embedded in this bilayer sheet, held by hydrophobic interactions between the membrane lipids and hydrophobic domains in the proteins. Some proteins protrude from only one side of the membrane; others have domains exposed on both sides. The orientation of proteins in the bilayer is asymmetric, giving the membrane "sidedness": the protein domains exposed on one side of the bilayer are different from those exposed on the other side, reflecting functional asymmetry. The individual lipid and protein units in a membrane form a fluid mosaic with a pattern that, unlike a mosaic of ceramic tile and mortar, is free to change constantly. The membrane mosaic is fluid because most of the interactions among its components are noncovalent, leaving individual lipid and protein molecules free to move laterally in the plane of the membrane.

We now look at some of these features of the fluid mosaic model in more detail and consider the experimental evidence that supports the basic model but has necessitated its refinement in several ways.

A Lipid Bilayer Is the Basic Structural Element of Membranes

Glycerophospholipids, sphingolipids, and sterols are virtually insoluble in water. When mixed with water, they spontaneously form microscopic lipid aggregates in a phase separate from their aqueous surroundings, clustering together, with their hydrophobic moieties in contact with each other and their hydrophilic groups interacting with the surrounding water. Recall that lipid clustering reduces the amount of hydrophobic surface

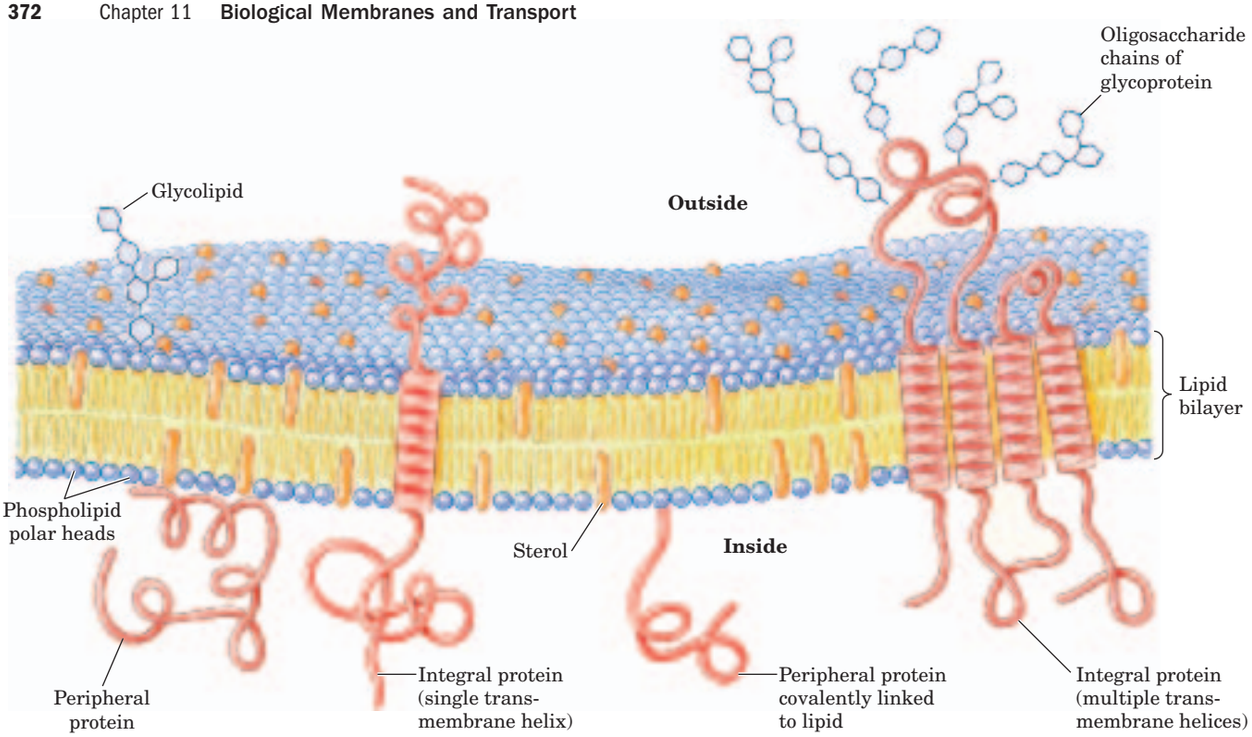

FIGURE 11–3 Fluid mosaic model for membrane structure. The fatty acyl chains in the interior of the membrane form a fluid, hydrophobic region. Integral proteins float in this sea of lipid, held by hydrophobic interactions with their nonpolar amino acid side chains. Both proteins and lipids are free to move laterally in the plane of the bilayer, but movement of either from one face of the bilayer to the other is restricted. The carbohydrate moieties attached to some proteins and lipids of the plasma membrane are exposed on the extracellular surface of the membrane.

exposed to water and thus minimizes the number of molecules in the shell of ordered water at the lipid-water interface (see Fig. 2–7), resulting in an increase in entropy. Hydrophobic interactions among lipid molecules provide the thermodynamic driving force for the formation and maintenance of these clusters.

Depending on the precise conditions and the nature of the lipids, three types of lipid aggregates can form when amphipathic lipids are mixed with water (Fig. 11–4). **Micelles** are spherical structures that contain anywhere from a few dozen to a few thousand amphipathic molecules. These molecules are arranged with

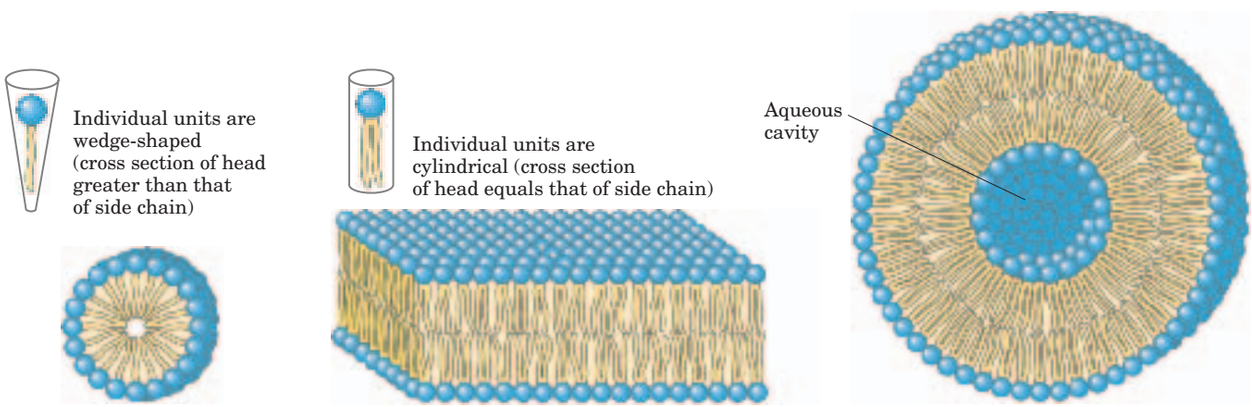

FIGURE 11–4 Amphipathic lipid aggregates that form in water. (a) In micelles, the hydrophobic chains of the fatty acids are sequestered at the core of the sphere. There is virtually no water in the hydrophobic interior. **(b)** In an open bilayer, all acyl side chains except those at the edges of the sheet are protected from interaction with water. **(c)** When a two-dimensional bilayer folds on itself, it forms a closed bilayer, a three-dimensional hollow vesicle (liposome) enclosing an aqueous cavity.

their hydrophobic regions aggregated in the interior, where water is excluded, and their hydrophilic head groups at the surface, in contact with water. Micelle formation is favored when the cross-sectional area of the head group is greater than that of the acyl side chain(s), as in free fatty acids, lysophospholipids (phospholipids lacking one fatty acid), and detergents such as sodium dodecyl sulfate (SDS; p. 92).

A second type of lipid aggregate in water is the **bilayer,** in which two lipid monolayers (leaflets) form a two-dimensional sheet. Bilayer formation occurs most readily when the cross-sectional areas of the head group and acyl side chain(s) are similar, as in glycerophospholipids and sphingolipids. The hydrophobic portions in each monolayer, excluded from water, interact with each other. The hydrophilic head groups interact with water at each surface of the bilayer. Because the hydrophobic regions at its edges (Fig. 11–4b) are transiently in contact with water, the bilayer sheet is relatively unstable and spontaneously forms a third type of aggregate: it folds back on itself to form a hollow sphere, a vesicle or **liposome** (Fig. 11–4c). By forming vesicles, bilayers lose their hydrophobic edge regions, achieving maximal stability in their aqueous environment. These bilayer vesicles enclose water, creating a separate aqueous compartment. It is likely that the precursors to the first living cells resembled liposomes, their aqueous contents segregated from the rest of the world by a hydrophobic shell.

Biological membranes are constructed of lipid bilayers 3 nm (30 Å) thick, with proteins protruding on each side. The hydrocarbon core of the membrane, made up of the —CH_2— and —CH_3 of the fatty acyl groups, is about as nonpolar as decane, and liposomes formed in the laboratory from pure lipids are essentially impermeable to polar solutes, as are biological membranes (although the latter, as we shall see, are permeable to solutes for which they have specific transporters).

Plasma membrane lipids are asymmetrically distributed between the two monolayers of the bilayer, although the asymmetry, unlike that of membrane proteins, is not absolute. In the plasma membrane of the erythrocyte, for example, choline-containing lipids (phosphatidylcholine and sphingomyelin) are typically found in the outer (extracellular or exoplasmic) leaflet (Fig. 11–5), whereas phosphatidylserine, phosphatidylethanolamine, and the phosphatidylinositols are much more common in the inner (cytoplasmic) leaflet. Changes in the distribution of lipids between plasma membrane leaflets have biological consequences. For example, only when the phosphatidylserine in the plasma membrane moves into the outer leaflet is a platelet able to play its role in formation of a blood clot. For many other cells types, phosphatidylserine exposure on the outer surface marks a cell for destruction by programmed cell death.

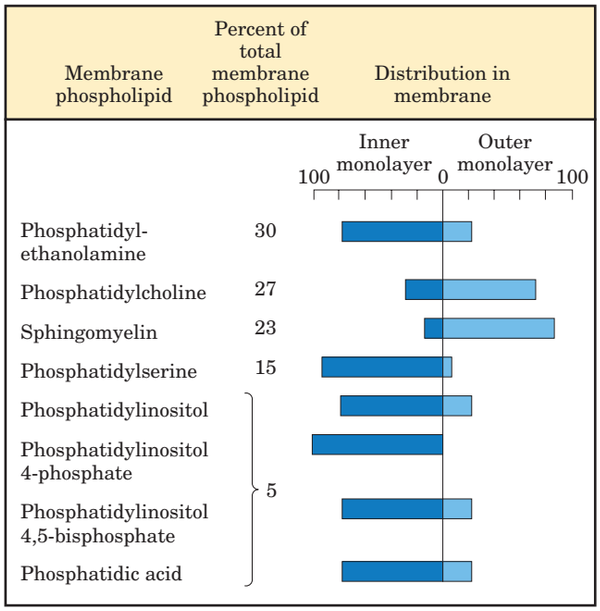

FIGURE 11–5 Asymmetric distribution of phospholipids between the inner and outer monolayers of the erythrocyte plasma membrane. The distribution of a specific phospholipid is determined by treating the intact cell with phospholipase C, which cannot reach lipids in the inner monolayer (leaflet) but removes the head groups of lipids in the outer monolayer. The proportion of each head group released provides an estimate of the fraction of each lipid in the outer monolayer.

Peripheral Membrane Proteins Are Easily Solubilized

Membrane proteins may be divided operationally into two groups (Fig. 11–6). **Integral proteins** are very firmly associated with the membrane, removable only by agents that interfere with hydrophobic interactions, such as detergents, organic solvents, or denaturants. **Peripheral proteins** associate with the membrane through electrostatic interactions and hydrogen bonding with the hydrophilic domains of integral proteins and with the polar head groups of membrane lipids. They can be released by relatively mild treatments that interfere with electrostatic interactions or break hydrogen bonds; a commonly used agent is carbonate at high pH. Peripheral proteins may serve as regulators of membrane-bound enzymes or may limit the mobility of integral proteins by tethering them to intracellular structures.

Many Membrane Proteins Span the Lipid Bilayer

Membrane protein topology (localization relative to the lipid bilayer) can be determined with reagents that react with protein side chains but cannot cross membranes—polar chemical reagents that react with primary amines of Lys residues, for example, or enzymes

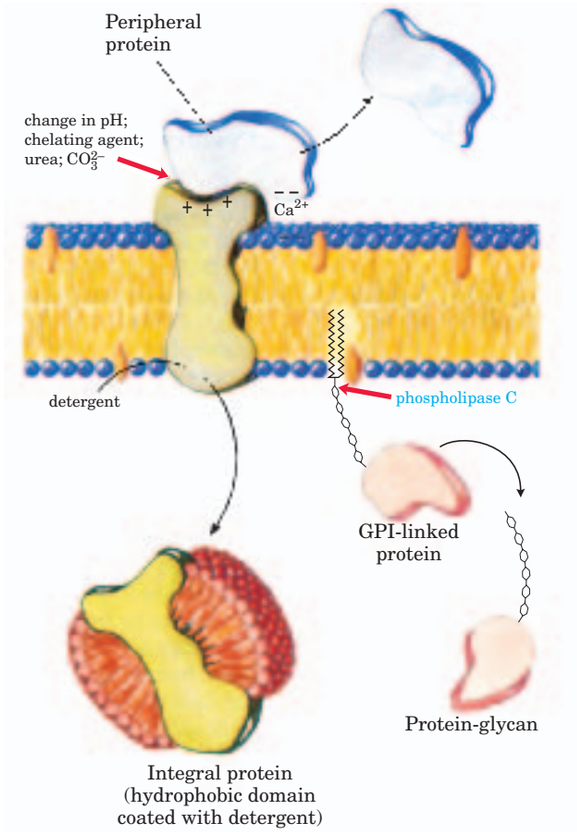

FIGURE 11–6 Peripheral and integral proteins. Membrane proteins can be operationally distinguished by the conditions required to release them from the membrane. Most peripheral proteins are released by changes in pH or ionic strength, removal of Ca^{2+} by a chelating agent, or addition of urea or carbonate. Integral proteins are extractable with detergents, which disrupt the hydrophobic interactions with the lipid bilayer and form micelle-like clusters around individual protein molecules. Integral proteins covalently attached to a membrane lipid, such as a glycosyl phosphatidylinositol (GPI; see Fig. 11–14), can be released by treatment with phospholipase C.

like trypsin that cleave proteins but cannot cross the membrane. The human erythrocyte is convenient for such studies because it has no membrane-bounded organelles; the plasma membrane is the only membrane present. If a membrane protein in an intact erythrocyte reacts with a membrane-impermeant reagent, that protein must have at least one domain exposed on the outer (extracellular) face of the membrane. Trypsin is found to cleave extracellular domains but does not affect domains buried within the bilayer or exposed on the inner surface only, unless the plasma membrane is broken to make these domains accessible to the enzyme.

Experiments with such topology-specific reagents show that the erythrocyte glycoprotein **glycophorin** spans the plasma membrane. Its amino-terminal domain (bearing the carbohydrate chains) is on the outer surface and is cleaved by trypsin. The carboxyl terminus protrudes on the inside of the cell, where it cannot react with impermeant reagents. Both the amino-terminal and carboxyl-terminal domains contain many polar or charged amino acid residues and are therefore quite hydrophilic. However, a segment in the center of the protein (residues 75 to 93) contains mainly hydrophobic amino acid residues, suggesting that glycophorin has a transmembrane segment arranged as shown in Figure 11–7.

One further fact may be deduced from the results of experiments with glycophorin: its disposition in the membrane is asymmetric. Similar studies of other membrane proteins show that each has a specific orientation

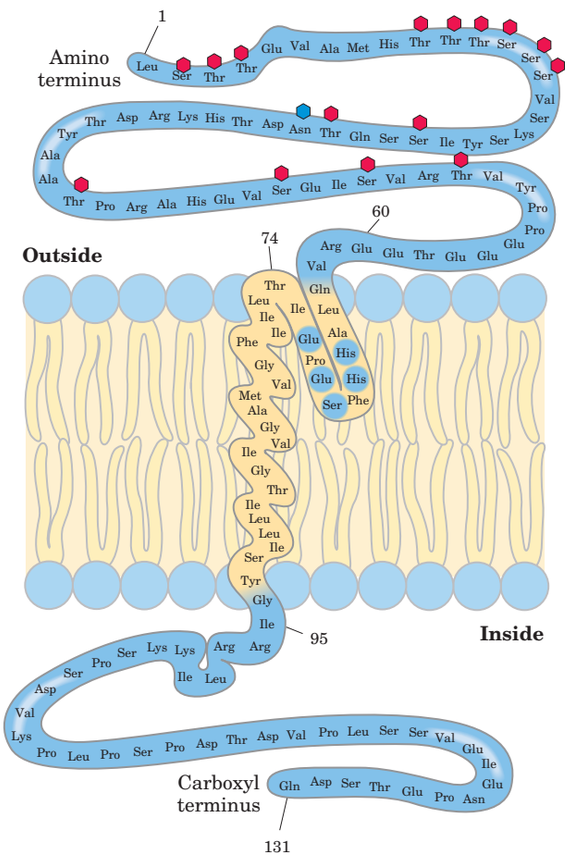

FIGURE 11–7 Transbilayer disposition of glycophorin in an erythrocyte. One hydrophilic domain, containing all the sugar residues, is on the outer surface, and another hydrophilic domain protrudes from the inner face of the membrane. Each red hexagon represents a tetrasaccharide (containing two Neu5Ac (sialic acid), Gal, and GalNAc) *O*-linked to a Ser or Thr residue; the blue hexagon represents an oligosaccharide chain *N*-linked to an Asn residue. The relative size of the oligosaccharide units is larger than shown here. A segment of 19 hydrophobic residues (residues 75 to 93) forms an α helix that traverses the membrane bilayer (see Fig. 11–11a). The segment from residues 64 to 74 has some hydrophobic residues and probably penetrates into the outer face of the lipid bilayer, as shown.

in the bilayer; one domain of a transmembrane protein always faces out, the other always faces in. Furthermore, glycoproteins of the plasma membrane are invariably situated with their sugar residues on the outer surface of the cell. As we shall see, the asymmetric arrangement of membrane proteins results in functional asymmetry. All the molecules of a given ion pump, for example, have the same orientation in the membrane and therefore pump in the same direction.

Integral Proteins Are Held in the Membrane by Hydrophobic Interactions with Lipids

The firm attachment of integral proteins to membranes is the result of hydrophobic interactions between membrane lipids and hydrophobic domains of the protein. Some proteins have a single hydrophobic sequence in the middle (as in glycophorin) or at the amino or carboxyl terminus. Others have multiple hydrophobic sequences, each of which, when in the α-helical conformation, is long enough to span the lipid bilayer (Fig. 11–8). The same techniques used to determine the three-dimensional structures of soluble proteins can, in principle, be applied to membrane proteins. In practice, however, membrane proteins have until recently proved difficult to crystallize. New techniques are overcoming this obstacle, and crystallographic structures of membrane proteins are regularly becoming available, yielding deep insights into membrane events at the molecular level.

One of the best-studied membrane-spanning proteins, bacteriorhodopsin, has seven very hydrophobic internal sequences and crosses the lipid bilayer seven times. Bacteriorhodopsin is a light-driven proton pump densely packed in regular arrays in the purple membrane of the bacterium *Halobacterium salinarum.* X-ray crystallography reveals a structure with seven α-helical segments, each traversing the lipid bilayer, connected by nonhelical loops at the inner and outer face of the membrane (Fig. 11–9). In the amino acid sequence of bacteriorhodopsin, seven segments of about 20 hydrophobic residues can be identified, each segment just long enough to form an α helix that spans the bilayer. Hydrophobic interactions between the nonpolar amino acids and the fatty acyl groups of the membrane lipids firmly anchor the protein in the membrane. The seven helices are clustered together and oriented not quite perpendicular to the bilayer plane, providing a transmembrane pathway for proton movement. As we shall see in Chapter 12, this pattern of seven hydrophobic membrane-spanning helices is a common motif in membrane proteins involved in signal reception.

The photosynthetic reaction center of a purple bacterium was the first membrane protein structure solved by crystallography. Although a more complex membrane protein than bacteriorhodopsin, it is constructed on the same principles. The reaction center has four protein subunits, three of which contain α-helical segments that span the membrane (Fig. 11–10). These segments are rich in nonpolar amino acids, their hydrophobic side chains oriented toward the outside of the molecule where they interact with membrane lipids. The architecture of the reaction center protein is therefore the inverse of that seen in most water-soluble proteins, in

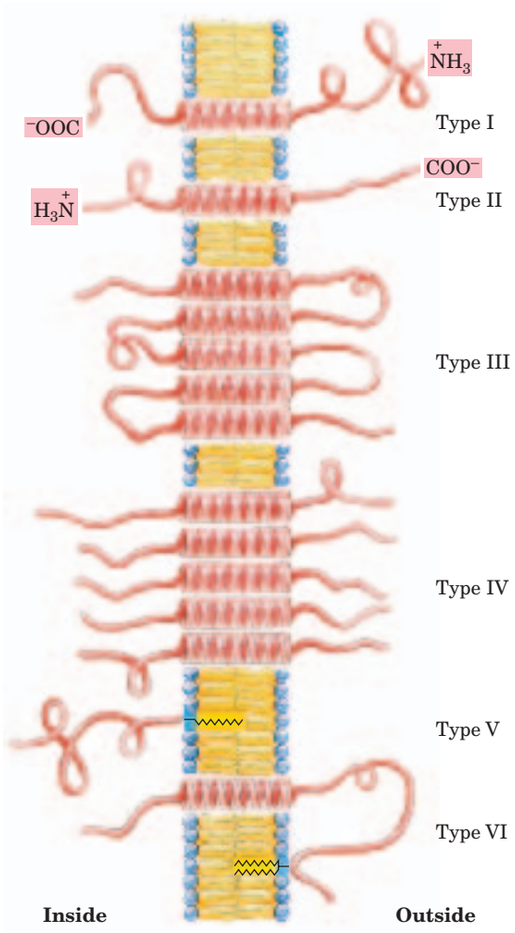

FIGURE 11–8 Integral membrane proteins. For known proteins of the plasma membrane, the spatial relationships of protein domains to the lipid bilayer fall into six categories. Types I and II have only one transmembrane helix; the amino-terminal domain is outside the cell in type I proteins and inside in type II. Type III proteins have multiple transmembrane helices in a single polypeptide. In type IV proteins, transmembrane domains of several different polypeptides assemble to form a channel through the membrane. Type V proteins are held to the bilayer primarily by covalently linked lipids (see Fig. 11–14), and type VI proteins have both transmembrane helices and lipid (GPI) anchors.

In this figure, and in figures throughout the book, we represent transmembrane protein segments in their most likely conformations: as α helices of six to seven turns. Sometimes these helices are shown simply as cylinders. As relatively few membrane protein structures have been deduced by x-ray crystallography, our representation of the extramembrane domains is arbitrary and not necessarily to scale.

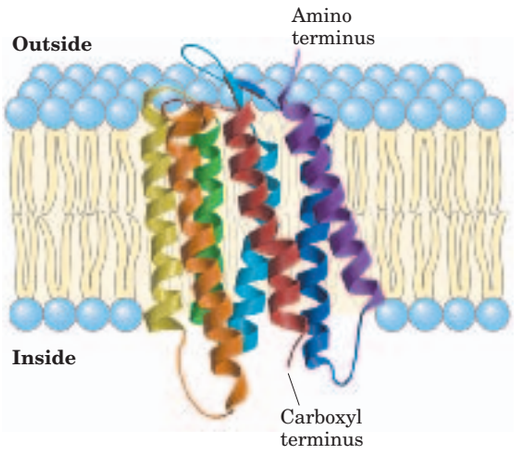

FIGURE 11–9 Bacteriorhodopsin, a membrane-spanning protein. (PDB ID 2AT9) The single polypeptide chain folds into seven hydrophobic α helices, each of which traverses the lipid bilayer roughly perpendicular to the plane of the membrane. The seven transmembrane helices are clustered, and the space around and between them is filled with the acyl chains of membrane lipids. The light-absorbing pigment retinal (see Fig. 10–21) is buried deep in the membrane in contact with several of the helical segments (not shown). The helices are colored to correspond with the hydropathy plot in Figure 11–11b.

which hydrophobic residues are buried within the protein core and hydrophilic residues are on the surface (recall the structures of myoglobin and hemoglobin, for example). In Chapter 19 we will encounter several complex membrane proteins having multiple transmembrane helical segments in which hydrophobic chains are positioned to interact with the lipid bilayer.

The Topology of an Integral Membrane Protein Can Be Predicted from Its Sequence

Determination of the three-dimensional structure of a membrane protein, or its topology, is generally much more difficult than determining its amino acid sequence, which can be accomplished by sequencing the protein or its gene. Thousands of sequences are known for membrane proteins, but relatively few three-dimensional structures have been established by crystallography or NMR spectroscopy. The presence of unbroken sequences of more than 20 hydrophobic residues in a membrane protein is commonly taken as evidence that these sequences traverse the lipid bilayer, acting as hydrophobic anchors or forming transmembrane channels. Virtually all integral proteins have at least one such sequence. Application of this logic to entire genomic sequences leads to the conclusion that in many species, 10% to 20% of all proteins are integral membrane proteins.

What can we predict about the secondary structure of the membrane-spanning portions of integral proteins? An α-helical sequence of 20 to 25 residues is just long enough to span the thickness (30 Å) of the lipid bilayer (recall that the length of an α helix is 1.5 Å (0.15 nm) per amino acid residue). A polypeptide chain surrounded by lipids, having no water molecules with which to hydrogen-bond, will tend to form α helices or β sheets, in which intrachain hydrogen bonding is maximized. If the side chains of all amino acids in a helix are nonpolar, hydrophobic interactions with the surrounding lipids further stabilize the helix.

Several simple methods of analyzing amino acid sequences yield reasonably accurate predictions of secondary structure for transmembrane proteins. The relative polarity of each amino acid has been determined experimentally by measuring the free-energy change accompanying the movement of that amino acid side chain from a hydrophobic solvent into water. This free energy of transfer ranges from very exergonic for charged or polar residues to very endergonic for amino acids with aromatic or aliphatic hydrocarbon side chains. The overall hydrophobicity of a sequence of amino acids is estimated by summing the free energies of transfer for

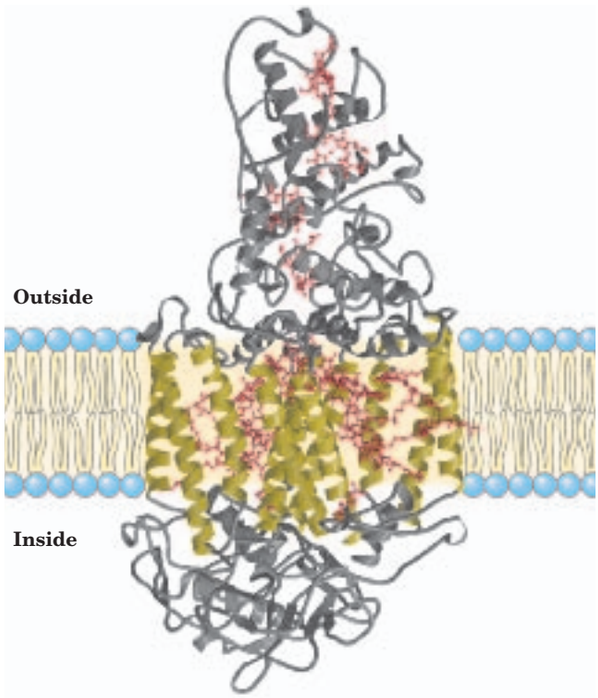

FIGURE 11–10 Three-dimensional structure of the photosynthetic reaction center of *Rhodopseudomonas viridis*, a purple bacterium. This was the first integral membrane protein to have its atomic structure determined by x-ray diffraction methods (PDB ID 1PRC). Eleven α-helical segments from three of the four subunits span the lipid bilayer, forming a cylinder 45 Å (4.5 nm) long; hydrophobic residues on the exterior of the cylinder interact with lipids of the bilayer. In this ribbon representation, residues that are part of the transmembrane helices are shown in yellow. The prosthetic groups (light-absorbing pigments and electron carriers; see Fig. 19–45) are red.

the residues in the sequence, which yields a **hydropathy index** for that region (see Table 3–1). To scan a polypeptide sequence for potential membrane-spanning segments, an investigator calculates the hydropathy index for successive segments (called windows) of a given size, from 7 to 20 residues. For a window of seven residues, for example, the indices for residues 1 to 7, 2 to 8, 3 to 9, and so on, are plotted as in Figure 11–11 (plotted for the middle residue in each window—residue 4 for residues 1 to 7, for example). A region with more than 20 residues of high hydropathy index is presumed to be a transmembrane segment. When the sequences of membrane proteins of known three-dimensional structure are scanned in this way, we find a reasonably good correspondence between predicted and known membrane-spanning segments. Hydropathy analysis predicts a single hydrophobic helix for glycophorin (Fig. 11–11a) and seven transmembrane segments for bacteriorhodopsin (Fig. 11–11b)—in agreement with experimental studies.

On the basis of their amino acid sequences and hydropathy plots, many of the transport proteins described in this chapter are believed to have multiple membrane-spanning helical regions—that is, they are type III or type IV integral proteins (Fig. 11–8). When predictions are consistent with chemical studies of protein localization (such as those described above for glycophorin and bacteriorhodopsin), the assumption that hydrophobic regions correspond to membrane-spanning domains is much better justified.

A further remarkable feature of many transmembrane proteins of known structure is the presence of Tyr and Trp residues at the interface between lipid and water (Fig. 11–12). The side chains of these residues apparently serve as membrane interface anchors, able to interact simultaneously with the central lipid phase and the aqueous phases on either side of the membrane.

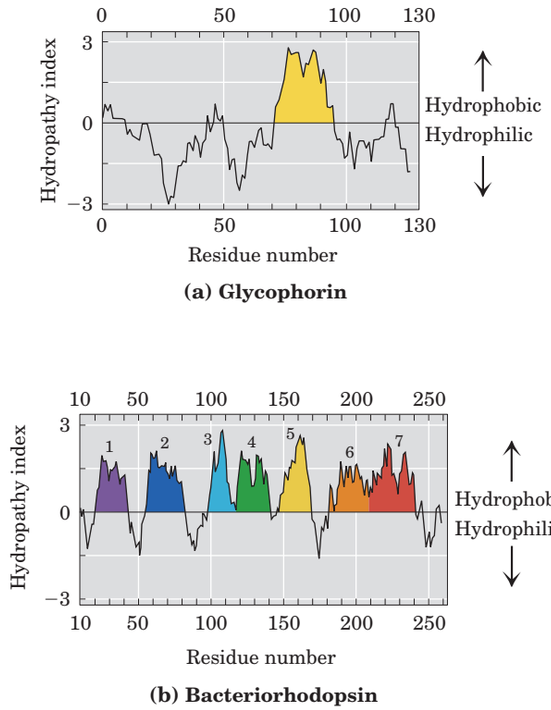

FIGURE 11–11 Hydropathy plots. Hydropathy index (see Table 3–1) is plotted against residue number for two integral membrane proteins. The hydropathy index for each amino acid residue in a sequence of defined length (called the window) is used to calculate the average hydropathy for the residues in that window. The horizontal axis shows the residue number in the middle of the window. **(a)** Glycophorin from human erythrocytes has a single hydrophobic sequence between residues 75 and 93 (yellow); compare this with Figure 11–7. **(b)** Bacteriorhodopsin, known from independent physical studies to have seven transmembrane helices (see Fig. 11–9), has seven hydrophobic regions. Note, however, that the hydropathy plot is ambiguous in the region of segments 6 and 7. Physical studies have confirmed that this region has two transmembrane segments.

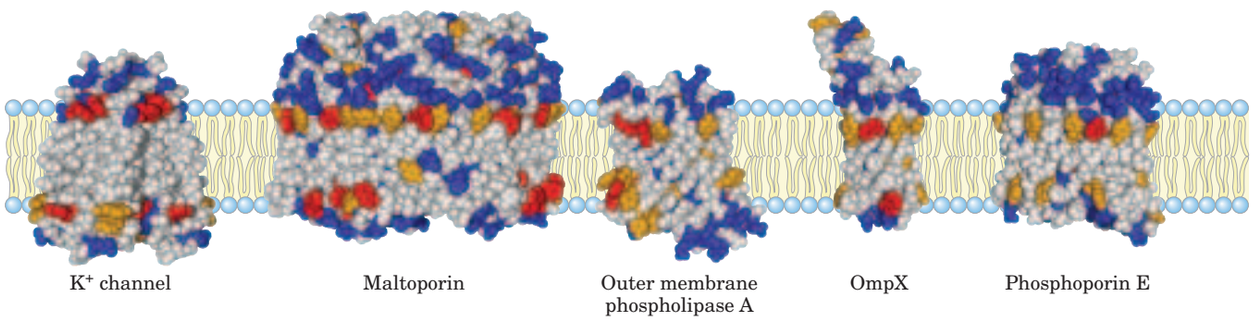

FIGURE 11–12 Tyr and Trp residues of membrane proteins clustering at the water-lipid interface. The detailed structures of these five integral membrane proteins are known from crystallographic studies. The K^+ channel (PDB ID 1BL8) is from the bacterium *Streptomyces lividans* (see Fig. 11–48); maltoporin (PDB ID 1AF6), outer membrane phospholipase A (PDB ID 1QD5), OmpX (PDB ID 1QJ9), and phosphoporin E (PDB ID 1PHO) are proteins of the outer membrane of *E. coli*. Residues of Tyr (orange) and Trp (red) are found predominantly where the nonpolar region of acyl chains meets the polar head group region. Charged residues (Lys, Arg, Glu, Asp) are shown in blue; they are found almost exclusively in the aqueous phases.

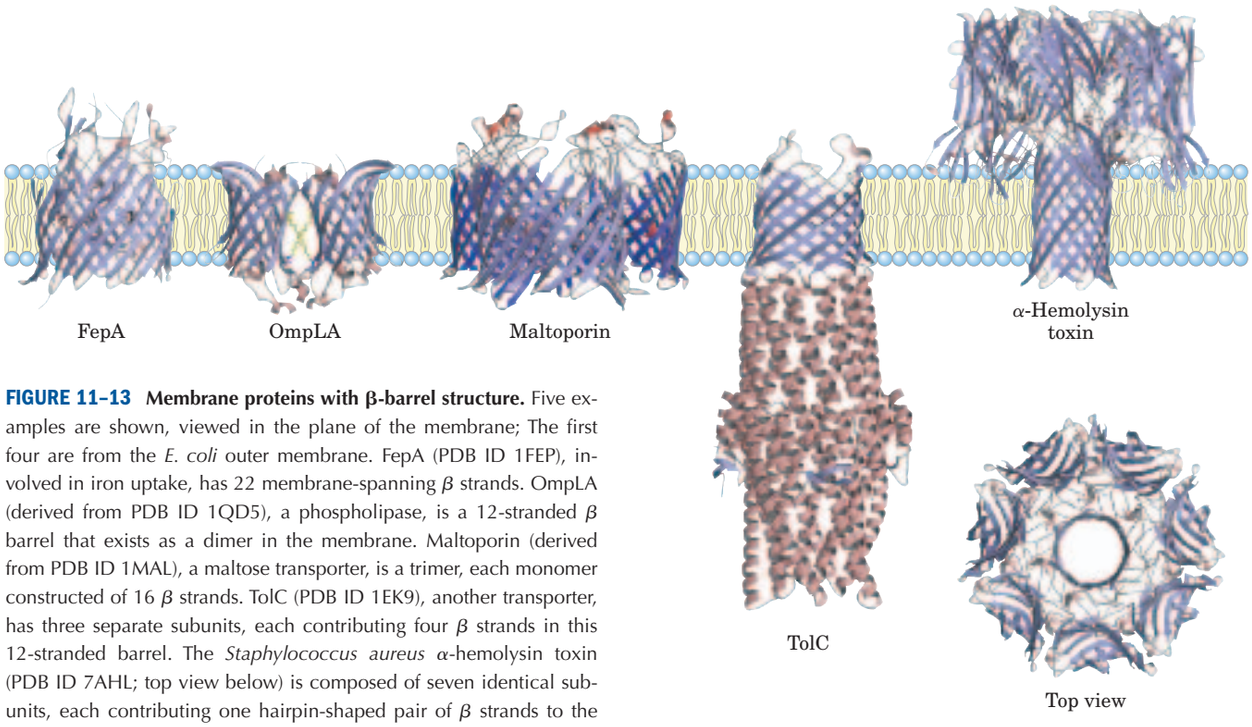

FIGURE 11–13 Membrane proteins with β-barrel structure. Five examples are shown, viewed in the plane of the membrane; The first four are from the *E. coli* outer membrane. FepA (PDB ID 1FEP), involved in iron uptake, has 22 membrane-spanning β strands. OmpLA (derived from PDB ID 1QD5), a phospholipase, is a 12-stranded β barrel that exists as a dimer in the membrane. Maltoporin (derived from PDB ID 1MAL), a maltose transporter, is a trimer, each monomer constructed of 16 β strands. TolC (PDB ID 1EK9), another transporter, has three separate subunits, each contributing four β strands in this 12-stranded barrel. The *Staphylococcus aureus* α-hemolysin toxin (PDB ID 7AHL; top view below) is composed of seven identical subunits, each contributing one hairpin-shaped pair of β strands to the 14-stranded barrel.

The hydrophobic domains of some integral membrane proteins penetrate only one leaflet of the bilayer. Cyclooxygenase, the target of aspirin action, is an example; its hydrophobic helices do not span the whole membrane but interact strongly with the acyl groups on one side of the bilayer (see Box 21–2, Fig. 1a).

Not all integral membrane proteins are composed of transmembrane α helices. Another structural motif common in membrane proteins is the ***β* barrel** (see Fig. 4–20d), in which 20 or more transmembrane segments form β sheets that line a cylinder (Fig. 11–13). The same factors that favor α-helix formation in the hydrophobic interior of a lipid bilayer also stabilize β barrels. When no water molecules are available to hydrogen-bond with the carbonyl oxygen and nitrogen of the peptide bond, maximal intrachain hydrogen bonding gives the most stable conformation. Planar β sheets do not maximize these interactions and are generally not found in the membrane interior; β barrels do allow all possible hydrogen bonds and are apparently common among membrane proteins. **Porins,** proteins that allow certain polar solutes to cross the outer membrane of gram-negative bacteria such as *E. coli,* have many-stranded β barrels lining the polar transmembrane passage.

A polypeptide is more extended in the β conformation than in an α helix; just seven to nine residues of β conformation are needed to span a membrane. Recall that in the β conformation, alternating side chains project above and below the sheet (see Fig. 4–7). In β strands of membrane proteins, every second residue in the membrane-spanning segment is hydrophobic and interacts with the lipid bilayer; aromatic side chains are commonly found at the lipid-protein interface. The other residues may or may not be hydrophilic. The hydropathy plot is not useful in predicting transmembrane segments for proteins with β barrel motifs, but as the database of known β barrel motifs increases, sequence-based predictions of transmembrane β conformations have become feasible. For example, a number of outer membrane proteins of gram-negative bacteria (Fig. 11–13) have been correctly predicted, by sequence analysis, to contain β barrels.

Covalently Attached Lipids Anchor Some Membrane Proteins

Some membrane proteins contain one or more covalently linked lipids of several types: long-chain fatty acids, isoprenoids, sterols, or *g*lycosylated derivatives of *p*hosphatidyl*i*nositol, GPI (Fig. 11–14). The attached lipid provides a hydrophobic anchor that inserts into the lipid bilayer and holds the protein at the membrane surface. The strength of the hydrophobic interaction between a bilayer and a single hydrocarbon chain linked to a protein is barely enough to anchor the protein securely, but many proteins have more than one attached

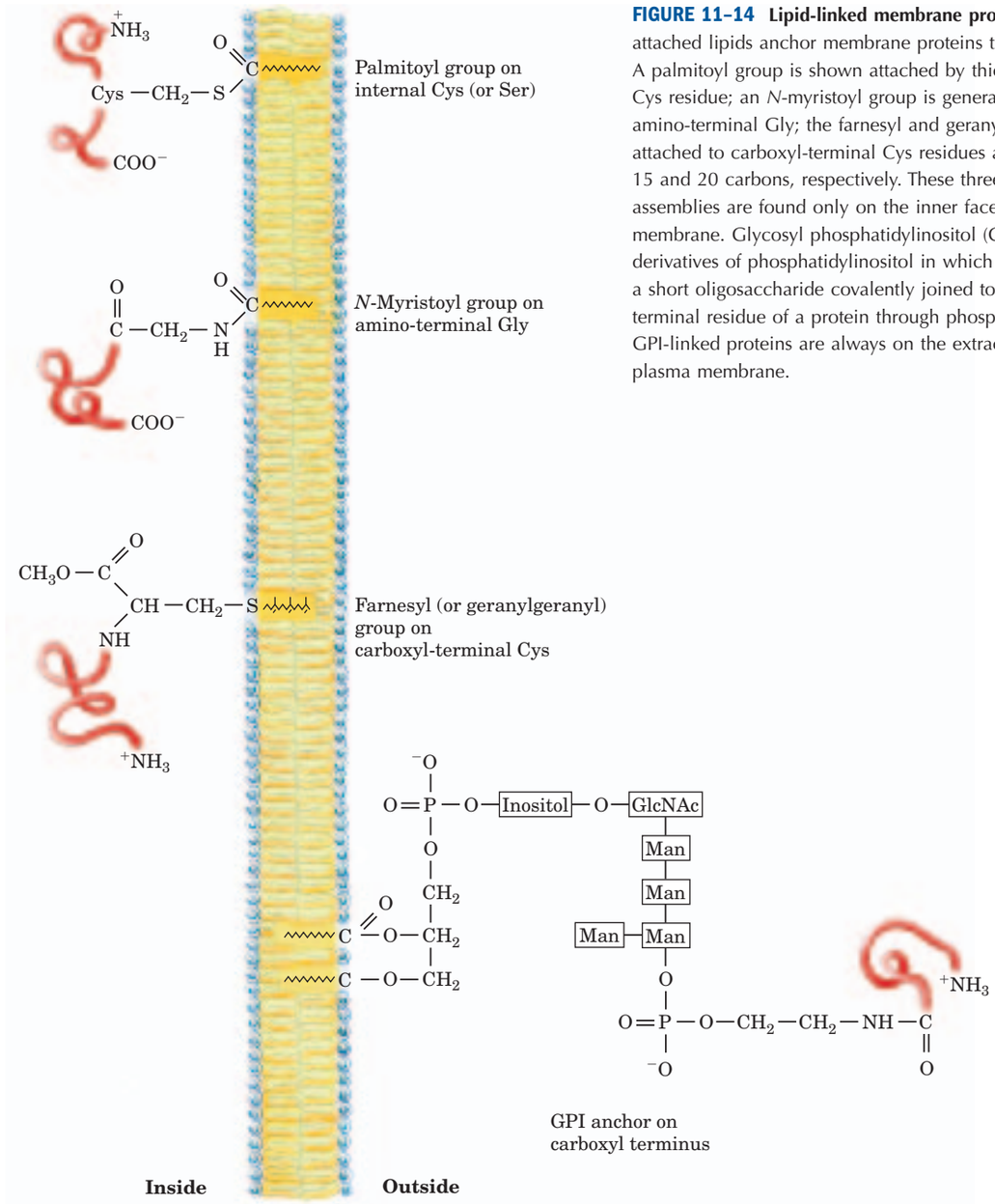

FIGURE 11–14 Lipid-linked membrane proteins. Covalently attached lipids anchor membrane proteins to the lipid bilayer. A palmitoyl group is shown attached by thioester linkage to a Cys residue; an *N*-myristoyl group is generally attached to an amino-terminal Gly; the farnesyl and geranylgeranyl groups attached to carboxyl-terminal Cys residues are isoprenoids of 15 and 20 carbons, respectively. These three lipid-protein assemblies are found only on the inner face of the plasma membrane. Glycosyl phosphatidylinositol (GPI) anchors are derivatives of phosphatidylinositol in which the inositol bears a short oligosaccharide covalently joined to the carboxyl-terminal residue of a protein through phosphoethanolamine. GPI-linked proteins are always on the extracellular face of the plasma membrane.

lipid moiety. Other interactions, such as ionic attractions between positively charged Lys residues in the protein and negatively charged lipid head groups, probably contribute to the stability of the attachment. The association of these lipid-linked proteins with the membrane is certainly weaker than that for integral membrane proteins and is, in at least some cases, reversible. But treatment with alkaline carbonate does not release GPI-linked proteins, which are therefore, by the working definition, integral proteins.

Beyond merely anchoring a protein to the membrane, the attached lipid may have a specific role. In the plasma membrane, proteins with GPI anchors are exclusively on the outer face and are confined within clusters, as we shall see below, whereas other types of lipid-linked proteins (with farnesyl or geranylgeranyl groups attached; Fig. 11–14) are exclusively on the inner face. Attachment of a specific lipid to a newly synthesized membrane protein therefore has a targeting function, directing the protein to its correct membrane location.

SUMMARY 11.1 The Composition and Architecture of Membranes

- Biological membranes define cellular boundaries, divide cells into discrete compartments, organize complex reaction sequences, and act in signal reception and energy transformations.
- Membranes are composed of lipids and proteins in varying combinations particular to each species, cell type, and organelle. The fluid mosaic model describes features common to all biological membranes. The lipid bilayer is the basic structural unit. Fatty acyl chains of phospholipids and the steroid nucleus of sterols are oriented toward the interior of the bilayer; their hydrophobic interactions stabilize the bilayer but give it flexibility.
- Peripheral proteins are loosely associated with the membrane through electrostatic interactions and hydrogen bonds or by covalently attached lipid anchors. Integral proteins associate firmly with membranes by hydrophobic interactions between the lipid bilayer and their nonpolar amino acid side chains, which are oriented toward the outside of the protein molecule.
- Some membrane proteins span the lipid bilayer several times, with hydrophobic sequences of about 20 amino acid residues forming transmembrane α helices. Detection of such hydrophobic sequences in proteins can be used to predict their secondary structure and transmembrane disposition. Multistranded β barrels are also common in integral membrane proteins. Tyr and Trp residues of transmembrane proteins are commonly found at the lipid-water interface.
- The lipids and proteins of membranes are inserted into the bilayer with specific sidedness; thus membranes are structurally and functionally asymmetric. Many membrane proteins contain covalently attached oligosaccharides. Plasma membrane glycoproteins are always oriented with the carbohydrate-bearing domain on the extracellular surface.

11.2 Membrane Dynamics

One remarkable feature of all biological membranes is their flexibility—their ability to change shape without losing their integrity and becoming leaky. The basis for this property is the noncovalent interactions among lipids in the bilayer and the motions allowed to individual lipids because they are not covalently anchored to one another. We turn now to the dynamics of membranes: the motions that occur and the transient structures allowed by these motions.

Acyl Groups in the Bilayer Interior Are Ordered to Varying Degrees

Although the lipid bilayer structure is quite stable, its individual phospholipid and sterol molecules have some freedom of motion (Fig. 11–15). The structure and flexibility of the lipid bilayer depend on temperature and on the kinds of lipids present. At relatively low temperatures, the lipids in a bilayer form a semisolid **gel phase,** in which all types of motion of individual lipid molecules are strongly constrained; the bilayer is paracrystalline (Fig. 11–15a). At relatively high temperatures, individual hydrocarbon chains of fatty acids are in constant motion produced by rotation about the carbon–carbon bonds of the long acyl side chains. In this **liquid-disordered state,** or fluid state (Fig. 11–15b), the interior of the bilayer is more fluid than solid and the bilayer is like a sea of constantly moving lipid. At intermediate temperatures, the lipids exist in a **liquid-ordered state;** there is less thermal motion in the acyl chains of the lipid bilayer, but lateral movement in the plane of the bilayer still takes place. These differences in bilayer state are easily observed in liposomes composed of a single lipid,

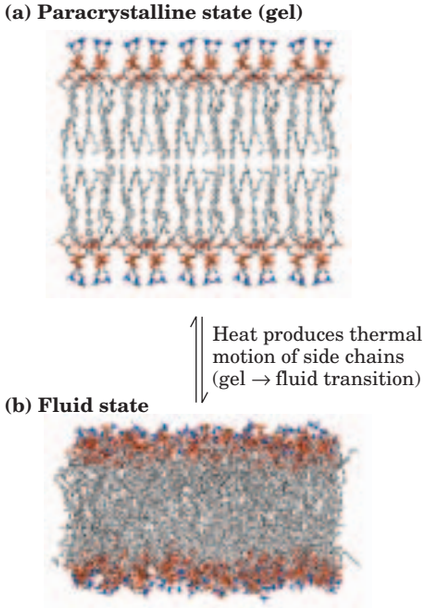

FIGURE 11–15 Two states of bilayer lipids. (a) In the paracrystalline state, or gel phase, polar head groups are uniformly arrayed at the surface, and the acyl chains are nearly motionless and packed with regular geometry; **(b)** in the liquid disordered state, or fluid state, acyl chains undergo much thermal motion and have no regular organization. Intermediate between these extremes is the liquid-ordered state, in which individual phospholipid molecules can diffuse laterally but the acyl groups remain extended and more or less ordered.

but biological membranes contain many lipids with a variety of fatty acyl chains and thus do not show sharp phase changes with temperature.

At temperatures in the physiological range (about 20 to 40 °C), long-chain saturated fatty acids (such as 16:0 and 18:0) pack well into a liquid-ordered array, but the kinks in unsaturated fatty acids (see Fig. 10–1) interfere with this packing, favoring the liquid-disordered state. Shorter-chain fatty acyl groups have the same effect. The sterol content of a membrane (which varies greatly with organism and organelle; Table 11–1) is another important determinant of lipid state. The rigid planar structure of the steroid nucleus, inserted between fatty acyl side chains, reduces the freedom of neighboring fatty acyl chains to move by rotation about their carbon–carbon bonds, forcing acyl chains into their fully extended conformation. The presence of sterols therefore reduces the fluidity in the core of the bilayer, thus favoring the liquid-ordered phase, and increases the thickness of the lipid leaflet (as described below).

Cells regulate their lipid composition to achieve a constant membrane fluidity under various growth conditions. For example, bacteria synthesize more unsaturated fatty acids and fewer saturated ones when cultured at low temperatures than when cultured at higher temperatures (Table 11–2). As a result of this adjustment in lipid composition, membranes of bacteria cultured at high or low temperatures have about the same degree of fluidity.

Transbilayer Movement of Lipids Requires Catalysis

At physiological temperature, transbilayer—or "flip-flop"—diffusion of a lipid molecule from one leaflet of the bilayer to the other (Fig. 11–16a) occurs very slowly if at all in most membranes. Transbilayer movement requires that a polar or charged head group leave its

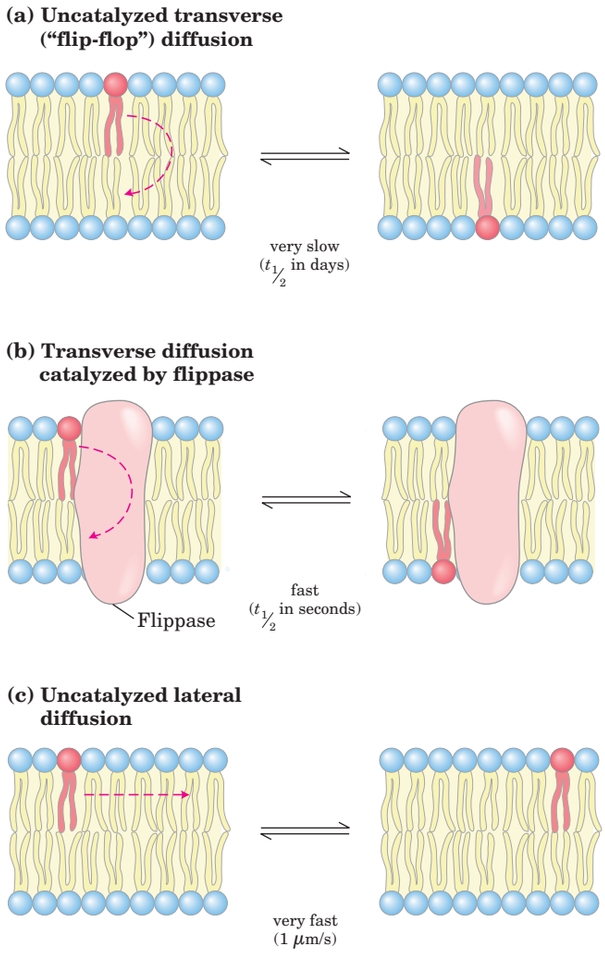

FIGURE 11–16 **Motion of single phospholipids in a bilayer.** **(a)** Movement from one leaflet to the other is very slow, unless **(b)** catalyzed by a flippase; in contrast, lateral diffusion within the leaflet **(c)** is very rapid and requires no protein catalysis.

TABLE 11–2 Fatty Acid Composition of *E. coli* Cells Cultured at Different Temperatures

	*Percentage of total fatty acids**			
	10 °C	*20 °C*	*30 °C*	*40 °C*
Myristic acid (14:0)	4	4	4	8
Palmitic acid (16:0)	18	25	29	48
Palmitoleic acid (16:1)	26	24	23	9
Oleic acid (18:1)	38	34	30	12
Hydroxymyristic acid	13	10	10	8
Ratio of unsaturated to saturated†	2.9	2.0	1.6	0.38

Source: Data from Marr, A.G. & Ingraham, J.L. (1962) Effect of temperature on the composition of fatty acids in *Escherichia coli*. *J. Bacteriol.* **84,** 1260.

*The exact fatty acid composition depends not only on growth temperature but on growth stage and growth medium composition.

†Ratios calculated as the total percentage of 16:1 plus 18:1 divided by the total percentage of 14:0 plus 16:0. Hydroxymyristic acid was omitted from this calculation.

aqueous environment and move into the hydrophobic interior of the bilayer, a process with a large, positive free-energy change. There are, however, situations in which such movement is essential. For example, during synthesis of the bacterial plasma membrane, phospholipids are produced on the inside surface of the membrane and must undergo flip-flop diffusion to enter the outer leaflet of the bilayer. Similar transbilayer diffusion must also take place in eukaryotic cells as membrane lipids synthesized in one organelle move from the inner to the outer leaflet and into other organelles. A family of proteins, the **flippases** (Fig. 11–16b), facilitates flip-flop diffusion, providing a transmembrane path that is energetically more favorable and much faster than the uncatalyzed movement.

Lipids and Proteins Diffuse Laterally in the Bilayer

Individual lipid molecules can move laterally in the plane of the membrane by changing places with neighboring lipid molecules (Fig. 11–16c). A molecule in one monolayer, or leaflet, of the lipid bilayer—the outer leaflet of the erythrocyte plasma membrane, for example—can diffuse laterally so fast that it circumnavigates the erythrocyte in seconds. This rapid lateral diffusion within the plane of the bilayer tends to randomize the positions of individual molecules in a few seconds.

Lateral diffusion can be shown experimentally by attaching fluorescent probes to the head groups of lipids and using fluorescence microscopy to follow the probes over time (Fig. 11–17). In one technique, a small region ($5\ \mu m^2$) of a cell surface with fluorescence-tagged lipids is bleached by intense laser radiation so that the irradiated patch no longer fluoresces when viewed in the much dimmer light of the fluorescence microscope. However, within milliseconds, the region recovers its fluorescence as unbleached lipid molecules diffuse into the bleached patch and bleached lipid molecules diffuse away from it. The rate of *f*luorescence *r*ecovery *a*fter *p*hotobleaching, or **FRAP,** is a measure of the rate of lateral diffusion of the lipids. Using the FRAP technique, researchers have shown that some membrane lipids diffuse laterally by up to 1 μm/s.

Another technique, single particle tracking, allows one to follow the movement of a *single* lipid molecule in the plasma membrane on a much shorter time scale. Results from these studies confirm the rapid lateral diffusion within small, discrete regions of the cell sur-

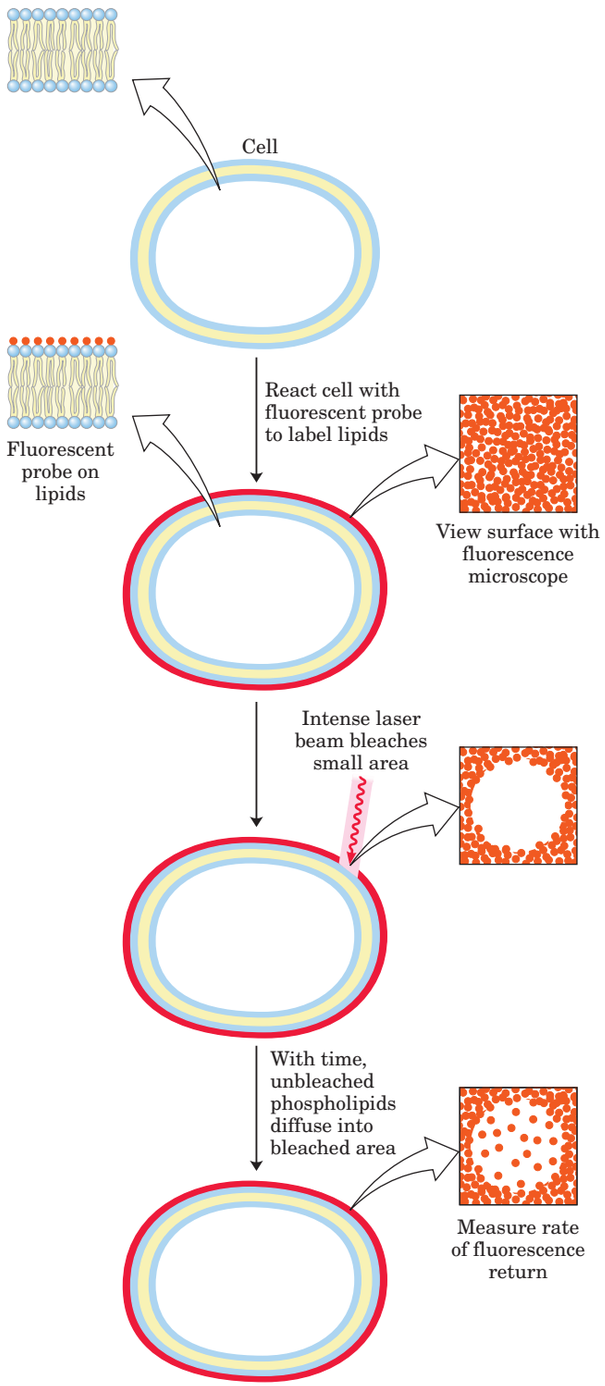

FIGURE 11–17 Measurement of lateral diffusion rates of lipids by fluorescence recovery after photobleaching (FRAP). The lipids in the outer leaflet of the plasma membrane are labeled by reaction with a membrane-impermeant fluorescent probe (red), so the surface is uniformly labeled when viewed with a fluorescence microscope. A small area is bleached by irradiation with an intense laser beam, leaving that area nonfluorescent. With the passage of time, labeled lipid molecules diffuse into the bleached region, and it again becomes fluorescent. From the time course of fluorescence return to this area, the diffusion coefficient for the labeled lipid is determined. The rates are typically high; a lipid moving at this speed could circumnavigate *E. coli* in one second. (The FRAP method can also be used to measure the lateral diffusion of membrane proteins.)

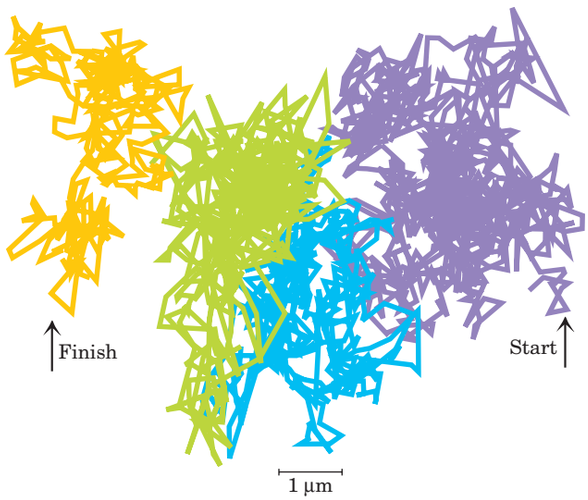

FIGURE 11–18 Hop diffusion of individual lipid molecules. The motion of a single fluorescent lipid molecule in a cell surface is recorded on video by fluorescence microscopy, with a time resolution of 25 μs (equivalent to 40,000 frames/s). The track shown here represents a molecule followed for 56 ms (a total of 2,250 frames); the trace begins in the purple area and continues through blue, green, and orange. The pattern of movement indicates rapid diffusion within a confined region (about 250 nm in diameter, shown by a single color), with occasional hops into an adjoining region. This finding suggests that the lipids are corralled by molecular fences that they occasionally jump.

face and show that movement from one such region to a nearby region is inhibited; lipids behave as though corralled by fences that they can occasionally jump (Fig. 11–18).

Many membrane proteins seem to be afloat in a sea of lipids. Like membrane lipids, these proteins are free to diffuse laterally in the plane of the bilayer and are in constant motion, as shown by the FRAP technique with fluorescence-tagged surface proteins. Some membrane proteins associate to form large aggregates ("patches") on the surface of a cell or organelle in which individual protein molecules do not move relative to one another; for example, acetylcholine receptors (see Fig. 11–51) form dense patches on neuron plasma membranes at synapses. Other membrane proteins are anchored to internal structures that prevent their free diffusion. In the erythrocyte membrane, both glycophorin and the chloride-bicarbonate exchanger (p. 395) are tethered to spectrin, a filamentous cytoskeletal protein (Fig. 11–19). One possible explanation for the pattern of lateral diffusion of lipid molecules shown in Figure 11–18 is that membrane proteins immobilized by their association with spectrin are the "fences" that define the regions of relatively unrestricted lipid motion.

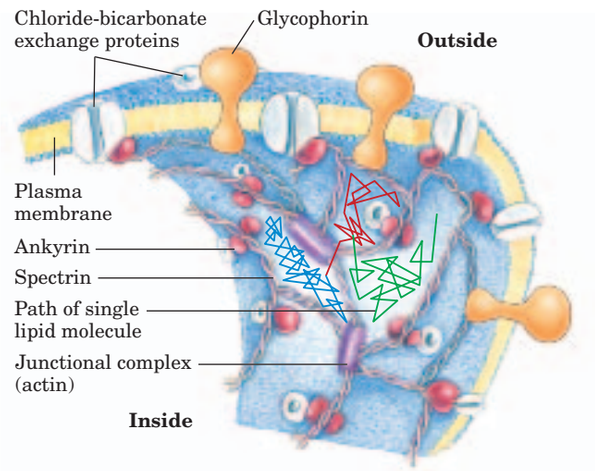

FIGURE 11–19 Restricted motion of the erythrocyte chloride-bicarbonate exchanger and glycophorin. The proteins span the membrane and are tethered to spectrin, a cytoskeletal protein, by another protein, ankyrin, limiting their lateral mobilities. Ankyrin is anchored in the membrane by a covalently bound palmitoyl side chain (see Fig. 11–14). Spectrin, a long, filamentous protein, is cross-linked at junctional complexes containing actin. A network of cross-linked spectrin molecules attached to the cytoplasmic face of the plasma membrane stabilizes the membrane against deformation. This network of anchored membrane proteins may be the "corral" suggested by the experiment shown in Figure 11–18; the lipid tracks shown here are confined to subregions defined by the tethered membrane proteins.

Sphingolipids and Cholesterol Cluster Together in Membrane Rafts

We have seen that diffusion of membrane lipids from one bilayer leaflet into the other is very slow unless catalyzed, and that the different lipid species of the plasma membrane are asymmetrically distributed in the two leaflets of the bilayer (Fig. 11–5). Even within a single leaflet, the lipid distribution is not random. Glycosphingolipids (cerebrosides and gangliosides), which typically contain long-chain saturated fatty acids, form transient clusters in the outer leaflet that largely exclude glycerophospholipids, which typically contain one unsaturated fatty acyl group and a shorter saturated fatty acyl group. The long, saturated acyl groups of sphingolipids can form more compact, more stable associations with the long ring system of cholesterol than can the shorter, often unsaturated, chains of phospholipids. The cholesterol-sphingolipid **microdomains** in the outer monolayer of the plasma membrane, visible with atomic-force microscopy (Box 11–1), are slightly thicker and more ordered (less fluid) than neighboring microdomains rich in phospholipids (Fig. 11–20) and are more difficult

BOX 11–1 WORKING IN BIOCHEMISTRY

Atomic Force Microscopy to Visualize Membrane Proteins

In atomic force microscopy (AFM), the sharp tip of a microscopic probe attached to a flexible cantilever is drawn across an uneven surface such as a membrane (Fig. 1). Electrostatic and van der Waals interactions between the tip and the sample produce a force that moves the probe up and down (in the z dimension) as it encounters hills and valleys in the sample. A laser beam reflected from the cantilever detects motions of as little as 1 Å. In one type of atomic force microscope, the force on the probe is held constant (relative to a standard force, on the order of piconewtons) by a feedback circuit that causes the platform holding the sample to rise or fall to keep the force constant. A series of scans in the x and y dimensions (the plane of the membrane) yields a three-dimensional contour map of the surface with resolution near the atomic scale—0.1 nm in the vertical dimension, 0.5 to 1.0 nm in the lateral dimensions. The membrane rafts shown in Figure 11–20b were visualized by this technique.

In favorable cases, AFM can be used to study single membrane protein molecules. Single molecules of bacteriorhodopsin in the purple membranes of the bacterium *Halobacterium salinarum* (see Fig. 11–9) are seen as highly regular structures (Fig. 2a). When a number of images of individual units are superimposed with the help of a computer, the real parts of the image reinforce each other and the noise in individual images is averaged out, yielding a high-resolution image of the protein (inset in Fig. 2a). AFM of purified *E. coli* aquaporin, reconstituted into lipid bilayers and viewed as if from the outside of a cell, shows the fine details of the protein's periplasmic domains (Fig. 2b). And AFM reveals that F_o, the proton-driven rotor of the chloroplast ATP synthase (p. 742), is composed of many subunits (14 in Fig. 2c) arranged in a circle.

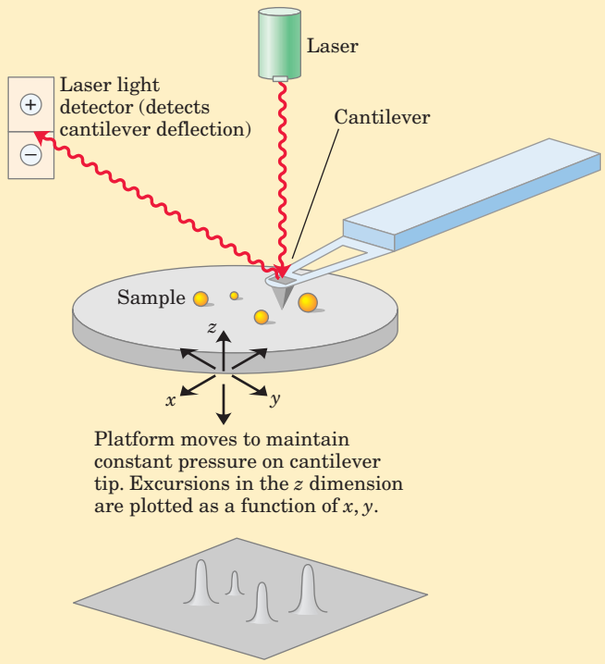

FIGURE 1

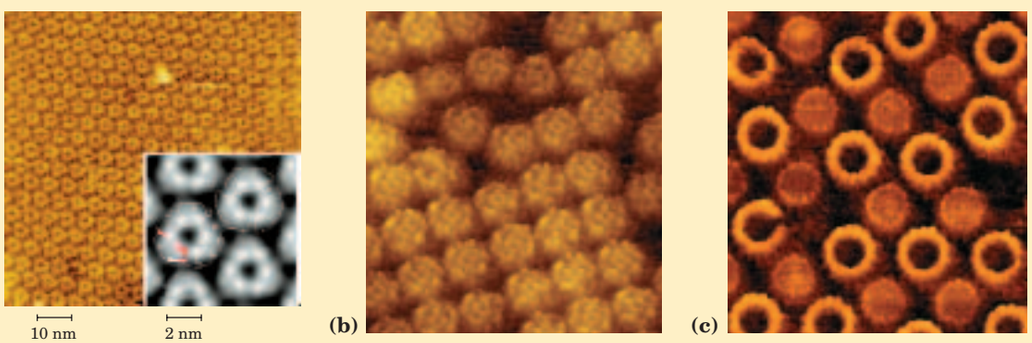

FIGURE 2

to dissolve with nonionic detergents; they behave like liquid-ordered sphingolipid **rafts** adrift in a sea of liquid-disordered phospholipids.

These lipid rafts are remarkably enriched in two classes of integral membrane proteins: those anchored to the membrane by two covalently attached long-chain saturated fatty acids (two palmitoyl groups or a palmitoyl and a myristoyl group) and GPI-anchored proteins (Fig. 11–14). Presumably these lipid anchors, like the acyl chains of sphingolipids, form more stable associations with the cholesterol and long acyl groups in rafts than with the surrounding phospholipids. (It is notable

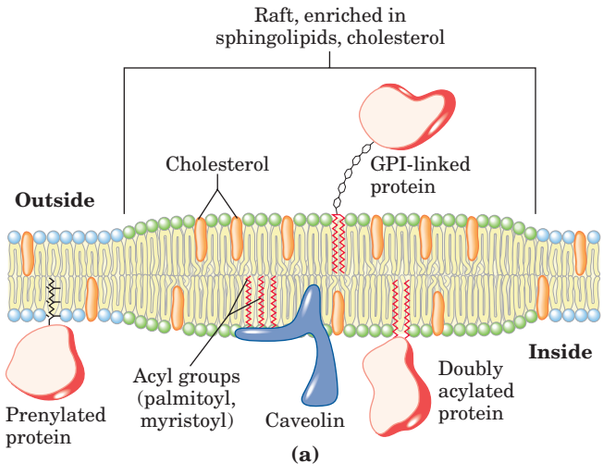

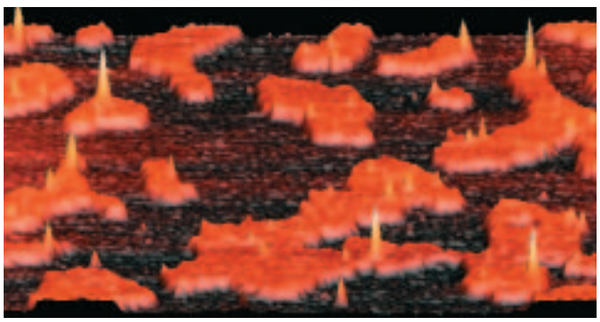

FIGURE 11–20 Microdomains (rafts) in the plasma membrane. **(a)** Stable associations of sphingolipids and cholesterol in the outer leaflet produce a microdomain, slightly thicker than other membrane regions, that is enriched with specific types of membrane proteins. GPI-linked proteins are commonly found in the outer leaflet of such rafts, and proteins with one or several covalently attached long-chain acyl groups are common in the inner leaflet. Caveolin is especially common in inwardly curved rafts called caveolae (see Fig. 11–21). Proteins with attached prenyl groups (such as Ras; see Fig. 12–6) tend to be excluded from rafts. **(b)** The greater thickness of raft regions can be visualized by atomic force microscopy (see Box 11–1). In this view of a membrane region, we can see the rafts protruding from a lipid bilayer ocean; in the rafts, sharp peaks represent GPI-linked proteins. Note that these peaks are found almost exclusively in rafts.

that other lipid-linked proteins, those with covalently attached isoprenyl groups such as farnesyl, are *not* preferentially associated with the outer leaflet of sphingolipid/cholesterol rafts (Fig. 11–20a).) The "raft" and "sea" domains of the plasma membrane are not rigidly separated; membrane proteins can move into and out of lipid rafts on a time scale of seconds. But in the shorter time scale (microseconds) more relevant to many membrane-mediated biochemical processes, many of these proteins reside primarily in a raft.

We can estimate the fraction of the cell surface occupied by rafts from the fraction of the plasma membrane that resists detergent solubilization, which can be as high as 50% in some cases: the rafts cover half of the ocean (Fig. 11–20b). Indirect measurements in cultured fibroblasts suggest a diameter of roughly 50 nm for an individual raft, which corresponds to a patch containing a few thousand sphingolipids and perhaps 10 to 50 membrane proteins. Because most cells express more than 50 different kinds of plasma membrane proteins, it is likely that a single raft contains only a subset of membrane proteins and that this segregation of membrane proteins is functionally significant. For a process that involves interaction of two membrane proteins, their presence in a single raft would hugely increase the likelihood of their collision. Certain membrane receptors and signaling proteins, for example, appear to be segregated together in membrane rafts. Experiments show that signaling through these proteins can be disrupted by manipulations that deplete the plasma membrane of cholesterol and destroy lipid rafts.

Caveolins Define a Special Class of Membrane Rafts

Caveolin is an integral membrane protein with two globular domains connected by a hairpin-shaped hydrophobic domain, which binds the protein to the cytoplasmic leaflet of the plasma membrane. Three palmitoyl groups attached to the carboxyl-terminal globular domain further anchor it to the membrane. Caveolin (actually, a family of related caveolins) binds cholesterol in the membrane, and the presence of caveolin forces the associated lipid bilayer to curve inward, forming **caveolae** ("little caves") in the surface of the cell (Fig. 11–21). Caveolae are unusual rafts: they involve *both* leaflets of the bilayer—the cytoplasmic leaflet, from which the caveolin globular domains project, and the exoplasmic leaflet, a typical sphingolipid/cholesterol raft with associated GPI-anchored proteins. Caveolae are implicated in a variety of cellular functions, including membrane trafficking within cells and the transduction of external signals into cellular responses. The receptors for insulin and other growth factors, as well as certain GTP-binding proteins and protein kinases associated with transmembrane signaling, appear to be localized in rafts and perhaps in caveolae. We discuss some possible roles of rafts in signaling in Chapter 12.

Certain Integral Proteins Mediate Cell-Cell Interactions and Adhesion

Several families of integral proteins in the plasma membrane provide specific points of attachment between cells, or between a cell and extracellular matrix proteins. **Integrins** are heterodimeric proteins (two unlike subunits, α and β) anchored to the plasma membrane by a single hydrophobic transmembrane helix in each subunit (Fig. 11–22; see also Fig. 7–30). The large extracellular domains of the α and β subunits combine to form a specific binding site for extracellular proteins

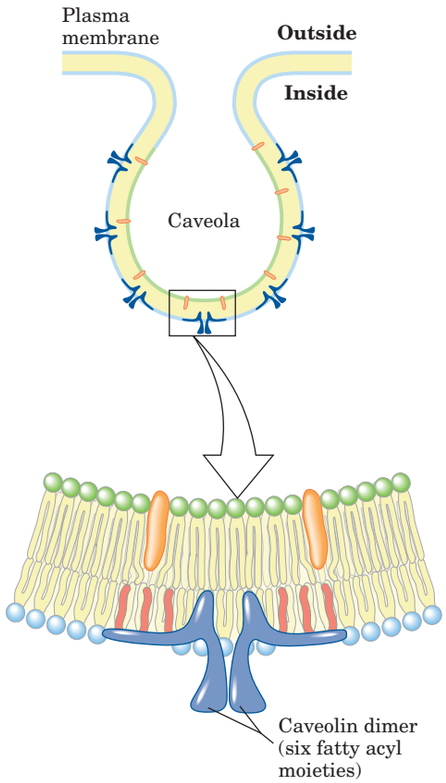

FIGURE 11–21 Caveolin forces inward curvature in membranes. The protein caveolin has a central hydrophobic domain and three long-chain acyl groups on each monomeric unit, which hold the molecule to the inside of the plasma membrane. When a number of caveolin dimers are concentrated in a small region (a raft), they force a curvature in the lipid bilayer, forming a caveola.

such as collagen and fibronectin. As there are 18 different α subunits and at least 8 different β subunits, a wide variety of specificities may be generated from various combinations of α and β. One common determinant of integrin binding in several extracellular partners of integrins is the sequence Arg–Gly–Asp (RGD).

Integrins are not merely adhesives; they serve as receptors and signal transducers, conveying information across the plasma membrane in both directions. Integrins regulate many processes, including platelet aggregation at the site of a wound, tissue repair, the activity of immune cells, and the invasion of tissue by a tumor. Mutation in an integrin gene encoding the β subunit known as CD18 is the cause of leukocyte adhesion deficiency in humans, a rare genetic disease in which leukocytes fail to pass out of blood vessels to reach sites of infection (see Fig. 7–33). Infants with a severe defect in CD18 commonly die of infections before the age of two. ■

At least three other families of plasma membrane proteins are also involved in surface adhesion (Fig. 11–22). **Cadherins** undergo homophilic ("with same kind") interactions with identical cadherins in an adjacent cell. **Immunoglobulin-like proteins** can undergo either homophilic interactions with their identical counterparts on another cell or heterophilic interactions with an integrin on a neighboring cell. **Selectins** have extracellular domains that, in the presence of Ca^{2+}, bind specific polysaccharides on the surface of an adjacent cell. Selectins are present primarily in the various types of blood cells and in the endothelial cells that line blood vessels (see Fig. 7–33). They are an essential part of the blood-clotting process.

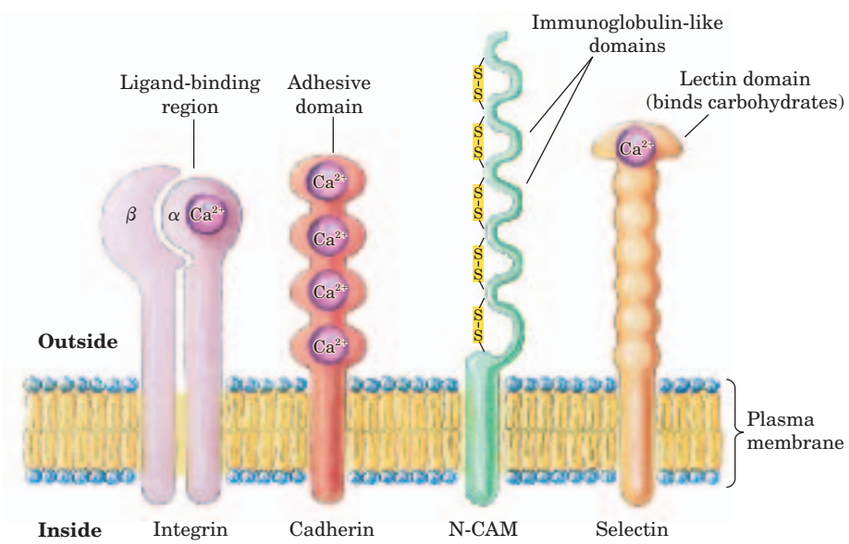

FIGURE 11–22 Four examples of integral protein types that function in cell-cell interactions. Integrins consist of α and β transmembrane polypeptides; their extracellular domains combine to form binding sites for divalent metal ions and proteins of the extracellular matrix (such as collagen and fibronectin) or for specific surface proteins of other cells. Cadherin has four extracellular Ca^{2+}-binding domains, the most distal of which contains the site that binds to cadherin on another cell surface. N-CAM (*n*euronal cell *a*dhesion *m*olecule) is one of a family of immunoglobulin-like proteins that mediate Ca^{2+}-independent interactions with surface proteins of nearby cells. Selectins bind tightly to carbohydrate moieties in neighboring cells; this binding is Ca^{2+}-dependent.

Integral proteins play a role in many other cellular processes. They serve as transporters and ion channels (discussed in Section 11.3) and as receptors for hormones, neurotransmitters, and growth factors (Chapter 12). They are central to oxidative phosphorylation and photosynthesis (Chapter 19) and to cell-cell and antigen-cell recognition in the immune system (Chapter 5). Integral proteins are also important players in the membrane fusion that accompanies exocytosis, endocytosis, and the entry of many types of viruses into host cells.

Membrane Fusion Is Central to Many Biological Processes

A remarkable feature of the biological membrane is its ability to undergo fusion with another membrane without losing its continuity. Although membranes are stable, they are by no means static. Within the eukaryotic endomembrane system (which includes the nuclear membrane, endoplasmic reticulum, Golgi, and various small vesicles), the membranous compartments constantly reorganize. Vesicles bud from the endoplasmic reticulum to carry newly synthesized lipids and proteins to other organelles and to the plasma membrane. Exocytosis, endocytosis, cell division, fusion of egg and sperm cells, and entry of a membrane-enveloped virus into its host cell all involve membrane reorganization in which the fundamental operation is fusion of two membrane segments without loss of continuity (Fig. 11–23).

Specific fusion of two membranes requires that (1) they recognize each other; (2) their surfaces become closely apposed, which requires the removal of water molecules normally associated with the polar head groups of lipids; (3) their bilayer structures become locally disrupted, resulting in fusion of the outer leaflet of each membrane (hemifusion); and (4) their bilayers fuse to form a single continuous bilayer. Receptor mediated endocytosis, or regulated secretion, also requires that (5) the fusion process is triggered at the appropriate time or in response to a specific signal. Integral proteins called **fusion proteins** mediate these events, bringing about specific recognition and a transient local distortion of the bilayer structure that favors membrane fusion. (Note that these fusion proteins are unrelated to the products of two fused genes, also called fusion proteins, discussed in Chapter 9.)

Two cases of membrane fusion are especially well studied: the entry into a host cell of an enveloped virus such as influenza virus, and the release of neurotransmitters by exocytosis. Both processes involve complexes of fusion proteins that undergo dramatic conformational changes.

The influenza virus is surrounded by a membrane containing, among other proteins, many molecules of the hemagglutination (HA) protein (named for its ability to cause erythrocytes to clump together). The virus enters a host cell by inducing endocytosis, which encloses the virus in an endosome, a small membrane vesicle with a pH of about 5 (Fig. 11–24). At this pH, a conformational change in the HA protein occurs, exposing a sequence within the HA protein called the **fusion peptide** and enabling the protein to penetrate the endosomal membrane. The endosomal membrane and the viral membrane are now connected through the HA protein. Next, the HA protein bends at its middle to form a hairpin shape, bringing its two ends together. This pulls the two membranes into close apposition and causes fusion of the viral membrane and the endosomal membrane. The HA protein functions as a trimer (Fig. 11–24). In its low-pH form, three HA domains at the closed end of the hairpin twist about each other to form a stable, coiled structure. The fusion process involves an intermediate stage (hemifusion) in which the outer leaflet of the viral membrane is fused with the inner leaflet of the endosomal membrane, while the other two leaflets maintain their continuity. At the point of hemifusion, the lipid bilayer must be temporarily disorganized, presumably caused by the HA fusion peptide

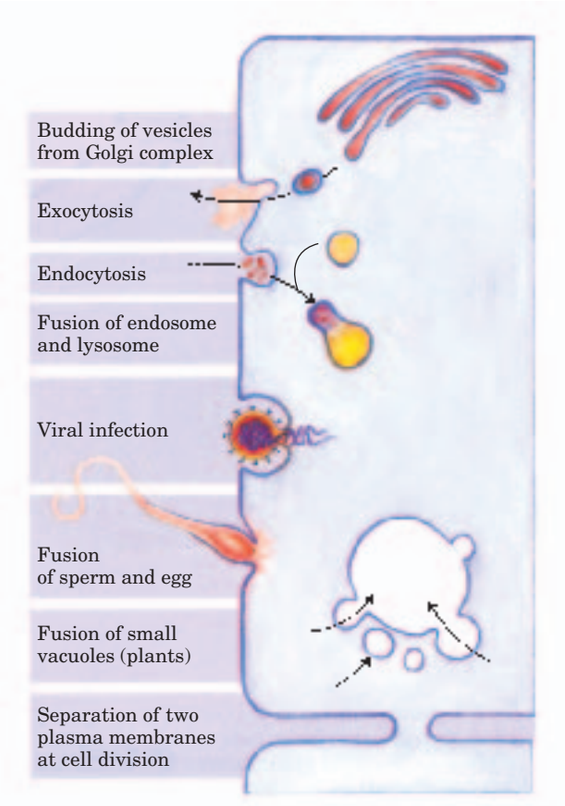

FIGURE 11–23 Membrane fusion. The fusion of two membranes is central to a variety of cellular processes involving both organelles and the plasma membrane.

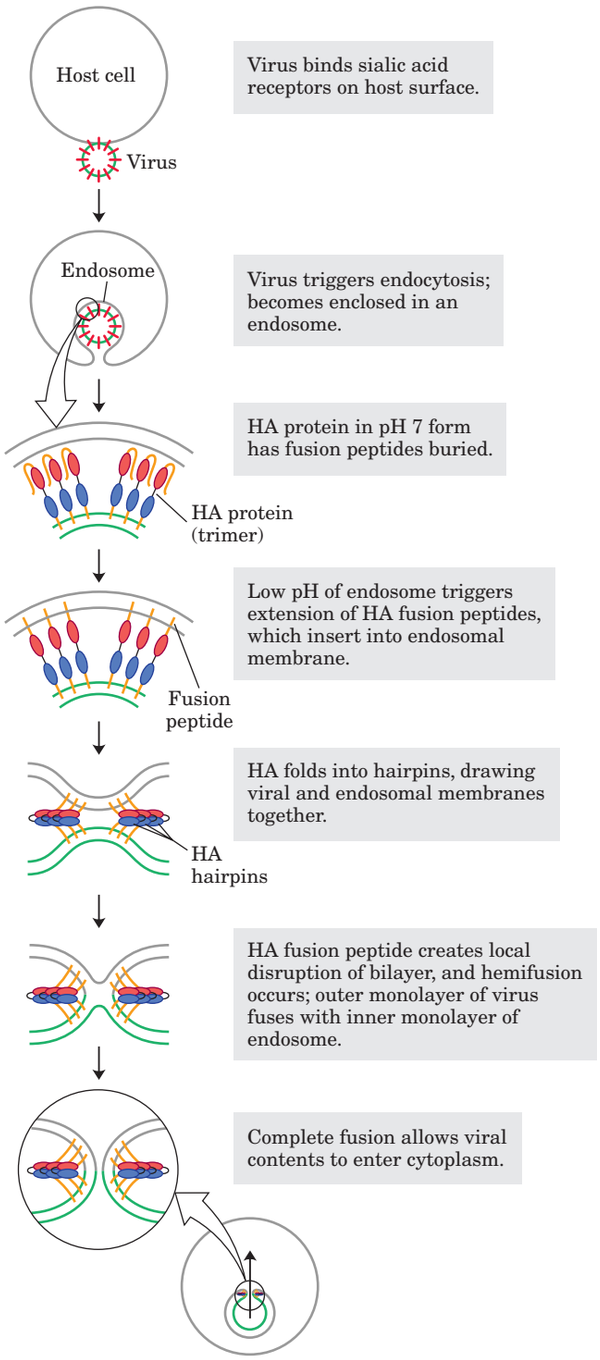

FIGURE 11–24 Fusion induced by the hemagglutinin (HA) protein during viral infection. HA protein is exposed on the membrane surface of the influenza virus. When the virus moves from the neutral pH of the interstitial fluid to the low-pH compartment (endosome) in the host cell, HA undergoes dramatic shape changes that mediate fusion of the viral and endosomal membranes, releasing the viral contents into the cytoplasm.

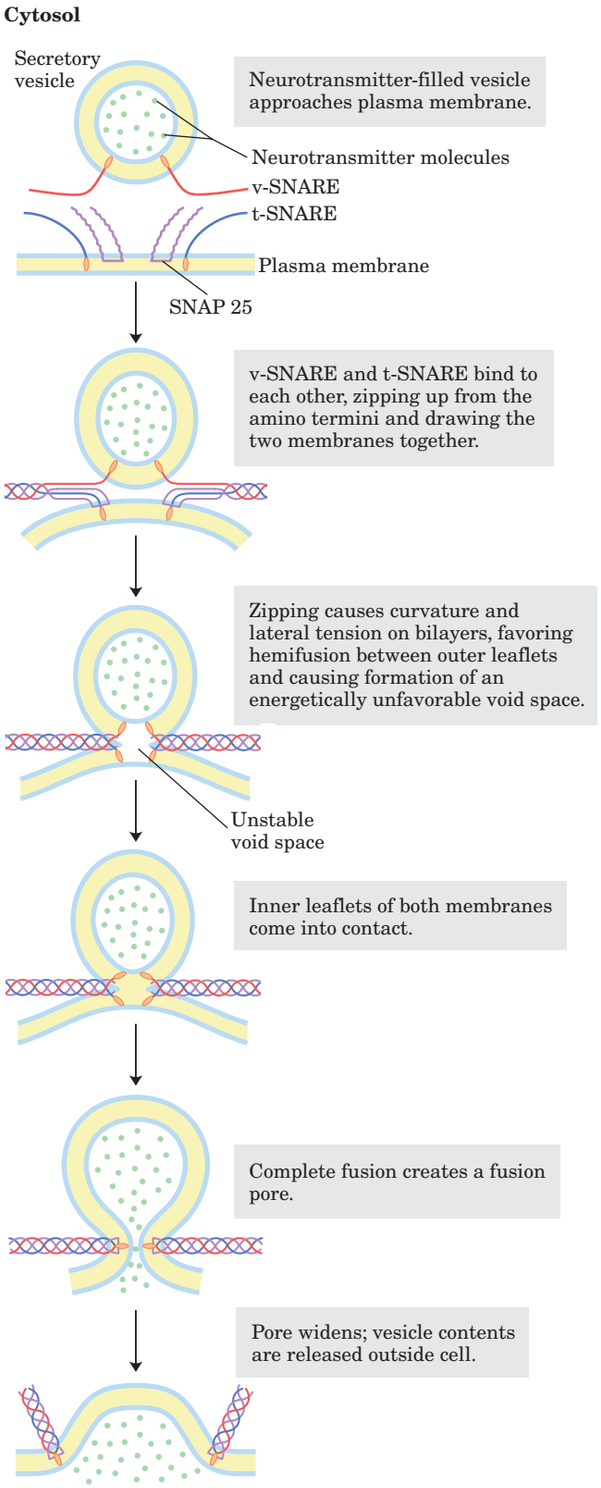

FIGURE 11–25 Fusion during neurotransmitter release at a synapse. The membrane of the secretory vesicle contains the v-SNARE synaptobrevin (red). The target (plasma) membrane contains the t-SNAREs syntaxin (blue) and SNAP25 (violet). When a local increase in $[Ca^{2+}]$ signals release of neurotransmitter, the v-SNARE, SNAP25, and t-SNARE interact, forming a coiled bundle of four α helices, pulling the two membranes together and disrupting the bilayer locally, which leads to membrane fusion and neurotransmitter release.

domains. Complete fusion results in release of the viral contents into the host cell cytoplasm.

Neurotransmitters are released at synapses when intracellular vesicles loaded with neurotransmitter fuse with the plasma membrane. This process involves a family of proteins called SNARES (Fig. 11–25). SNAREs in the cytoplasmic face of the intracellular vesicles are called **v-SNAREs;** those in the target membranes with which the vesicles fuse (the plasma membrane during exocytosis) are **t-SNAREs.** Two other proteins, SNAP25 and NSF, are also involved. During fusion, v- and t-SNAREs bind to each other and undergo a structural change that produces a bundle of long thin rods made up of helices from both v- and t-SNARES and two helices from SNAP25 (Fig. 11–25). The two SNAREs initially interact at their ends, then zip up into the bundle of helices. This structural change pulls the two membranes into contact and initiates the fusion of their lipid bilayers.

The complex of SNAREs and SNAP25 is the target of the powerful *Clostridium botulinum* toxin, a protease that cleaves specific bonds in these proteins, preventing neurotransmission and causing the death of the organism. Because of its very high specificity for these proteins, purified botulinum toxin has served as a powerful tool for dissecting the mechanism of neurotransmitter release in vivo and in vitro.

SUMMARY 11.2 Membrane Dynamics

- Lipids in a biological membrane can exist in liquid-ordered or liquid-disordered states; in the latter state, thermal motion of acyl chains makes the interior of the bilayer fluid. Fluidity is affected by temperature, fatty acid composition, and sterol content.
- Flip-flop diffusion of lipids between the inner and outer leaflets of a membrane is very slow except when specifically catalyzed by flippases.
- Lipids and proteins can diffuse laterally within the plane of the membrane, but this mobility is limited by interactions of membrane proteins with internal cytoskeletal structures and interactions of lipids with lipid rafts. One class of lipid rafts consists of sphingolipids and cholesterol with a subset of membrane proteins that are GPI-linked or attached to several long-chain fatty acyl moieties.
- Caveolin is an integral membrane protein that associates with the inner leaflet of the plasma membrane, forcing it to curve inward to form caveolae, probably involved in membrane transport and signaling.
- Integrins are transmembrane proteins of the plasma membrane that act both to attach cells to each other and to carry messages between the extracellular matrix and the cytoplasm.
- Specific proteins mediate the fusion of two membranes, which accompanies processes such as viral invasion and endocytosis and exocytosis.

11.3 Solute Transport across Membranes

Every living cell must acquire from its surroundings the raw materials for biosynthesis and for energy production, and must release to its environment the byproducts of metabolism. A few nonpolar compounds can dissolve in the lipid bilayer and cross the membrane unassisted, but for polar or charged compounds or ions, a membrane protein is essential for transmembrane movement. In some cases a membrane protein simply facilitates the diffusion of a solute down its concentration gradient, but transport often occurs against a gradient of concentration, electrical charge, or both, in which case solutes must be "pumped" in a process that requires energy (Fig. 11–26). The energy may come directly from ATP hydrolysis or may be supplied in the form of movement of another solute down its electrochemical gradient with enough energy to carry another solute up its gradient. Ions may also move across membranes via ion channels formed by proteins, or they may be carried across by ionophores, small molecules that mask the charge of the ions and allow them to diffuse through the lipid bilayer. With very few exceptions, the traffic of small molecules across the plasma membrane is mediated by proteins such as transmembrane channels, carriers, or pumps. Within the eukaryotic cell, different compartments have different concentrations of metabolic intermediates and products and of ions, and these, too, must move across intracellular membranes in tightly regulated, protein-mediated processes.

Passive Transport Is Facilitated by Membrane Proteins

When two aqueous compartments containing unequal concentrations of a soluble compound or ion are separated by a permeable divider (membrane), the solute moves by **simple diffusion** from the region of higher concentration, through the membrane, to the region of lower concentration, until the two compartments have equal solute concentrations (Fig. 11–27a). When ions of opposite charge are separated by a permeable membrane, there is a transmembrane electrical gradient, a **membrane potential, V_m** (expressed in volts or millivolts). This membrane potential produces a force opposing ion movements that increase V_m and driving ion movements that reduce V_m (Fig. 11–27b). Thus the direction in which a charged solute tends to move spontaneously across a membrane depends on both the

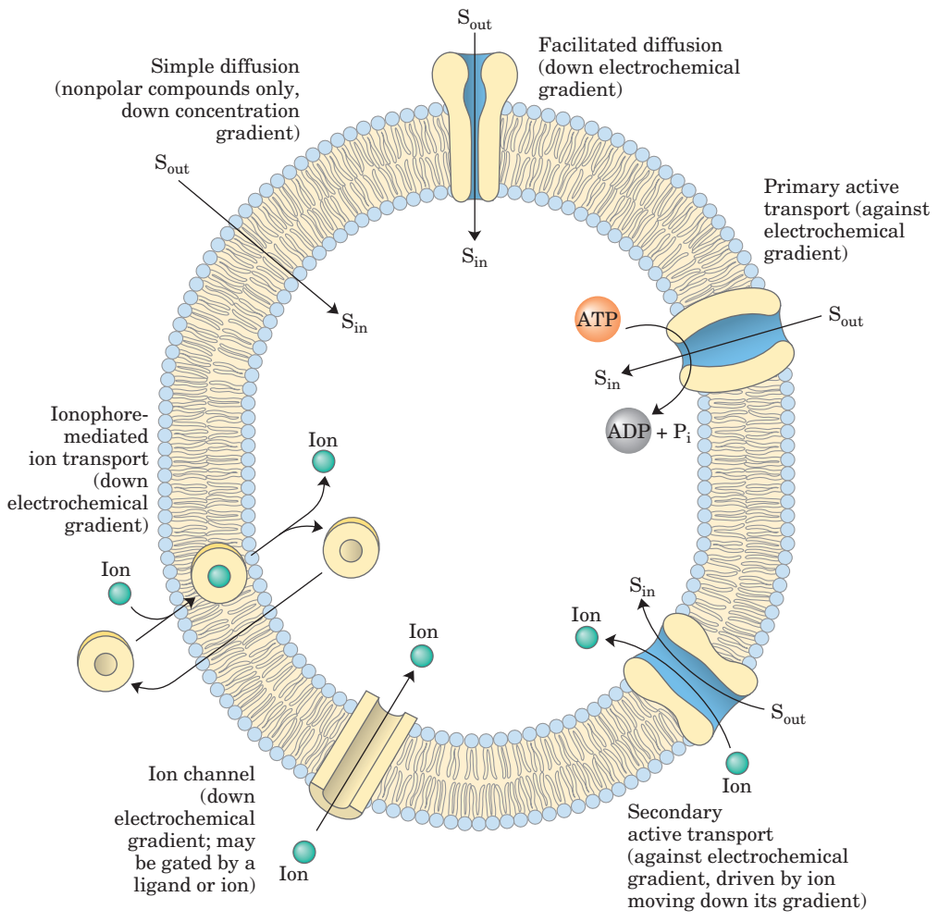

FIGURE 11–26 **Summary of transport types.**

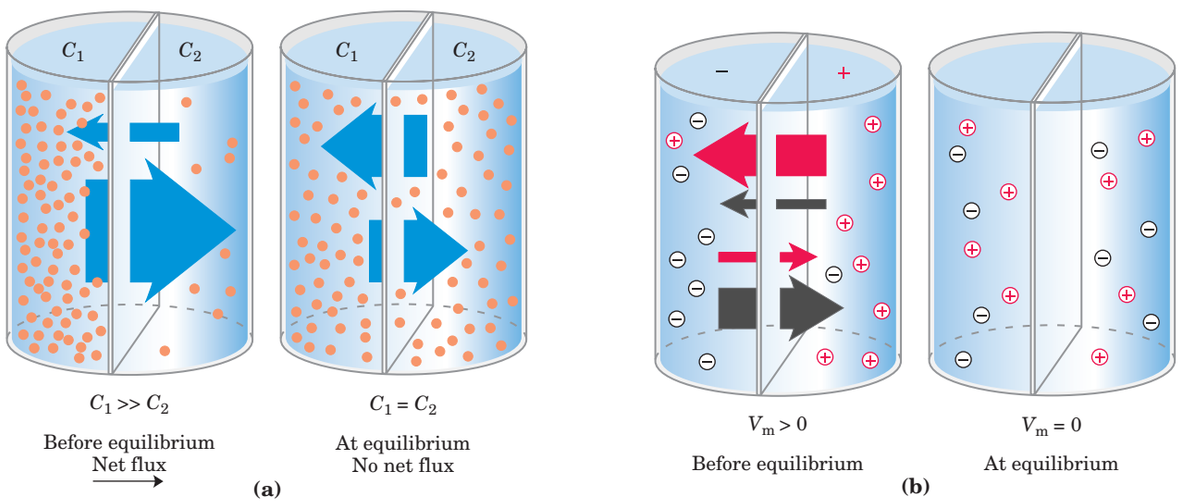

FIGURE 11–27 **Movement of solutes across a permeable membrane.** **(a)** Net movement of electrically neutral solutes is toward the side of lower solute concentration until equilibrium is achieved. The solute concentrations on the left and right sides of the membrane are designated C_1 and C_2. The rate of transmembrane movement (indicated by the large arrows) is proportional to the concentration gradient, C_1/C_2. **(b)** Net movement of electrically charged solutes is dictated by a combination of the electrical potential (V_m) and the chemical concentration difference across the membrane; net ion movement continues until this electrochemical potential reaches zero.

chemical gradient (the difference in solute concentration) and the electrical gradient (V_m) across the membrane. Together, these two factors are referred to as the **electrochemical gradient** or **electrochemical potential.** This behavior of solutes is in accord with the second law of thermodynamics: molecules tend to spontaneously assume the distribution of greatest randomness and lowest energy.

To pass through a lipid bilayer, a polar or charged solute must first give up its interactions with the water molecules in its hydration shell, then diffuse about 3 nm (30 Å) through a solvent (lipid) in which it is poorly soluble (Fig. 11–28). The energy used to strip away the hydration shell and to move the polar compound from water into and through lipid is regained as the compound leaves the membrane on the other side and is rehydrated. However, the intermediate stage of transmembrane passage is a high-energy state comparable to the transition state in an enzyme-catalyzed chemical reaction. In both cases, an activation barrier must be overcome to reach the intermediate stage (Fig. 11–28; compare with Fig. 6–3). The energy of activation ($\Delta G^{\ddagger}$) for

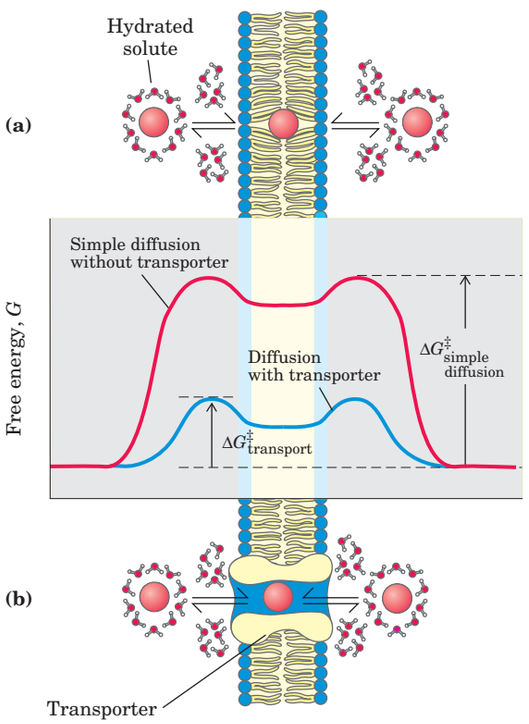

FIGURE 11–28 Energy changes accompanying passage of a hydrophilic solute through the lipid bilayer of a biological membrane. (a) In simple diffusion, removal of the hydration shell is highly endergonic, and the energy of activation ($\Delta G^{\ddagger}$) for diffusion through the bilayer is very high. **(b)** A transporter protein reduces the $\Delta G^{\ddagger}$ for transmembrane diffusion of the solute. It does this by forming noncovalent interactions with the dehydrated solute to replace the hydrogen bonding with water and by providing a hydrophilic transmembrane passageway.

translocation of a polar solute across the bilayer is so large that pure lipid bilayers are virtually impermeable to polar and charged species over periods of time relevant to cell growth and division.

Membrane proteins lower the activation energy for transport of polar compounds and ions by providing an alternative path through the bilayer for specific solutes. Proteins that bring about this **facilitated diffusion,** or **passive transport,** are not enzymes in the usual sense; their "substrates" are moved from one compartment to another, but are not chemically altered. Membrane proteins that speed the movement of a solute across a membrane by facilitating diffusion are called **transporters** or **permeases.**

Like enzymes, transporters bind their substrates with stereochemical specificity through multiple weak, noncovalent interactions. The negative free-energy change associated with these weak interactions, $\Delta G_{\text{binding}}$, counterbalances the positive free-energy change that accompanies loss of the water of hydration from the substrate, $\Delta G_{\text{dehydration}}$, thereby lowering $\Delta G^{\ddagger}$ for transmembrane passage (Fig. 11–28). Transporters span the lipid bilayer several times, forming a transmembrane channel lined with hydrophilic amino acid side chains. The channel provides an alternative path for a specific substrate to move across the lipid bilayer without its having to dissolve in the bilayer, further lowering $\Delta G^{\ddagger}$ for transmembrane diffusion. The result is an increase of several orders of magnitude in the rate of transmembrane passage of the substrate.

Transporters Can Be Grouped into Superfamilies Based on Their Structures

We know from genomic studies that transporters constitute a significant fraction of all proteins encoded in the genomes of both simple and complex organisms. There are probably a thousand or more different transporters in the human genome. A few hundred transporters from various species have been studied with biochemical, genetic, and electrophysiological tools, but investigators have determined the three-dimensional structures for only a handful of these. Examination of the many transporter genes reveals obvious sequence similarities among subsets of transporters. And as experience has shown, similar amino acid sequences in proteins generally reflect similar three-dimensional structures and, often, similar mechanisms of action. It is reasonable to hope that by determining the structure and mechanism of action of at least one member of each transporter family, we can learn much about the other members of the family—about their structures, substrate specificities, transport rates, and mechanisms of energy coupling. A phylogenetic tree in which proteins are grouped together based on sequence homologies has the potential to tell us much about the transport properties of individual proteins on that tree. When this

TABLE 11–3 The Transporter Classification (TC) System

1.A. α Helix type channels	
1.A.1.	Voltage-gated ion channel VIC superfamily
	Voltage-gated K^+ channel
1.A.3.	Ryanodine/IP_3 receptor Ca^{2+} channel
1.A.8.	Major intrinsic protein family
	Aquaporins
1.A.9.	Ligand-gated ion channel (LIC) of neurotransmitter receptors
	Acetylcholine receptor/channel
1.B. β Barrel porins	
1.B.1.	General bacterial porin (GBP) family
1.C. Pore-forming toxins	
1.C.7.	Diphtheria toxin family
1.C.18.	Mellitin family (bee venoms)
2.A. Porters: uniporters, symporters, and antiporters	
2.A.1.	Major facilitator superfamily (MFS)
	Lactose transporter/permease of *E. coli*
2.A.1.1.	Sugar porter family
	GLUT1 glucose transporter of erythrocyte
2.A.1.9.	P_i-H^+ symporter
2.A.12.	ATP-ADP antiporter (AAA) family
2.A.13.	C_4-dicarboxylate uptake (Dcu) family
2.A.21.	Solute-Na^+ symporter (SSS) family
	Na^+-glucose symporter in epithelial cells
2.A.73.	HCO_3^- transporters
	HCO_3^--Cl^- antiporter
2.B. Nonribosomally synthesized porters	
2.B.1.	Valinomycin carrier family
	Valinomycin
3.A. Diphosphate bond hydrolysis–driven transporters (use PP_i, not ATP)	
3.A.1.	ATP-binding cassette (ABC) superfamily
	CFTR Cl^- channel; multidrug transporter MDR1
3.A.2.	H^+- or Na^+-translocating F-type, V-type, A-type ATPase superfamily
	F_OF_1 ATPase proton pump; V_OV_1 ATPase; A_OA_1 ATPase
3.A.3.	P-type ATPase superfamily
	Na^+K^+ ATPase antiporter; SERCA Ca^{2+} pump

Note: The three broad groups correspond to groups 1, 2, and 3 in Figure 11-29. The individual transporters listed here (screened in yellow) are discussed in this chapter.

phylogeny is combined with knowledge of structure, specificity, or mechanism, we have a very useful and relatively simple representation of the huge group of transporters (Table 11–3).

Transporters can usefully be classified into superfamilies, whose members have considerable similarity of sequence and might therefore be expected to share structural and functional properties. There are two very broad categories of transporters: carriers and channels (Fig. 11–29). **Carriers** bind their substrates with high stereospecificity, catalyze transport at rates well below the limits of free diffusion, and are saturable in the same sense as are enzymes: there is some substrate concentration above which further increases will not produce a greater rate of activity. **Channels** generally allow transmembrane movement at rates several orders of magnitude greater than those typical of carriers, rates approaching the limit of unhindered diffusion. Channels typically show less stereospecificity than carriers and are usually not saturable. Most channels are oligomeric complexes of several, often identical, subunits, whereas many carriers function as monomeric proteins. The classification as carrier or channel is the broadest distinction among transporters. Within each of these categories

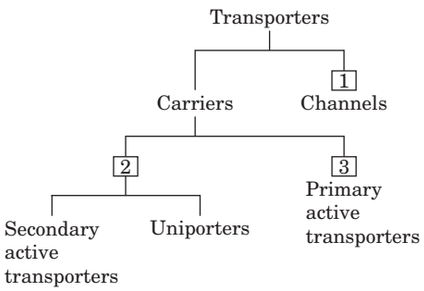

FIGURE 11–29 Classification of transporters. The numbers here correspond to the main subdivisions in Table 11–3.

are superfamilies of various types, defined not only by their primary sequences but by their secondary structures. Some channels are constructed primarily of helical transmembrane segments, others have β-barrel structures (Table 11–3). Among the carriers, some simply facilitate diffusion down a concentration gradient; they are the uniporter superfamily. Others (active transporters) can drive substrates across the membrane against a concentration gradient, some using energy provided directly by a chemical reaction (primary active transporters) and some coupling uphill transport of one substrate with the downhill transport of another (secondary active transporters). We now consider some well-studied representatives of the main transporter superfamilies. You will encounter some of these transporters again in later chapters in the context of the metabolic pathways in which they participate.

The Glucose Transporter of Erythrocytes Mediates Passive Transport

Energy-yielding metabolism in erythrocytes depends on a constant supply of glucose from the blood plasma, where the glucose concentration is maintained at about 5 mM. Glucose enters the erythrocyte by facilitated diffusion via a specific glucose transporter, at a rate about 50,000 times greater than the uncatalyzed diffusion rate. The glucose transporter of erythrocytes (called GLUT1 to distinguish it from related glucose transporters in other tissues) is a type III integral protein (M_r ~45,000) with 12 hydrophobic segments, each of which is believed to form a membrane-spanning helix. The detailed structure of GLUT1 is not yet known, but one plausible model suggests that the side-by-side assembly of several helices produces a transmembrane channel lined with hydrophilic residues that can hydrogen-bond with glucose as it moves through the channel (Fig. 11–30).

The process of glucose transport can be described by analogy with an enzymatic reaction in which the "substrate" is glucose outside the cell (S_{out}), the "product" is glucose inside (S_{in}), and the "enzyme" is the transporter, T. When the rate of glucose uptake is measured

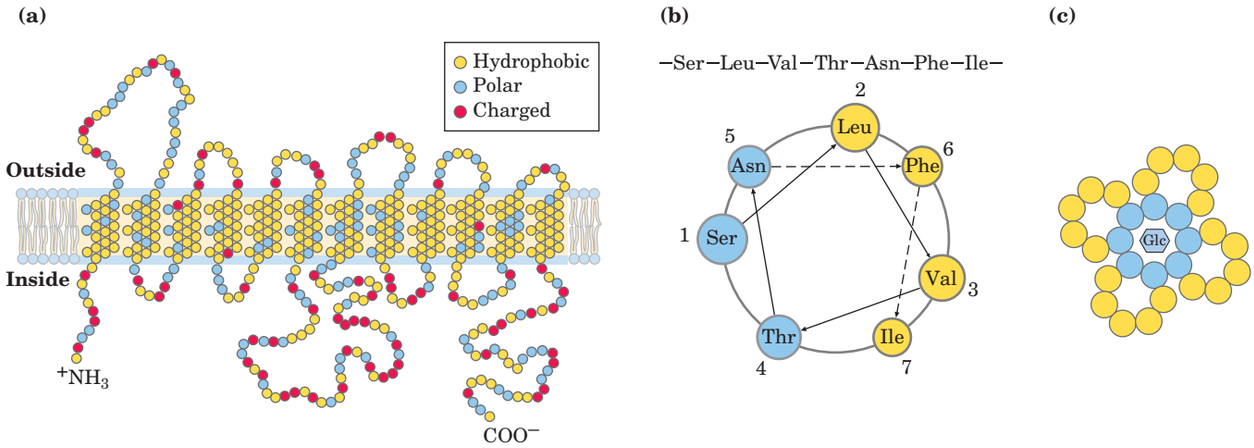

FIGURE 11–30 Proposed structure of GLUT1. (a) Transmembrane helices are represented as oblique (angled) rows of three or four amino acid residues, each row depicting one turn of the α helix. Nine of the 12 helices contain three or more polar or charged amino acid residues, often separated by several hydrophobic residues. **(b)** A helical wheel diagram shows the distribution of polar and nonpolar residues on the surface of a helical segment. The helix is diagrammed as though observed along its axis from the amino terminus. Adjacent residues in the linear sequence are connected with arrows, and each residue is placed around the wheel in the position it occupies in the helix; recall that 3.6 residues are required to make one complete turn of the α helix. In this example, the polar residues (blue) are on one side of the helix and the hydrophobic residues (yellow) on the other. This is, by definition, an amphipathic helix. **(c)** Side-by-side association of five or six amphipathic helices, each with its polar face oriented toward the central cavity, can produce a transmembrane channel lined with polar and charged residues. This channel provides many opportunities for hydrogen bonding with glucose as it moves through the transporter. The three-dimensional structure of GLUT1 has not yet been determined by x-ray crystallography, but researchers expect that the hydrophilic transmembrane channels of this and many other transporters and ion channels will resemble this model.

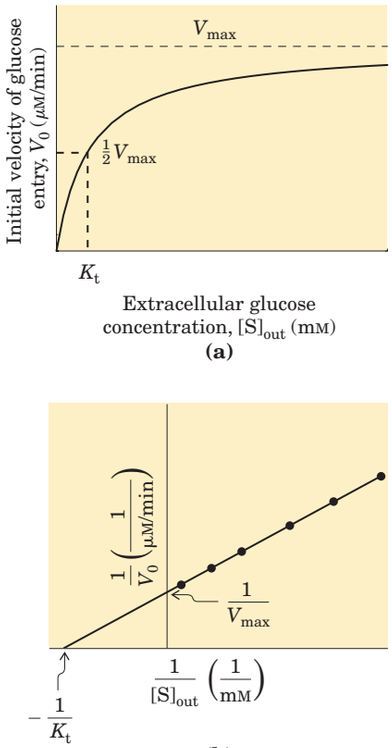

FIGURE 11–31 **Kinetics of glucose transport into erythrocytes. (a)** The initial rate of glucose entry into an erythrocyte, V_0, depends upon the initial concentration of glucose on the outside, $[S]_{out}$. **(b)** Double-reciprocal plot of the data in **(a).** The kinetics of facilitated diffusion is analogous to the kinetics of an enzyme-catalyzed reaction. Compare these plots with Figure 6–11, and Figure 1 in Box 6–1. Note that K_t is analogous to K_m, the Michaelis constant.

as a function of external glucose concentration (Fig. 11–31), the resulting plot is hyperbolic; at high external glucose concentrations the rate of uptake approaches V_{max}. Formally, such a transport process can be described by the equations

$$\begin{array}{ccc} S_{out} + T_1 & \underset{k_{-1}}{\overset{k_1}{\rightleftharpoons}} & S_{out} \bullet T_1 \\ k_{-4}\downarrow\uparrow k_4 & & k_{-2}\downarrow\uparrow k_2 \\ S_{in} + T_2 & \underset{k_{-3}}{\overset{k_3}{\rightleftharpoons}} & S_{in} \bullet T_2 \end{array}$$

in which k_1, k_{-1}, and so forth, are the forward and reverse rate constants for each step; T_2 is the transporter conformation that faces out, and T_2 the one that faces in. The steps are summarized in Figure 11–32.

The rate equations for this process can be derived exactly as for enzyme-catalyzed reactions (Chapter 6), yielding an expression analogous to the Michaelis-Menten equation:

$$V_0 = \frac{V_{max}[S]_{out}}{K_t + [S]_{out}}$$

in which V_0 is the initial velocity of accumulation of glucose inside the cell when its concentration in the surrounding medium is $[S]_{out}$, and K_t ($K_{transport}$) is a constant analogous to the Michaelis constant, a combination of rate constants that is characteristic of each transport system. This equation describes the *initial* velocity, the rate observed when $[S]_{in} = 0$. As is the case for enzyme-catalyzed reactions, the slope-intercept form of the equation describes a linear plot of $1/V_0$ against $1/[S]_{out}$, from which we can obtain values of K_t and V_{max} (Fig. 11–31b). When $[S] = K_t$, the rate of uptake is $\frac{1}{2}\ V_{max}$; the transport process is half-saturated. The concentration of blood glucose, 4.5 to 5 mM, is about

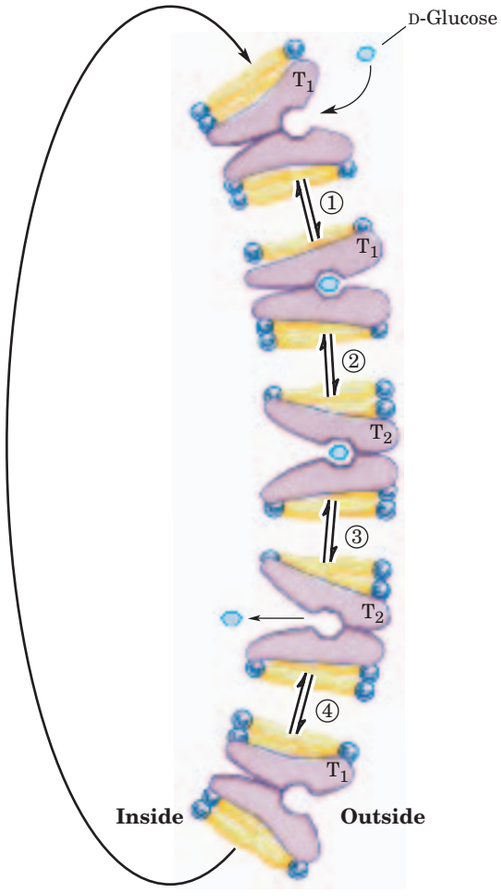

FIGURE 11–32 **Model of glucose transport into erythrocytes by GLUT1.** The transporter exists in two conformations: T_1, with the glucose-binding site exposed on the outer surface of the plasma membrane, and T_2, with the binding site exposed on the inner surface. Glucose transport occurs in four steps. ① Glucose in blood plasma binds to a stereospecific site on T_1; this lowers the activation energy for ② a conformational change from $S_{out} \cdot T_1$ to $S_{in} \cdot T_2$, effecting the transmembrane passage of the glucose. ③ Glucose is now released from T_2 into the cytoplasm, and ④ the transporter returns to the T_1 conformation, ready to transport another glucose molecule.

three times K_t, which ensures that GLUT1 is nearly saturated with substrate and operates near V_{max}.

Because no chemical bonds are made or broken in the conversion of S_{out} to S_{in}, neither "substrate" nor "product" is intrinsically more stable, and the process of entry is therefore fully reversible. As $[S]_{in}$ approaches $[S]_{out}$, the rates of entry and exit become equal. Such a system is therefore incapable of accumulating the substrate (glucose) within a cell at concentrations above that in the surrounding medium; it simply achieves equilibration of glucose on the two sides of the membrane much faster than would occur in the absence of a specific transporter. GLUT1 is specific for D-glucose, having a measured K_t of 1.5 mM. For the close analogs D-mannose and D-galactose, which differ only in the position of one hydroxyl group, the values of K_t are 20 and 30 mM, respectively; and for L-glucose, K_t exceeds 3,000 mM. Thus GLUT1 shows the three hallmarks of passive transport: high rates of diffusion down a concentration gradient, saturability, and specificity.

Twelve glucose transporters are encoded in the human genome, each with unique kinetic properties, patterns of tissue distribution, and function (Table 11–4). In liver, GLUT2 transports glucose out of hepatocytes when liver glycogen is broken down to replenish blood glucose. GLUT2 has a K_t of about 66 mM and can therefore respond to increased levels of intracellular glucose (produced by glycogen breakdown) by increasing outward transport. Skeletal muscle and adipose tissue have yet another glucose transporter, GLUT4 (K_t = 5 mM), which is distinguished by its stimulation by insulin: its activity increases when release of insulin signals a high blood glucose concentration, thus increasing the rate of glucose uptake into muscle and adipose tissue (Box 11–2 describes some malfunctions of this transporter).

The Chloride-Bicarbonate Exchanger Catalyzes Electroneutral Cotransport of Anions across the Plasma Membrane

The erythrocyte contains another facilitated diffusion system, an anion exchanger that is essential in CO_2 transport to the lungs from tissues such as skeletal muscle and liver. Waste CO_2 released from respiring tissues into the blood plasma enters the erythrocyte, where it is converted to bicarbonate (HCO_3^-) by the enzyme carbonic anhydrase. (Recall that HCO_3^- is the primary buffer of blood pH; see Box 2–4). The HCO_3^- reenters the blood plasma for transport to the lungs (Fig. 11–33). Because HCO_3^- is much more soluble in blood plasma than is CO_2, this roundabout route increases the capacity of the blood to carry carbon dioxide from the tissues to the lungs. In the lungs, HCO_3^- reenters the erythrocyte and is converted to CO_2, which is eventually released into the lung space and exhaled. To be effective, this shuttle requires very rapid movement of HCO_3^- across the erythrocyte membrane.

The **chloride-bicarbonate exchanger,** also called the **anion exchange (AE) protein,** increases the permeability of the erythrocyte membrane to HCO_3^- more than a millionfold. Like the glucose transporter, it is an integral protein that probably spans the membrane at least 12 times. This protein mediates the simultaneous movement of two anions: for each HCO_3^- ion that moves in one direction, one Cl^- ion moves in the opposite direction (Fig. 11–33), with no net transfer of charge; the exchange is **electroneutral.** The coupling of Cl^- and HCO_3^- movements is obligatory; in the absence of chloride, bicarbonate transport stops. In this respect, the anion exchanger is typical of all systems, called **cotransport systems,** that simultaneously carry

TABLE 11–4 Glucose Transporters in the Human Genome

Transporter	*Tissue(s) where expressed*	*Gene*	*Role*[*]
GLUT1	Ubiquitous	*SLC2A1*	Basal glucose uptake
GLUT2	Liver, pancreatic islets, intestine	*SLC2A2*	In liver, removal of excess glucose from blood; in pancreas, regulation of insulin release
GLUT3	Brain (neuronal)	*SLC2A3*	Basal glucose uptake
GLUT4	Muscle, fat, heart	*SLC2A4*	Activity increased by insulin
GLUT5	Intestine, testis, kidney, sperm	*SLC2A5*	Primarily fructose transport
GLUT6	Spleen, leukocytes, brain	*SLC2A6*	Possibly no transporter function
GLUT7	Liver microsomes	*SLC2A7*	—
GLUT8	Testis, blastocyst, brain	*SLC2A8*	—
GLUT9	Liver, kidney	*SLC2A9*	—
GLUT10	Liver, pancreas	*SLC2A10*	—
GLUT11	Heart, skeletal muscle	*SLC2A11*	—
GLUT12	Skeletal muscle, adipose, small intestine	*SLC2A12*	—

[*]Dash indicates role uncertain.

Defective Glucose and Water Transport in Two Forms of Diabetes

When ingestion of a carbohydrate-rich meal causes blood glucose to exceed the usual concentration between meals (about 5 mM), excess glucose is taken up by the myocytes of cardiac and skeletal muscle (which store it as glycogen) and by adipocytes (which convert it to triacylglycerols). Glucose uptake into myocytes and adipocytes is mediated by the glucose transporter GLUT4. Between meals, some GLUT4 is present in the plasma membrane, but most is sequestered in the membranes of small intracellular vesicles (Fig. 1). Insulin released from the pancreas in response to high blood glucose triggers the movement of these intracellular vesicles to the plasma membrane, where they fuse, thus exposing GLUT4 molecules on the outer surface of the cell (see Fig. 12–8). With more GLUT4 molecules in action, the rate of glucose uptake increases 15-fold or more. When blood glucose levels return to normal, insulin release slows and most GLUT4 molecules are removed from the plasma membrane and stored in vesicles.

In type I (juvenile onset) diabetes mellitus, the inability to release insulin (and thus to mobilize glucose transporters) results in low rates of glucose uptake into muscle and adipose tissue. One consequence is a prolonged period of high blood glucose after a carbohydrate-rich meal. This condition is the basis for the glucose tolerance test used to diagnose diabetes (Chapter 23).

The water permeability of epithelial cells lining the renal collecting duct in the kidney is due to the presence of an aquaporin (AQP-2) in their apical plasma membranes (facing the lumen of the duct). Antidiuretic hormone (ADH) regulates the retention of water by mobilizing AQP-2 molecules stored in vesicle membranes within the epithelial cells, much as insulin mobilizes GLUT4 in muscle and adipose tissue. When the vesicles fuse with the epithelial cell plasma membrane, water permeability greatly increases and more water is reabsorbed from the collecting duct and returned to the blood. When the ADH level drops, AQP-2 is resequestered within vesicles, reducing water retention. In the relatively rare human disease diabetes insipidus, a genetic defect in AQP-2 leads to impaired water reabsorption by the kidney. The result is excretion of copious volumes of very dilute urine.

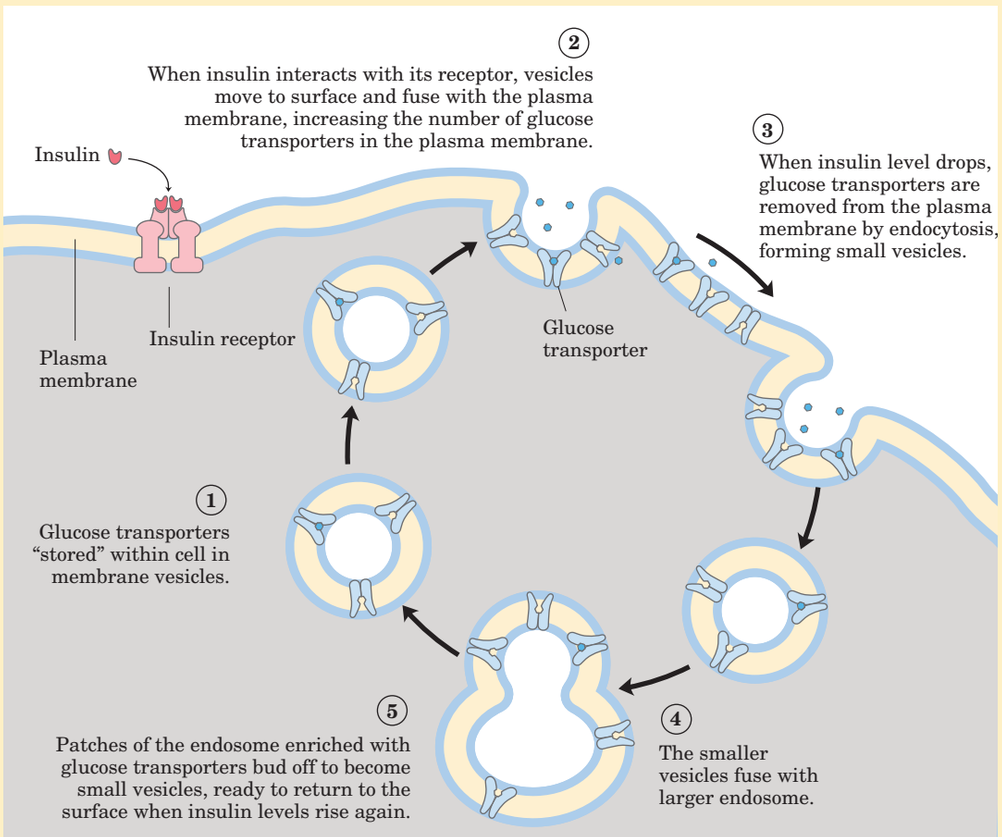

FIGURE 1 Regulation by insulin of glucose transport by GLUT4 into a myocyte.

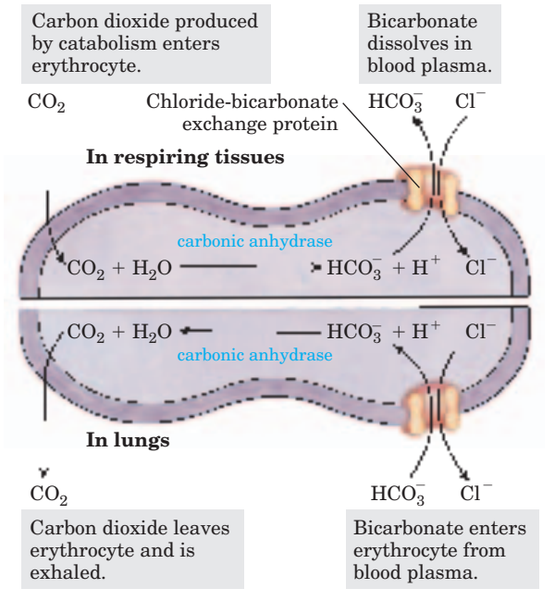

FIGURE 11–33 Chloride-bicarbonate exchanger of the erythrocyte membrane. This cotransport system allows the entry and exit of HCO_3^- without changes in the transmembrane electrical potential. Its role is to increase the CO_2-carrying capacity of the blood.

two solutes across a membrane. When, as in this case, the two substrates move in opposite directions, the process is **antiport.** In **symport,** two substrates are moved simultaneously in the same direction. As we noted earlier, transporters that carry only one substrate, such as the erythrocyte glucose transporter, are **uniport** systems (Fig. 11–34).

The human genome has genes for three closely related chloride-bicarbonate exchangers, all with the same predicted transmembrane topology. Erythrocytes contain the AE1 transporter, AE2 is prominent in liver, and AE3 is present in plasma membranes of the brain, heart, and retina. Similar anion exchangers are also found in plants and microorganisms.

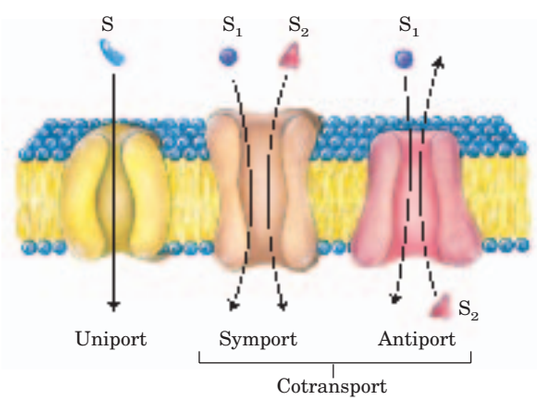

FIGURE 11–34 Three general classes of transport systems. Transporters differ in the number of solutes (substrates) transported and the direction in which each is transported. Examples of all three types of transporters are discussed in the text. Note that this classification tells us nothing about whether these are energy-requiring (active transport) or energy-independent (passive transport) processes.

Active Transport Results in Solute Movement against a Concentration or Electrochemical Gradient

In passive transport, the transported species always moves down its electrochemical gradient and is not accumulated above the equilibrium concentration. Active transport, by contrast, results in the accumulation of a solute above the equilibrium point. Active transport is thermodynamically unfavorable (endergonic) and takes place only when coupled (directly or indirectly) to an exergonic process such as the absorption of sunlight, an oxidation reaction, the breakdown of ATP, or the concomitant flow of some other chemical species down its electrochemical gradient. In **primary active transport,** solute accumulation is coupled directly to an exergonic chemical reaction, such as conversion of ATP to ADP + P_i (Fig. 11–35). **Secondary active transport** occurs when endergonic (uphill) transport of one solute is coupled to the exergonic (downhill) flow of a different solute that was originally pumped uphill by primary active transport.

The amount of energy needed for the transport of a solute against a gradient can be calculated from the initial concentration gradient. The general equation for the free-energy change in the chemical process that converts S to P is

$$\Delta G = \Delta G'^{\circ} + RT \ln [P]/[S] \qquad (11–1)$$

where R is the gas constant, 8.315 J/mol · K, and T is the absolute temperature. When the "reaction" is simply

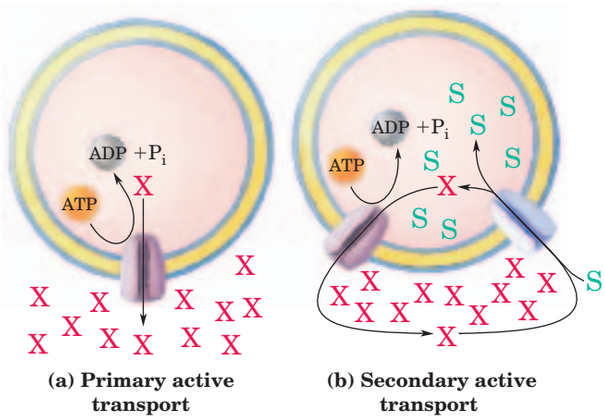

FIGURE 11–35 Two types of active transport. (a) In primary active transport, the energy released by ATP hydrolysis drives solute movement against an electrochemical gradient. **(b)** In secondary active transport, a gradient of ion X (often Na^+) has been established by primary active transport. Movement of X down its electrochemical gradient now provides the energy to drive cotransport of a second solute (S) against its electrochemical gradient.

transport of a solute from a region where its concentration is C_1 to a region where its concentration is C_2, no bonds are made or broken and the standard free-energy change, $\Delta G'^{\circ}$, is zero. The free-energy change for transport, ΔG_t, is then

$$\Delta G_t = RT \ln \frac{C_2}{C_1} \qquad (11\text{–}2)$$

If there is a tenfold difference in concentration between two compartments, the cost of moving 1 mol of an uncharged solute at 25 °C across a membrane separating the compartments is therefore

$$\Delta G_t = (8.315 \text{ J/mol} \cdot \text{K})(298 \text{ K})(\ln 10/1) = 5{,}700 \text{ J/mol} = 5.7 \text{ kJ/mol}$$

Equation 11–2 holds for all uncharged solutes.

When the solute is an ion, its movement without an accompanying counterion results in the endergonic separation of positive and negative charges, producing an electrical potential; such a transport process is said to be **electrogenic.** The energetic cost of moving an ion depends on the electrochemical potential (p. 391), the sum of the chemical and electrical gradients:

$$\Delta G_t = RT \ln \left(\frac{C_2}{C_1}\right) + Z\mathcal{F}\Delta\psi \qquad (11\text{–}3)$$

where Z is the charge on the ion, $\mathcal{F}$ is the Faraday constant (96,480 J/V · mol), and $\Delta\psi$ is the transmembrane electrical potential (in volts). Eukaryotic cells typically have electrical potentials across their plasma membranes of about 0.05 to 0.1 V (with the inside negative relative to the outside), so the second term of Equation 11–3 can make a significant contribution to the total free-energy change for transporting an ion. Most cells maintain more than tenfold differences in ion concentrations across their plasma or intracellular membranes, and for many cells and tissues active transport is therefore a major energy-consuming process.

The mechanism of active transport is of fundamental importance in biology. As we shall see in Chapter 19, the formation of ATP in mitochondria and chloroplasts occurs by a mechanism that is essentially ATP-driven ion transport operating in reverse. The energy made available by the spontaneous flow of protons across a membrane is calculable from Equation 11–3; remember that ΔG for flow *down* an electrochemical gradient has a negative value, and ΔG for transport of ions *against* an electrochemical gradient has a positive value.

P-Type ATPases Undergo Phosphorylation during Their Catalytic Cycles

The family of active transporters called **P-type ATPases** are ATP-driven cation transporters that are reversibly phosphorylated by ATP as part of the transport cycle; phosphorylation forces a conformational change that is central to moving the cation across the membrane. All P-type transport ATPases have similarities in amino acid sequence, especially near the Asp residue that undergoes phosphorylation, and all are sensitive to inhibition by the phosphate analog **vanadate.**

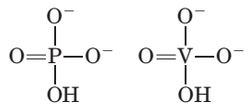

Phosphate Vanadate

Each P-type ATPase transporter is an integral protein with ten predicted membrane-spanning regions in a single polypeptide; some also have a second subunit. The P-type transporters are very widely distributed. In animal tissues, the Na^+K^+ ATPase (an antiporter for Na^+ and K^+) and the Ca^{2+} ATPase (a uniporter for Ca^{2+}) are ubiquitous P-type ATPases that maintain differences in the ionic composition of the cytosol and the extracellular medium. Parietal cells in the lining of the mammalian stomach have a P-type ATPase that pumps H^+ and K^+ across the plasma membrane, thereby acidifying the stomach contents. In vascular plants, a P-type ATPase pumps protons out of the cell, establishing an electrochemical difference of as much as 2 pH units and 250 mV across the plasma membrane. A similar P-type ATPase in the bread mold *Neurospora* pumps protons out of cells to establish an inside-negative membrane potential, which is used to drive the uptake of substrates and ions from the surrounding medium by secondary active transport. Bacteria use P-type ATPases to pump out toxic heavy metal ions such as Cd^{2+} and Cu^{2+}.

In virtually every animal cell type, the concentration of Na^+ is lower in the cell than in the surrounding medium, and the concentration of K^+ is higher (Fig. 11–36). This imbalance is maintained by a primary active transport system in the plasma membrane. The enzyme **Na^+K^+ ATPase,** discovered by Jens Skou in 1957, couples breakdown of ATP to the simultaneous movement of both Na^+ and K^+ against their electrochemical gradients. For each molecule of ATP converted to ADP and P_i, the transporter moves two K^+ ions inward and three Na^+ ions outward across the plasma membrane. The Na^+K^+ ATPase is an integral protein with two subunits (M_r ~50,000 and ~110,000), both of which span the membrane.

Jens Skou

The detailed mechanism by which ATP hydrolysis is coupled to transport awaits determination of the protein's three-dimensional structure, but a current model (Fig. 11–37) proposes that the ATPase cycles between two forms, a phosphorylated form (designated $P\text{-}Enz_{II}$) with high affinity for K^+ and low affinity for Na^+, and a dephosphorylated form (Enz_I) with high affinity for Na^+

and low affinity for K^+. The conversion of ATP to ADP and P_i takes place in two steps catalyzed by the enzyme, involving formation then hydrolysis of the phosphoenzyme:

$$(1) \quad ATP + Enz_I \longrightarrow ADP + P\text{-}Enz_{II}$$
$$(2) \quad P\text{-}Enz_{II} + H_2O \longrightarrow Enz_I + P_i$$
$$Sum: \quad ATP + H_2O \longrightarrow ADP + P_i$$

Because three Na^+ ions move outward for every two K^+ ions that move inward, the process is electrogenic—it creates a net separation of charge across the membrane. The result is a transmembrane potential of −50 to −70 mV (inside negative relative to outside), which is characteristic of most animal cells and essential to the conduction of action potentials in neurons. The central role of the Na^+K^+ ATPase is reflected in the energy invested in this single reaction: about 25% of the total energy consumption of a human at rest!

The steroid derivative **ouabain** (pronounced wah'-bane; from *waa bayyo,* Somali for "arrow poison") is a potent and specific inhibitor of the Na^+K^+ ATPase. Oubain binds preferentially to the form of the enzyme that is open to the extracellular side, locking in two Na^+ ions and preventing the changes of conformation necessary to ion transport. Another very potent toxin, palytoxin (produced by a coral on the Hawaiian shoreline), also targets the Na^+K^+ ATPase, but it binds to the protein so as to lock it into a position in which the ion-binding sites are permanently accessible from both sides, converting the transporter into a nonspecific ion channel. This allows exit of K^+ from cells and deflates the (essential) ion gradient across the plasma membrane, which accounts for the high toxicity of this compound.

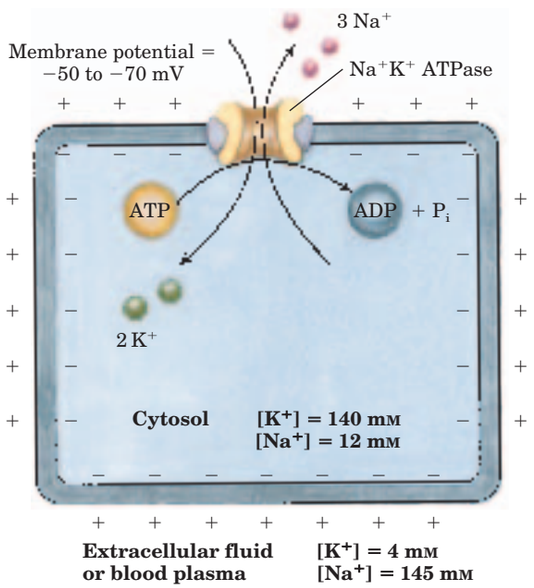

FIGURE 11–36 **Na^+K^+ ATPase.** In animal cells, this active transport system is primarily responsible for setting and maintaining the intracellular concentrations of Na^+ and K^+ and for generating the transmembrane electrical potential. It does this by moving three Na^+ out of the cell for every two K^+ it moves in. The electrical potential is central to electrical signaling in neurons, and the gradient of Na^+ is used to drive the uphill cotransport of solutes in many cell types.

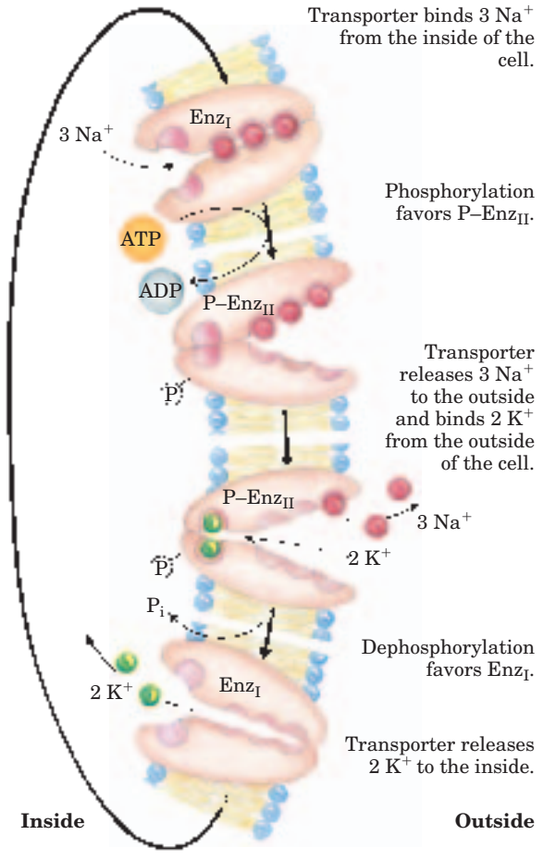

FIGURE 11–37 **Postulated mechanism of Na^+ and K^+ transport by the Na^+K^+ ATPase.**

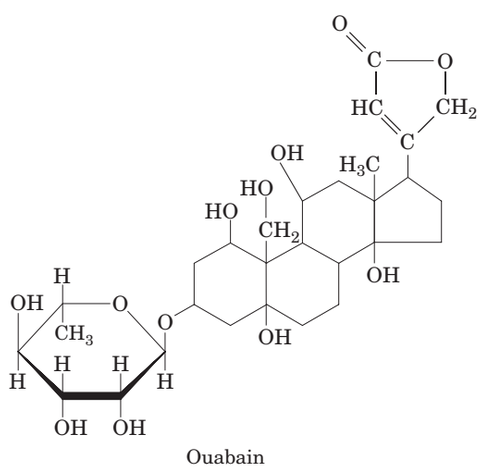

Ouabain

Ouabain and another steroid derivative, **digitoxigenin,** are the active ingredients of digitalis, an extract of the leaves of the foxglove plant. (Ouabain is found in lower concentrations in a number of other plants, presumably serving to discourage herbivores.) Digitalis has been used to treat congestive heart failure since its introduction for that purpose (treatment of "dropsy") by the British physician William Withering in 1785. It strengthens heart muscle contractions without increasing the heart rate and thus increases the efficiency of the heart. Digitalis inhibits the efflux of Na^+, raising the intracellular [Na^+] enough to activate a Na^+-Ca^{2+} antiporter in cardiac muscle. The increased influx of Ca^{2+} through this antiporter produces elevated cytosolic [Ca^{2+}], which strengthens the contractions of the heart. The potency of ouabain in animals led to the suggestion (50 years ago) that this plant product might act by mimicking a normal regulator of the Na^+K^+ ATPase produced in animals, and it now appears that this may be so. Ouabain itself has been isolated from bovine adrenal glands and has been detected in the blood plasma and hypothalamus of mammals. ■

P-Type Ca^{2+} Pumps Maintain a Low Concentration of Calcium in the Cytosol

The cytosolic concentration of free Ca^{2+} is generally at or below 100 nM, far lower than that in the surrounding medium, whether pond water or blood plasma. The ubiquitous occurrence of inorganic phosphates (P_i and PP_i) at millimolar concentrations in the cytosol necessitates a low cytosolic Ca^{2+} concentration, because inorganic phosphate combines with calcium to form relatively insoluble calcium phosphates. Calcium ions are pumped out of the cytosol by a P-type ATPase, the **plasma membrane Ca^{2+} pump.** Another P-type Ca^{2+} pump in the endoplasmic reticulum moves Ca^{2+} into the ER lumen, a compartment separate from the cytosol. In myocytes, Ca^{2+} is normally sequestered in a specialized form of endoplasmic reticulum called the sarcoplasmic reticulum. **The sarcoplasmic and endoplasmic reticulum calcium (SERCA) pumps** are closely related in structure and mechanism, and both are inhibited by the tumor-promoting agent thapsigargin, which does not affect the plasma membrane Ca^{2+} pump.

The plasma membrane Ca^{2+} pump and SERCA pumps are integral proteins that cycle between phosphorylated and dephosphorylated conformations in a mechanism similar to that for Na^+K^+ ATPase (Fig. 11–37). Phosphorylation favors a conformation with a high-affinity Ca^{2+}-binding site exposed on the cytoplasmic side, and dephosphorylation favors one with a low-affinity Ca^{2+}-binding site on the lumenal side. By this mechanism, the energy released by hydrolysis of ATP during one phosphorylation-dephosphorylation cycle drives Ca^{2+} across the membrane against a large electrochemical gradient.

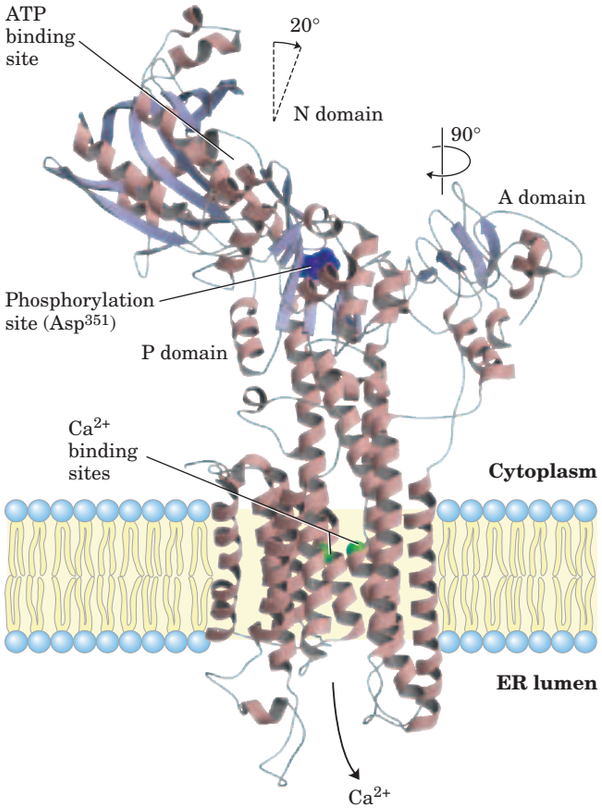

FIGURE 11–38 Structure of the Ca^{2+} pump of sarcoplasmic reticulum. (PDB ID 1EUL) Ten transmembrane helices surround the path for Ca^{2+} movement through the membrane. Two of the helices are interrupted near the middle of the bilayer, and their nonhelical regions form the binding sites for two Ca^{2+} ions (green). The carboxylate groups of an Asp residue in one helix and a Glu residue in another are central to the Ca^{2+}-binding sites. Three globular domains extend from the cytoplasmic side: the N (nucleotide-binding) domain has the binding site for ATP; the P (phosphorylation) domain contains the Asp^{351} residue (blue) that undergoes reversible phosphorylation, and the A (actuator) domain somehow mediates the structural changes that alter the Ca^{2+} affinity of the Ca^{2+}-binding site and its exposure to cytoplasm or lumen. Note the long distance between the phosphorylation site and the Ca^{2+}-binding site. There is strong evidence that during one transport cycle, the N domain tips about 20° to the right, bringing the ATP site close to Asp^{351}, and that during each catalytic cycle the A domain twists by about 90° around the normal (perpendicular) to the membrane. These conformational changes must expose the Ca^{2+}-binding site first on one side of the membrane, then on the other, changing the Ca^{2+} affinity of the site from high on the cytoplasmic side to lower on the lumenal side. A complete understanding of the coupling between phosphorylation and Ca^{2+} transport awaits determination of all the conformations involved in the cycle.

The Ca^{2+} pump of the sarcoplasmic reticulum, which comprises 80% of the protein in that membrane, consists of a single polypeptide (M_r ~100,000) that spans the membrane ten times and has three cytoplasmic domains formed by loops that connect the transmembrane helices (Fig. 11–38). The two Ca^{2+}-binding sites are located near the middle of the membrane bi-

layer, 40 to 50 Å from the phosphorylated Asp residue characteristic of all P-type ATPases, so the effects of Asp phosphorylation are not direct. They must be mediated by conformational changes that alter the affinity for Ca^{2+} and open a path for Ca^{2+} release on the lumenal side of the membrane.

The amino acid sequences of the SERCA pumps and the Na^+K^+ ATPase share 30% identity and 65% sequence similarity, and their topology relative to the membrane is also the same. Thus it seems likely that the Na^+K^+ ATPase structure is similar to that of the SERCA pumps and that all P-type ATPase transporters share the same basic structure.

F-Type ATPases Are Reversible, ATP-Driven Proton Pumps

The **F-type ATPase** active transporters play a central role in energy-conserving reactions in mitochondria, bacteria, and chloroplasts; we discuss that role in detail in our description of oxidative phosphorylation and photophosphorylation in Chapter 19. The F-type ATPases catalyze the uphill transmembrane passage of protons driven by ATP hydrolysis ("F-type" originated in the identification of these ATPases as energy-coupling *f*actors). The F_o integral membrane protein complex (Fig. 11–39; subscript *o* denoting its inhibition by the drug oligomycin) provides a transmembrane pore for protons, and the peripheral protein F_1 (subscript *1* indicating that it was the first of several factors isolated from mitochondria) is a molecular machine that uses the energy

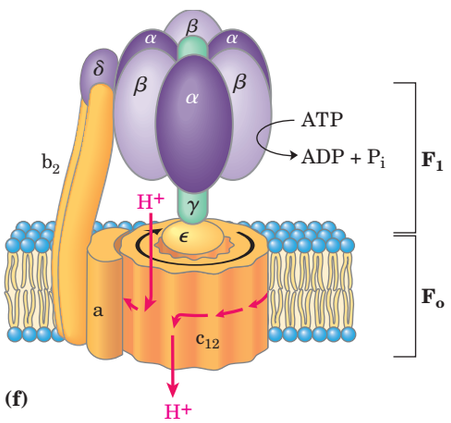

FIGURE 11–39 Structure of the F_oF_1 ATPase/ATP synthase. F-type ATPases have a peripheral domain, F_1, consisting of three α subunits, three β subunits, one δ subunit (purple), and a central shaft (the γ subunit, green). The integral portion of F-type ATPases, F_o (yellow), has multiple copies of c, one a, and two b subunits. F_o provides a transmembrane channel through which about four protons are pumped (red arrows) for each ATP hydrolyzed on the β subunits of F_1. The remarkable mechanism by which these two events are coupled is described in detail in Chapter 19. It involves rotation of F_o relative to F_1 (black arrow). The structures of V_oV_1 and A_oA_1 are essentially similar to that of F_oF_1, and the mechanisms are probably similar, too.

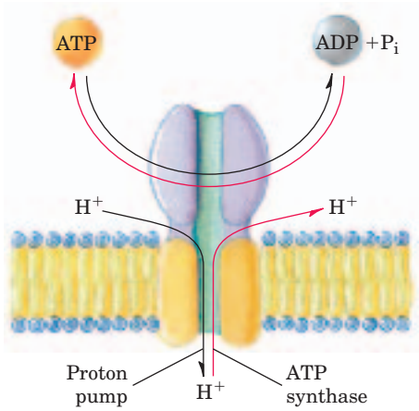

FIGURE 11–40 Reversibility of F-type ATPases. An ATP-driven proton transporter also can catalyze ATP synthesis (red arrows) as protons flow *down* their electrochemical gradient. This is the central reaction in the processes of oxidative phosphorylation and photophosphorylation, both described in detail in Chapter 19.

of ATP to drive protons uphill (into a region of higher H^+ concentration). The F_oF_1 organization of proton-pumping transporters must have developed very early in evolution. Eubacteria such as *E. coli* use an F_oF_1 ATPase complex in their plasma membrane to pump protons outward, and archaebacteria have a closely homologous proton pump, the A_oA_1 ATPase.

The reaction catalyzed by F-type ATPases is reversible, so a proton gradient can supply the energy to drive the reverse reaction, ATP synthesis (Fig. 11–40). When functioning in this direction, the F-type ATPases are more appropriately named **ATP synthases.** ATP synthases are central to ATP production in mitochondria during oxidative phosphorylation and in chloroplasts during photophosphorylation, as well as in eubacteria and archaebacteria. The proton gradient needed to drive ATP synthesis is produced by other types of proton pumps powered by substrate oxidation or sunlight. As noted above, we return to a detailed description of these processes in Chapter 19.

V-type ATPases, a class of proton-transporting ATPases structurally (and possibly mechanistically) related to the F-type ATPases, are responsible for acidifying intracellular compartments in many organisms (thus *V* for *v*acuolar). Proton pumps of this type maintain the vacuoles of fungi and higher plants at a pH between 3 and 6, well below that of the surrounding cytosol (pH 7.5). V-type ATPases are also responsible for the acidification of lysosomes, endosomes, the Golgi complex, and secretory vesicles in animal cells. All V-type ATPases have a similar complex structure, with an integral (transmembrane) domain (V_o) that serves as a proton channel and a peripheral domain (V_1) that contains the ATP-binding site and the ATPase activity. The mechanism by which V-type ATPases couple ATP hydrolysis to the uphill transport of protons is not understood in detail.

ABC Transporters Use ATP to Drive the Active Transport of a Wide Variety of Substrates

ABC transporters (Fig. 11–41) constitute a large family of ATP-dependent transporters that pump amino acids, peptides, proteins, metal ions, various lipids, bile salts, and many hydrophobic compounds, including drugs, out of cells against a concentration gradient. One ABC transporter in humans, the **multidrug transporter (MDR1),** is responsible for the striking resistance of certain tumors to some generally effective antitumor drugs. MDR1 has a broad substrate specificity for hydrophobic compounds, including, for example, the chemotherapeutic drugs adriamycin, doxorubicin, and vinblastine. By pumping these drugs out of the cell, the transporter prevents their accumulation within a tumor and thus blocks their therapeutic effects. MDR1 is an integral membrane protein (M_r 170,000) with 12 transmembrane segments and two ATP-binding domains ("cassettes"), which give the family its name: *A*TP-*b*inding *c*assette transporters.

All ABC transporters have two nucleotide-binding domains (NBDs) and two transmembrane domains (Fig. 11–41). In some cases, all these domains are in a single long polypeptide; other ABC transporters have two subunits, each contributing an NBD and a domain with six (or in some cases ten) transmembrane helices. Although many of the ABC transporters are in the plasma membrane, some types are also found in the endoplasmic reticulum and in the membranes of mitochondria and lysosomes. Most ABC transporters act as pumps, but at least some members of the superfamily act as ion channels that are opened and closed by ATP hydrolysis. The CFTR transporter (Box 11–3) is a Cl^- channel operated by ATP hydrolysis.

The NBDs of all ABC proteins are similar in sequence and presumably in three-dimensional structure; they are the conserved molecular motor that can be coupled to a wide variety of pumps and channels. When coupled with a pump, the ATP-driven motor moves solutes against a concentration gradient; when coupled with an ion channel, the motor opens and closes the channel using ATP as energy source. The stoichiometry of ABC pumps is about one ATP hydrolyzed per molecule of substrate transported, but neither the mechanism of coupling nor the site of substrate binding are known.

Some ABC transporters have very high specificity for a single substrate; others are more promiscuous. The human genome contains at least 48 genes that encode ABC transporters, many of which are involved in maintaining the lipid bilayer and in transporting sterols, sterol derivatives, and fatty acids throughout the body. The flippases that move membrane lipids from one leaflet of the bilayer to the other are ABC transporters, and the cellular machinery for exporting excess cholesterol includes an ABC transporter. Mutations in the genes that encode some of these proteins contribute to several genetic diseases, including cystic fibrosis (Box 11–3), Tangier disease (p. 827), retinal degeneration, anemia, and liver failure.

ABC transporters are also present in simpler animals and in plants and microorganisms. Yeast has 31 genes that encode ABC transporters, *Drosophila* has 56, and *E. coli* has 80, representing 2% of its entire genome. The presence of ABC transporters that confer antibiotic resistance in pathogenic microbes (*Pseudomonas aeruginosa, Staphylococcus aureus, Candida albicans, Neisseria gonorrhoeae,* and *Plasmodium falciparum*) is a serious public health concern and makes these transporters attractive targets for drug design. ■

Ion Gradients Provide the Energy for Secondary Active Transport

The ion gradients formed by primary transport of Na^+ or H^+ can in turn provide the driving force for cotransport of other solutes. Many cell types contain transport

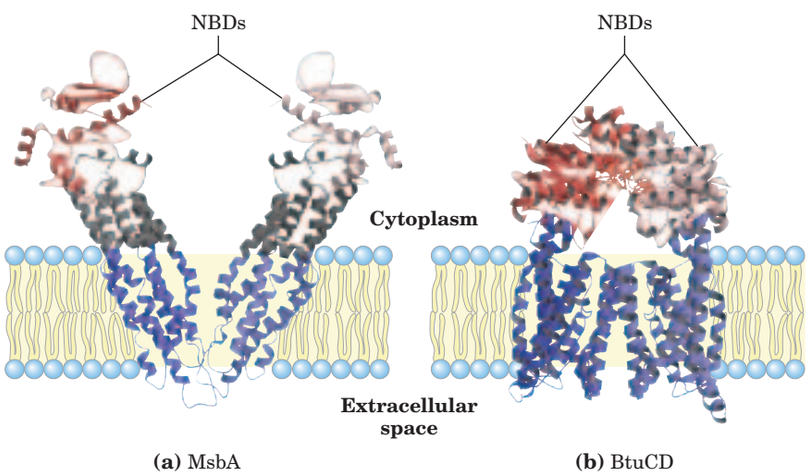

FIGURE 11–41 Structures of two ABC transporters of *E. coli*. **(a)** The lipid A flippase MsbA (PDB ID 1JSQ) and **(b)** the vitamin B_{12} importer BtuCD (PDB ID 1L7V). Both structures are homodimers. The two nucleotide-binding domains (NBDs, in red) extend into the cytoplasm. In **(b)**, residues involved in ATP binding and hydrolysis are shown as ball-and-stick structures. Each monomer of MsbA has six transmembrane helical segments (blue), and each monomer of BtuCD has ten.

BOX 11–3 BIOCHEMISTRY IN MEDICINE

A Defective Ion Channel in Cystic Fibrosis

Cystic fibrosis (CF) is a serious and relatively common hereditary disease of humans. About 5% of white Americans are carriers, having one defective and one normal copy of the gene. Only individuals with two defective copies show the severe symptoms of the disease: obstruction of the gastrointestinal and respiratory tracts, commonly leading to bacterial infection of the airways and death due to respiratory insufficiency before the age of 30. In CF, the thin layer of mucus that normally coats the internal surfaces of the lungs is abnormally thick, obstructing air flow and providing a haven for pathogenic bacteria, particularly *Staphylococcus aureus* and *Pseudomonas aeruginosa*.

The defective gene in CF patients was discovered in 1989. It encodes a membrane protein called *c*ystic *f*ibrosis *t*ransmembrane conductance *r*egulator, or CFTR. Hydropathy analysis predicted that CFTR has 12 transmembrane helices and is structurally related to the multidrug (MDR1) transporters of drug-resistant tumors (Fig. 1). The normal CFTR protein proved to be an ion channel specific for Cl^- ions. The Cl^- channel activity increases greatly when phosphoryl groups are transferred from ATP to several side chains of the protein, catalyzed by cAMP-dependent protein kinase (Chapter 12). The mutation responsible for CF in 70% of cases results in deletion of a Phe residue at position 508, with the effect that the mutant protein is not correctly folded and inserted in the plasma membrane. Other mutations yield a protein that is inserted properly but cannot be activated by phosphorylation. In each case, the fundamental problem is a nonfunctional Cl^- channel in the epithelial cells that line the airways (Fig. 2), the digestive tract, and exocrine glands (pancreas, sweat glands, bile ducts, and vas deferens).

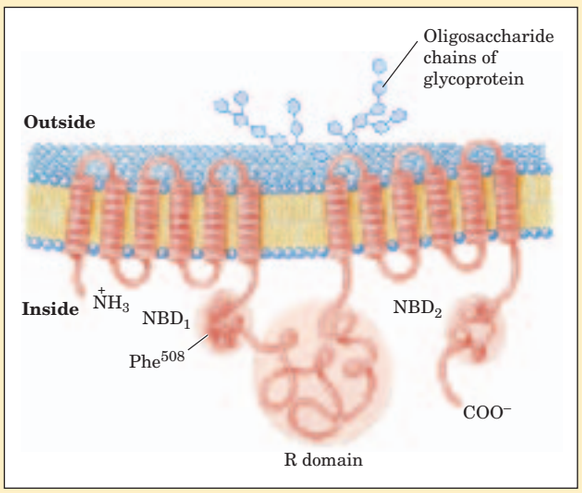

FIGURE 1 Topology of the cystic fibrosis transmembrane conductance regulator, CFTR. It has 12 transmembrane helices, and three functionally significant domains extend from the cytoplasmic surface: NBD_1 and NBD_2 are nucleotide-binding domains to which ATP binds, and a regulatory domain (R domain) is the site of phosphorylation by cAMP-dependent protein kinase. Oligosaccharide chains are attached to several residues on the outer surface of the segment between helices 7 and 8. The most commonly occurring mutation leading to CF is the deletion of Phe^{508}, in the NBD_1 domain. The structure of CFTR is very similar to that of the multidrug transporter of tumors, described in the text.

Normally, epithelial cells that line the inner surface of the lungs secrete a substance that traps and kills bacteria, and the cilia on the epithelial cells constantly sweep away the resulting debris. When CFTR is defective or missing, this process is less efficient, and frequent infections by bacteria such as *S. aureus* and *P. aeruginosa* progressively damage the lungs and reduce respiratory efficiency.

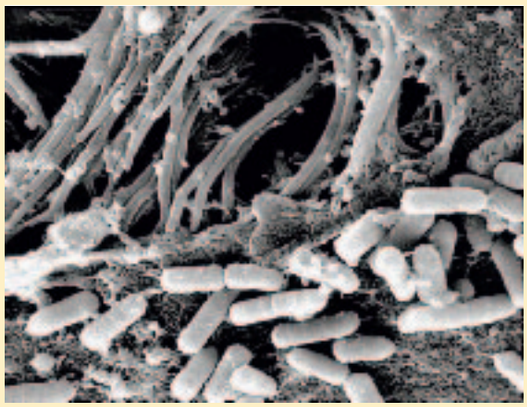

FIGURE 2 Mucus lining the surface of the lungs traps bacteria. In healthy lungs, these bacteria are killed and swept away by the action of cilia. In CF, the bactericidal activity is impaired, resulting in recurring infections and progressive damage to the lungs.

systems that couple the spontaneous, downhill flow of these ions to the simultaneous uphill pumping of another ion, sugar, or amino acid (Table 11–5). The **lactose transporter (lactose permease)** of *E. coli* is the well-studied prototype for proton-driven cotransporters. This protein consists of a single polypeptide chain (417 residues) that functions as a monomer to transport one proton and one lactose molecule into the

TABLE 11–5 Cotransport Systems Driven by Gradients of Na^+ or H^+

Organism/tissue/cell type	*Transported solute (moving against its gradient)*	*Cotransported solute (moving down its gradient)*	*Type of transport*
E. coli	Lactose	H^+	Symport
	Proline	H^+	Symport
	Dicarboxylic acids	H^+	Symport
Intestine, kidney (vertebrates)	Glucose	Na^+	Symport
	Amino acids	Na^+	Symport
Vertebrate cells (many types)	Ca^{2+}	Na^+	Antiport
Higher plants	K^+	H^+	Antiport
Fungi (*Neurospora*)	K^+	H^+	Antiport

cell, with the net accumulation of lactose (Fig. 11–42). *E. coli* normally produces a gradient of protons and charge across its plasma membrane by oxidizing fuels and using the energy of oxidation to pump protons outward. (This mechanism is discussed in detail in Chapter 19.) The lipid bilayer is impermeable to protons, but the lactose transporter provides a route for proton reentry, and lactose is simultaneously carried into the cell by symport. The endergonic accumulation of lactose is thereby coupled to the exergonic flow of protons into the cell, with a negative overall free-energy change.

The lactose transporter is one member of the **major facilitator superfamily (MFS)** of transporters, which comprises 28 families. Almost all proteins in this superfamily have 12 transmembrane domains (the few exceptions have 14). The proteins share relatively little sequence homology, but the similarity of their secondary structures and topology suggests a common tertiary structure. The crystallographic solution of the *E. coli* lactose transporter by Ron Kaback and So Iwata in 2003 may provide a glimpse of this general structure (Fig. 11–43a). The protein has 12 transmembrane helices, and connecting loops that protrude into the cytoplasm or the periplasmic space. All six amino-terminal and six carboxyl-terminal helices form very similar domains, to produce a structure with a rough twofold symmetry. In the crystallized form of the protein, a large aqueous cavity is exposed on the cytoplasmic side of the membrane. The substrate-binding site is in this cavity, more or less in the middle of the membrane. The side of the transporter facing outward (the periplasmic face) is closed tightly, with no channel big enough for lactose to enter. The proposed mecha-

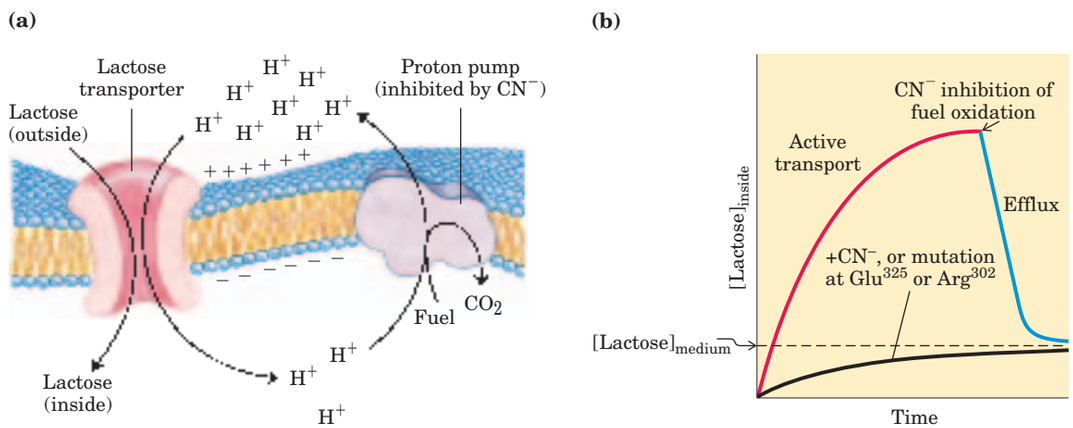

FIGURE 11–42 Lactose uptake in *E. coli*. **(a)** The primary transport of H^+ out of the cell, driven by the oxidation of a variety of fuels, establishes both a proton gradient and an electrical potential (inside negative) across the membrane. Secondary active transport of lactose into the cell involves symport of H^+ and lactose by the lactose transporter. The uptake of lactose against its concentration gradient is entirely dependent on this inflow of H^+, driven by the electrochemical gradient. **(b)** When the energy-yielding oxidation reactions of metabolism are blocked by cyanide (CN^-), the lactose transporter allows equilibration of lactose inside and outside the cell via passive transport. Mutations that affect Glu^{325} or Arg^{302} have the same effect as cyanide. The dashed line represents the concentration of lactose in the surrounding medium.

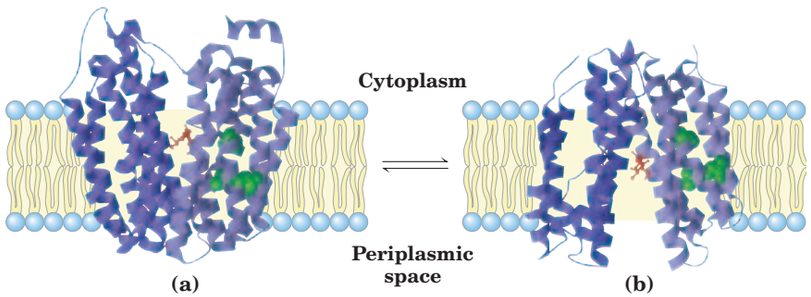

FIGURE 11–43 Structure of the lactose transporter (lactose permease) of *E. coli*. **(a)** Ribbon representation viewed parallel to the plane of the membrane shows the 12 transmembrane helices arranged in two nearly symmetrical domains shown in different shades of blue. In the form of the protein for which the crystal structure was determined, the substrate sugar (red) is bound near the middle of the membrane where it is exposed to the cytoplasm (derived from PDB ID 1PV7). **(b)** The structural changes postulated to take place during one transport cycle. The two halves of the transporter undergo a large, reversible conformational change in which the two domains tilt relative to each other, exposing the substrate-binding site first to the periplasm (structure on the right), where lactose is picked up, then to the cytoplasm (left), where the lactose is released. The interconversion of the two forms is driven by changes in the pairing of charged (protonatable) side chains such as those of Glu^{325} and Arg^{302} (green), which is affected by the transmembrane proton gradient.

nism for transmembrane passage of the substrate (Fig. 11–43b) involves a rocking motion between the two domains, driven by substrate binding and proton movement, alternately exposing the substrate-binding domain to the cytoplasm and to the periplasm. This so-called rocking banana model is similar to that shown in Figure 11–32 for GLUT1.

How is proton movement into the cell coupled with lactose uptake? Extensive genetic studies of the lactose transporter have established that of the 417 residues in the protein, only 6 are absolutely essential for cotransport of H^+ and lactose—some for lactose binding, others for proton transport. Mutation in either of two residues (Glu^{325} and Arg^{302}; Fig. 11–43) results in a protein still able to catalyze facilitated diffusion of lactose but incapable of coupling H^+ flow to uphill lactose transport. A similar effect is seen in wild-type (unmutated) cells when their ability to generate a proton gradient is blocked with CN^-: the transporter carries out facilitated diffusion normally, but it cannot pump lactose against a concentration gradient (Fig. 11–42b). The balance between the two conformations of the lactose transporter is affected by changes in charge pairing between side chains.

In intestinal epithelial cells, glucose and certain amino acids are accumulated by symport with Na^+, down the Na^+ gradient established by the Na^+K^+ ATPase of the plasma membrane (Fig. 11–44). The apical surface of the intestinal epithelial cell is covered with microvilli, long thin projections of the plasma membrane

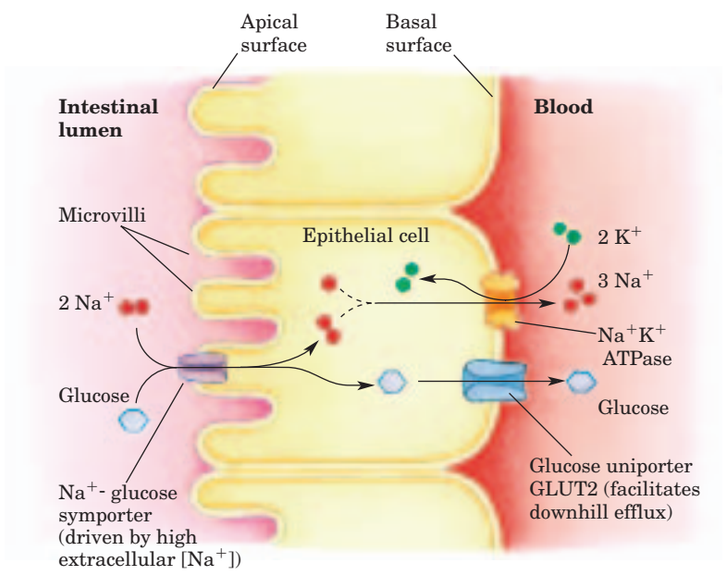

FIGURE 11–44 Glucose transport in intestinal epithelial cells. Glucose is cotransported with Na^+ across the apical plasma membrane into the epithelial cell. It moves through the cell to the basal surface, where it passes into the blood via GLUT2, a passive glucose transporter. The Na^+K^+ ATPase continues to pump Na^+ outward to maintain the Na^+ gradient that drives glucose uptake.

that greatly increase the surface area exposed to the intestinal contents. **Na^+-glucose symporters** in the apical plasma membrane take up glucose from the intestine in a process driven by the downhill flow of Na^+:

$$2Na^+_{out} + glucose_{out} \longrightarrow 2Na^+_{in} + glucose_{in}$$

The energy required for this process comes from two sources: the greater concentration of Na^+ outside than inside (the chemical potential) and the transmembrane potential (the electrical potential), which is inside-negative and therefore draws Na^+ inward. The electrochemical potential of Na^+ is

$$\Delta G = RT \ln \frac{[Na^+]_{in}}{[Na^+]_{out}} + n\mathcal{F}\Delta E$$

where $n = 2$, the number of Na^+ ions cotransported with each glucose molecule. Given the typical membrane potential of -50 mV, an intracellular $[Na^+]$ of 12 mM, and an extracellular $[Na^+]$ of 145 mM, the energy, ΔG, made available as two Na^+ ions reenter the cell is 22.5 kJ, enough to pump glucose against a large concentration gradient:

$$\Delta G_t = -22.5 \text{ kJ} = RT \ln \frac{[glucose]_{in}}{[glucose]_{out}}$$

and thus

$$\frac{[Glucose]_{in}}{[Glucose]_{out}} \approx 9{,}000$$

That is, the cotransporter can pump glucose inward until its concentration within the epithelial cell is about 9,000 times that in the intestine. As glucose is pumped from the intestine into the epithelial cell at the apical surface, it is simultaneously moved from the cell into the blood by passive transport through a glucose transporter (GLUT2) in the basal surface (Fig. 11–44). The crucial role of Na^+ in symport and antiport systems such as these requires the continued outward pumping of Na^+ to maintain the transmembrane Na^+ gradient.

Because of the essential role of ion gradients in active transport and energy conservation, compounds that collapse ion gradients across cellular membranes are effective poisons, and those that are specific for infectious microorganisms can serve as antibiotics. One such substance is valinomycin, a small cyclic peptide that neutralizes the K^+ charge by surrounding it with six carbonyl oxygens (Fig. 11–45). The hydrophobic peptide then acts as a shuttle, carrying K^+ across membranes down its concentration gradient and deflating that gradient. Compounds that shuttle ions across membranes in this way are called **ionophores** ("ion bearers"). Both valinomycin and monensin (a Na^+-carrying ionophore) are antibiotics; they kill microbial cells by disrupting secondary transport processes and energy-conserving reactions.

Aquaporins Form Hydrophilic Transmembrane Channels for the Passage of Water

A family of integral proteins discovered by Peter Agre, the **aquaporins (AQPs),** provide channels for rapid movement of water molecules across all plasma membranes (Table 11–6 lists a few examples). Ten aquaporins are known in humans, each with its specialized role. Erythrocytes, which swell or shrink rapidly in response to abrupt changes in extracellular osmolarity as blood travels through the renal medulla, have a high density of aquaporin in their plasma membranes (2×10^5 copies of AQP-1 per cell). In the nephron (the functional unit of the kidney), the plasma membranes of proximal renal tubule cells have five different aquaporin types.

Peter Agre

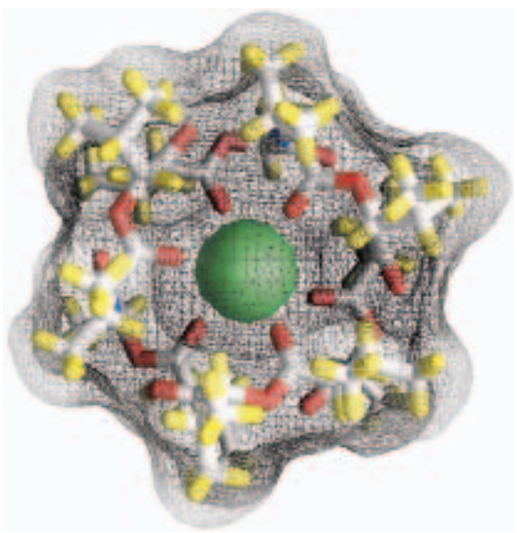

FIGURE 11–45 Valinomycin, a peptide ionophore that binds K^+. In this image, the surface contours are shown as a transparent mesh, through which a stick structure of the peptide and a K^+ atom (green) are visible. The oxygen atoms (red) that bind K^+ are part of a central hydrophilic cavity. Hydrophobic amino acid side chains (yellow) coat the outside of the molecule. Because the exterior of the K^+-valinomycin complex is hydrophobic, the complex readily diffuses through membranes, carrying K^+ down its concentration gradient. The resulting dissipation of the transmembrane ion gradient kills microbial cells, making valinomycin a potent antibiotic.

These cells reabsorb water during urine formation, a process for which water movement across membranes is essential (Box 11–3). The plant *Arabidopsis thaliana* has 38 genes that encode various types of aquaporins, reflecting the critical roles of water movement in plant physiology. Changes in turgor pressure, for example, require rapid movement of water across a membrane.

Water molecules flow through an AQP-1 channel at the rate of about 10^9 s^{-1}. For comparison, the highest known turnover number for an enzyme is that for catalase, 4×10^7 s^{-1}, and many enzymes have turnover numbers between 1 s^{-1} and 10^4 s^{-1} (see Table 6–7). The low activation energy for passage of water through aquaporin channels ($\Delta G^{\ddagger} < 15$ kJ/mol) suggests that water moves through the channels in a continuous stream, in the direction dictated by the osmotic gradient. (For a discussion of osmosis, see p. 57.) It is essential that aquaporins not allow passage of protons (hydronium ions, H_3O^+), which would collapse membrane electrochemical potentials. And they do not. What is the basis for this extraordinary selectivity?

We find an answer in the structure of AQP-1, as determined by x-ray diffraction analysis (Fig. 11–46). AQP-1 has four monomers (each M_r 28,000) associated in a tetramer, each monomer forming a transmembrane pore with a diameter (2 to 3 Å) sufficient to allow passage of water molecules in single file. Each monomer consists of six transmembrane helical segments and two shorter helices, each of which contains the sequence Asn–Pro–Ala (NPA). The NPA-containing short helices extend toward the middle of the bilayer from opposite

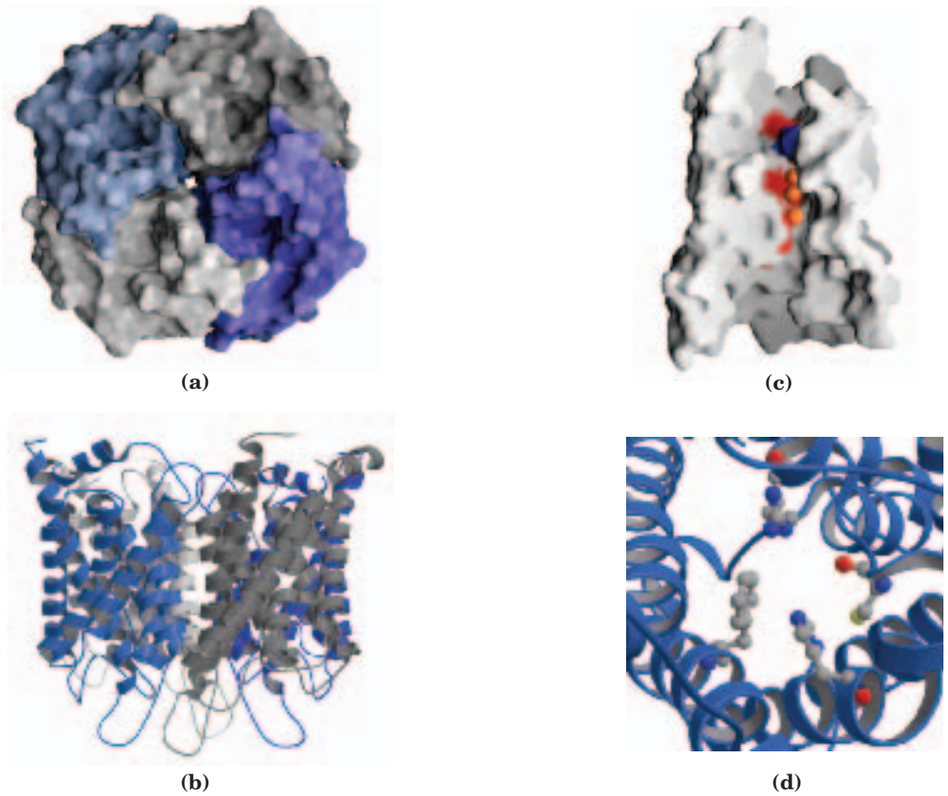

FIGURE 11–46 **Structure of an aquaporin, AQP-1.** The protein is a tetramer of identical monomeric units, each of which forms a transmembrane pore (derived from PBD ID 1J4N). **(a)** Surface model viewed perpendicular to the plane of the membrane. The protein contains four pores, one in each subunit. (The opening at the junction of the subunits is not a pore.) **(b)** An AQP-1 tetramer, viewed in the plane of the membrane. The helices of each subunit cluster around a central transmembrane pore. In each monomer, two short helical loops, one between helices 2 and 3 and the other between 5 and 6, contain the Asn–Pro–Ala (NPA) sequences found in all aquaporins, and form part of the water channel. **(c)** Surface representation of a single subunit, viewed in the plane of the membrane. The near side of the AQP-1 monomer has been cut away to reveal the channel running from top to bottom. The series of water molecules (orange spheres) shows the likely path of water molecules through the aquaporin channel, as predicted by molecular dynamics simulations in which investigators use the properties of water and aquaporin to calculate the lowest energy states. Hydrophilic atoms that provide selective interactions with water in the channel are colored red. A Phe residue (Phe^{58}) at the constriction is shown in blue. **(d)** A view down the channel, showing the constriction region of the specificity pore, which lets only a molecule as small as water pass. The side chains of Phe^{58}, His^{182}, Cys^{191}, and Arg^{197} create this constriction.

TABLE 11–6 Aquaporins

Aquaporin	*Roles and/or location*
AQP-1	Fluid reabsorption in proximal renal tubule; secretion of aqueous humor in eye and cerebrospinal fluid in central nervous system; water homeostasis in lung
AQP-2	Water permeability in renal collecting duct (mutations produce nephrogenic diabetes insipidus)
AQP-3	Water retention in renal collecting duct
AQP-4	Cerebrospinal fluid reabsorption in central nervous system; regulation of brain edema
AQP-5	Fluid secretion in salivary glands, lachrymal glands, and alveolar epithelium of lung
AQP-6	Kidney
AQP-7	Renal proximal tubule, intestine
AQP-8	Liver, pancreas, colon, placenta
AQP-9	Liver, leukocytes
TIP	Regulation of turgor pressure in plant tonoplast
PIP	Plant plasma membrane
AQY	Yeast plasma membrane

sides, with their NPA regions overlapping in the middle of the membrane to form part of the specificity filter—the structure that allows only water to pass.

The residues that line the channel of each AQP-1 monomer are generally nonpolar, but carbonyl oxygens in the peptide backbone, projecting into the narrow part of the channel at intervals, can form hydrogen bonds with individual water molecules as they pass through; the two Asn residues (Asn^{76} and Asn^{192}) in the NPA loops also hydrogen-bond with the water. The structure does not admit closely spaced water molecules that might form a chain to allow proton hopping (see Fig. 2–14), which would effectively move protons across the membrane. Critical Arg and His residues and electric dipoles formed by the short helices of the NPA loops provide positive charges in positions that repel any protons that might leak through the pore.

Ion-Selective Channels Allow Rapid Movement of Ions across Membranes

Ion-selective channels—first recognized in neurons and now known to be present in the plasma membranes of all cells, as well as in the intracellular membranes of eukaryotes—provide another mechanism for moving inorganic ions across membranes. Ion channels, together with ion pumps such as the Na^+K^+ ATPase, determine a plasma membrane's permeability to specific ions and regulate the cytosolic concentration of ions and the membrane potential. In neurons, very rapid changes in the activity of ion channels cause the changes in membrane potential (the action potentials) that carry signals from one end of a neuron to the other. In myocytes, rapid opening of Ca^{2+} channels in the sarcoplasmic reticulum releases the Ca^{2+} that triggers muscle contraction. We discuss the signaling functions of ion channels in Chapter 12. Here we describe the structural basis for ion-channel function, using as examples a bacterial K^+ channel, the neuronal Na^+ channel, and the acetylcholine receptor ion channel.

Ion channels are distinguished from ion transporters in at least three ways. First, the rate of flux through channels can be several orders of magnitude greater than the turnover number for a transporter—10^7 to 10^8 ions/s for an ion channel, near the theoretical maximum for unrestricted diffusion. Second, ion channels are not saturable: rates do not approach a maximum at high substrate concentration. Third, they are "gated"—opened or closed in response to some cellular event. In **ligand-gated channels** (which are generally oligomeric), binding of an extracellular or intracellular small molecule forces an allosteric transition in the protein, which opens or closes the channel. In **voltage-gated ion channels,** a change in transmembrane electrical potential (V_m) causes a charged protein domain to move relative to the membrane, opening or closing the ion channel. Both types of gating can be very fast. A channel typically opens in a fraction of a millisecond and may remain open for only milliseconds, making these molecular devices effective for very fast signal transmission in the nervous system.

Ion-Channel Function Is Measured Electrically

Because a single ion channel typically remains open for only a few milliseconds, monitoring this process is be-

Erwin Neher

Bert Sakmann

yond the limit of most biochemical measurements. Ion fluxes must therefore be measured electrically, either as changes in V_m (in the millivolt range) or as electric currents I (in the microampere or picoampere range), using microelectrodes and appropriate amplifiers. In patch-clamping, a technique developed by Erwin Neher and Bert Sakmann in 1976, very small currents are measured through a tiny region of the membrane surface containing only one or a few ion-channel molecules (Fig. 11–47). The researcher can measure the size and duration of the current that flows during one opening of an ion channel and can determine how often a channel opens and how that frequency is affected by transmembrane potential, regulatory ligands, toxins, and other agents. Patch-clamp studies have revealed that as many as 10^4 ions can move through a single ion channel in 1 ms. Such an ion flux represents a huge amplification of the initial signal; for example, only two acetylcholine molecules are needed to open an acetylcholine receptor channel (as described below).

The Structure of a K^+ Channel Reveals the Basis for Its Specificity

The structure of a potassium channel from the bacterium *Streptomyces lividans*, determined crystallographically by Roderick MacKinnon in 1998, provides much insight into the way ion channels work. This bacterial ion channel is related in sequence to all other known K^+ channels and serves as the prototype for such channels, including the voltage-gated K^+ channel of neurons. Among the members of this protein family, the similarities in sequence are greatest in the "pore region," which contains the ion selectivity filter that allows K^+ (radius 1.33 Å) to pass 10,000 times more readily than Na^+ (radius 0.95 Å)—at a rate (about 10^8 ions/s) approaching the theoretical limit for unrestricted diffusion.

Roderick MacKinnon

The K^+ channel consists of four identical subunits that span the membrane and form a cone within a cone surrounding the ion channel, with the wide end of the double cone facing the extracellular space (Fig. 11–48).

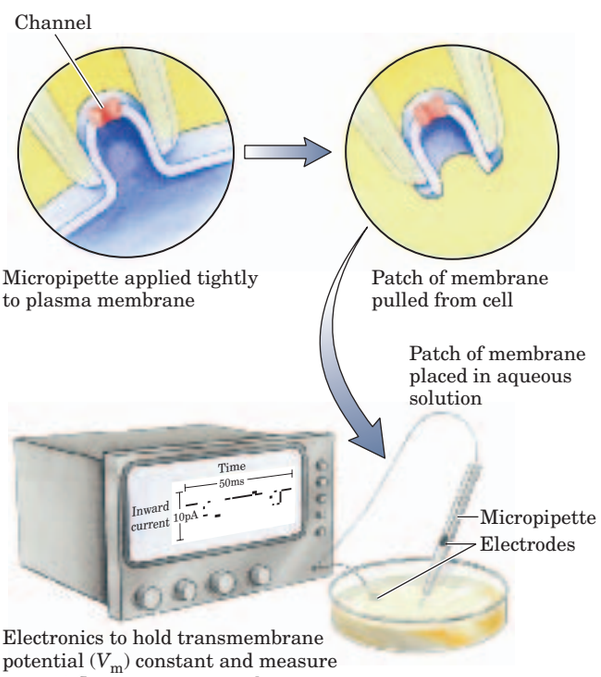

FIGURE 11–47 Electrical measurements of ion-channel function. The "activity" of an ion channel is estimated by measuring the flow of ions through it, using the patch-clamp technique. A finely drawn-out pipette (micropipette) is pressed against the cell surface, and negative pressure in the pipette forms a pressure seal between pipette and membrane. As the pipette is pulled away from the cell, it pulls off a tiny patch of membrane (which may contain one or a few ion channels). After placing the pipette and attached patch in an aqueous solution, the researcher can measure channel activity as the electric current that flows between the contents of the pipette and the aqueous solution. In practice, a circuit is set up that "clamps" the transmembrane potential at a given value and measures the current that must flow to maintain this voltage. With highly sensitive current detectors, researchers can measure the current flowing through a single ion channel, typically a few picoamperes. The trace showing the current as a function of time (in milliseconds) reveals how fast the channel opens and closes, how frequently it opens, and how long it stays open. Clamping the V_m at different values permits determination of the effect of membrane potential on these parameters of channel function.

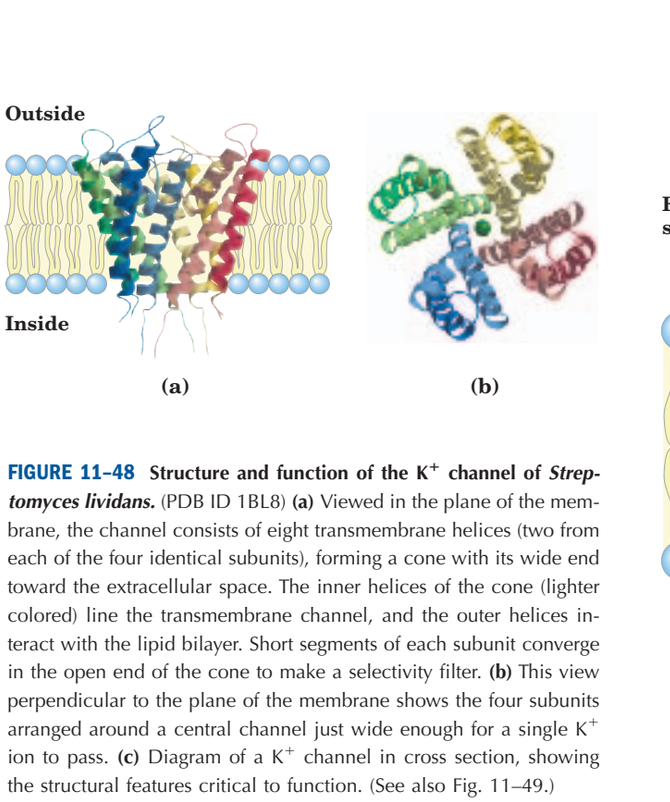

FIGURE 11–48 Structure and function of the K^+ channel of *Streptomyces lividans*. (PDB ID 1BL8) **(a)** Viewed in the plane of the membrane, the channel consists of eight transmembrane helices (two from each of the four identical subunits), forming a cone with its wide end toward the extracellular space. The inner helices of the cone (lighter colored) line the transmembrane channel, and the outer helices interact with the lipid bilayer. Short segments of each subunit converge in the open end of the cone to make a selectivity filter. **(b)** This view perpendicular to the plane of the membrane shows the four subunits arranged around a central channel just wide enough for a single K^+ ion to pass. **(c)** Diagram of a K^+ channel in cross section, showing the structural features critical to function. (See also Fig. 11–49.)

Each subunit has two transmembrane α helices as well as a third, shorter helix that contributes to the pore region. The outer cone is formed by one of the transmembrane helices of each subunit. The inner cone, formed by the other four transmembrane helices, surrounds the ion channel and cradles the ion selectivity filter.

Both the ion specificity and the high flux through the channel are understandable from what we know of the channel's structure. At the inner and outer plasma membrane surfaces, the entryways to the channel have several negatively charged amino acid residues, which presumably increase the local concentration of cations such as K^+ and Na^+. The ion path through the membrane begins (on the inner surface) as a wide, water-filled channel in which the ion can retain its hydration sphere. Further stabilization is provided by the short α helices in the pore region of each subunit, with the partial negative charges of their electric dipoles pointed at K^+ in the channel. About two-thirds of the way through the membrane, this channel narrows in the region of the selectivity filter, forcing the ion to give up its hydrating water molecules. Carbonyl oxygen atoms in the backbone of the selectivity filter replace the water molecules in the hydration sphere, forming a series of perfect coordination shells through which the K^+ moves. This favorable interaction with the filter is not possible for Na^+, which is too small to make contact with all the potential oxygen ligands. The preferential stabilization of K^+ is the basis for the ion selectivity of the filter, and mutations that change residues in this part of the protein eliminate the channel's ion selectivity.

There are four potential K^+-binding sites along the selectivity filter, each composed of an oxygen "cage" that provides ligands for the K^+ ions (Fig. 11–49). In the crystal structure, two K^+ ions are visible within the selectivity filter, about 7.5 Å apart, and two water molecules occupy the unfilled positions. K^+ ions pass through the filter in single file; their mutual electrostatic repulsion most likely just balances the interaction of each ion with the selectivity filter and keeps them moving. Movement of the two K^+ ions is concerted: first they occupy positions 1 and 3, then they hop to positions 2 and 4 (Fig. 11–48c). The energetic difference between these two configurations (1, 3 and 2, 4) is very small; energetically, the selectivity pore is not a series of hills and valleys but a flat surface, which is ideal for rapid ion movement through the channel. The structure of the channel appears to have been optimized during evolution to give maximal flow rates and high specificity.

The Neuronal Na^+ Channel Is a Voltage-Gated Ion Channel

Sodium ion channels in the plasma membranes of neurons and of myocytes of heart and skeletal muscle sense

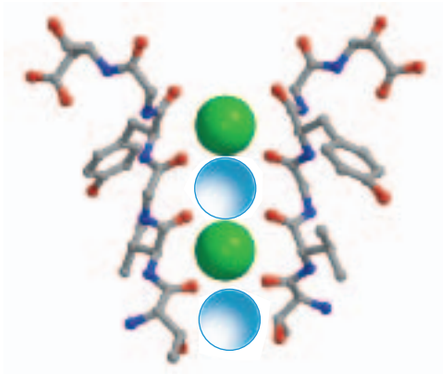

FIGURE 11–49 K^+ binding sites in the selectivity pore of the K^+ channel. (PDB ID 1J95) Carbonyl oxygens (red) of the peptide backbone in the selectivity filter protrude into the channel, interacting with and stabilizing a K^+ ion passing through. These ligands are perfectly positioned to interact with each of four K^+ ions, but not with the smaller Na^+ ions. This preferential interaction with K^+ is the basis for the ion selectivity. The mutual repulsion between K^+ ions results in occupation of only two of the four K^+ sites at a time (both green or both blue) and counteracts the tendency for a lone K^+ to stay bound in one site. The combined effect of K^+ binding to carbonyl oxygens and repulsion between K^+ ions ensures that an ion keeps moving, changing positions within 10 to 100 ns, and that there are no large energy barriers to ion flow along the path through the membrane.

electrical gradients across the membrane and respond by opening or closing. These voltage-gated ion channels are typically very selective for Na^+ over other monovalent or divalent cations (by factors of 100 or more) and have a very high flux rate ($>10^7$ ions/s). Normally (in the resting state) in the closed conformation, Na^+ channels are opened—activated—by a reduction in the transmembrane electrical potential, then they undergo very rapid inactivation. Within milliseconds of the opening, the channel closes and remains inactive for many milliseconds. Activation followed by inactivation of Na^+ channels is the basis for signaling by neurons (see Fig. 12–5).

The essential component of a Na^+ channel is a single, large polypeptide (1,840 amino acid residues) organized into four domains clustered around a central channel (Fig. 11–50a, b), providing a path for Na^+ through the membrane. The path is made Na^+-specific by a "pore region" composed of the segments between transmembrane helices 5 and 6 of each domain, which fold into the channel. Helix 4 of each domain has a high density of positively charged residues; this segment is believed to move within the membrane in response to changes in the transmembrane voltage, from the "resting" potential of about −60 mV (inside negative) to about +30 mV. The movement of helix 4 triggers opening of the channel, and this is the basis for voltage gating (Fig. 11–50c).

Inactivation of the channel is thought to occur by a ball-and-chain mechanism. A protein domain on the cytosolic surface of the Na^+ channel, the inactivation gate (the ball), is tethered to the channel by a short segment of the polypeptide (the chain) (Fig. 11–50b). This domain is free to move about when the channel is closed, but when it opens, a site on the inner face of the channel becomes available for the tethered ball to bind, blocking the channel. The length of the tether appears to determine how long an ion channel stays open; the longer the tether, the longer the open period. Inactivation of other ion channels may proceed by a similar mechanism.

The Acetylcholine Receptor Is a Ligand-Gated Ion Channel

Another very well-studied ion channel is the **nicotinic acetylcholine receptor,** essential in the passage of an electrical signal from a motor neuron to a muscle fiber at the neuromuscular junction (signaling the muscle to contract). (Nicotinic receptors were originally distinguished from muscarinic receptors by the sensitivity of the former to nicotine, the latter to the mushroom alkaloid muscarine. They are structurally and functionally different.) Acetylcholine released by the motor neuron diffuses a few micrometers to the plasma membrane of a myocyte, where it binds to the acetylcholine receptor. This forces a conformational change in the receptor, causing its ion channel to open. The resulting inward movement of positive charges depolarizes the plasma membrane, triggering contraction. The acetylcholine receptor allows Na^+, Ca^{2+}, and K^+ to pass through with equal ease, but other cations and all anions are unable to pass. Movement of Na^+ through an acetylcholine receptor ion channel is unsaturable (its rate is linear with respect to extracellular $[Na^+]$) and very fast—about 2×10^7 ions/s under physiological conditions.

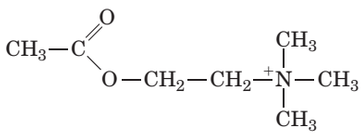

Acetylcholine

This receptor channel is typical of many other ion channels that produce or respond to electrical signals: it has a "gate" that opens in response to stimulation by a signal molecule (in this case acetylcholine) and an intrinsic timing mechanism that closes the gate after a split second. Thus the acetylcholine signal is transient—an essential feature of electrical signal conduction. We understand the structural changes underlying gating in the acetylcholine receptor, but not the exact mechanism of "desensitization"—of closing the gate even in the continued presence of acetylcholine.

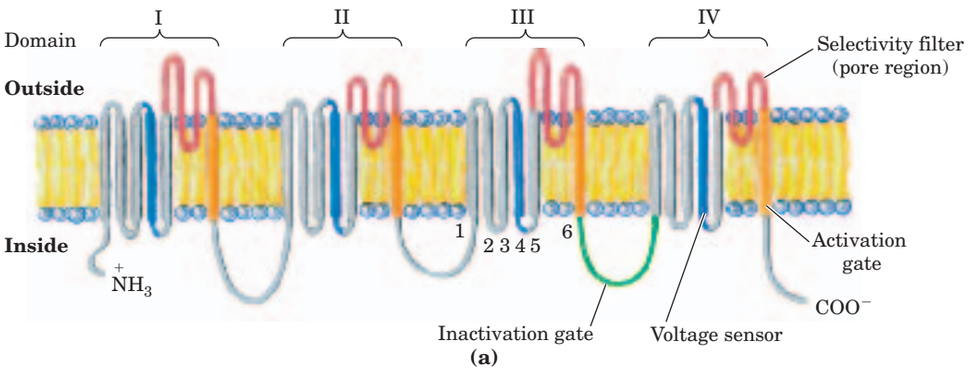

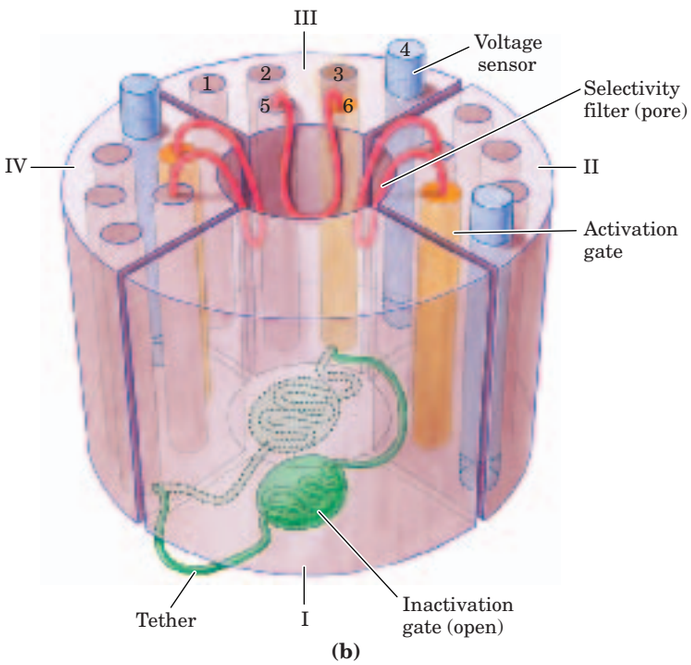

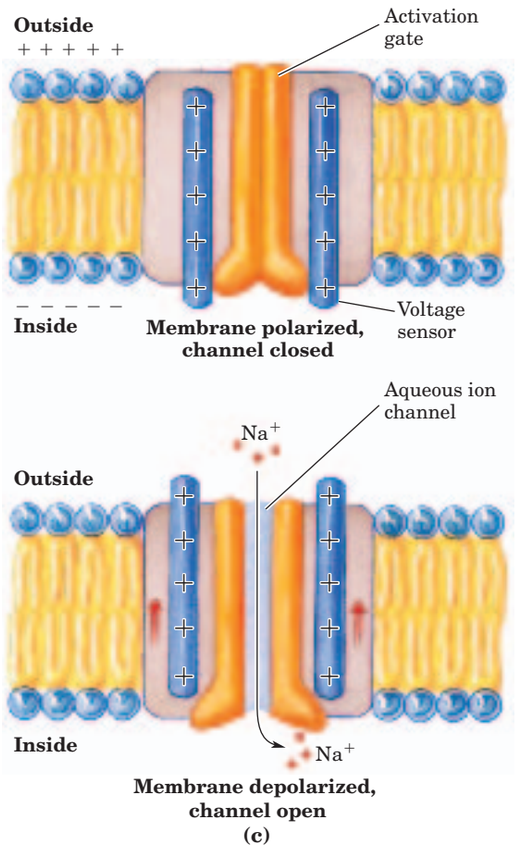

FIGURE 11–50 Voltage-gated Na^+ channels of neurons. Sodium channels of different tissues and organisms have a variety of subunits, but only the principal subunit (α) is essential. **(a)** The α subunit is a large protein with four homologous domains (I to IV), each containing six transmembrane helices (1 to 6). Helix 4 in each domain (blue) is the voltage sensor; helix 6 (orange) is thought to be the activation gate. The segments between helices 5 and 6, the pore region (red), form the selectivity filter, and the segment connecting domains III and IV (green) is the inactivation gate. **(b)** The four domains are wrapped about a central transmembrane channel lined with polar amino acid residues. The segments linking helices 5 and 6 (red) in each domain come together near the extracellular surface to form the selectivity filter, which is conserved in all Na^+ channels. The filter gives the channel its ability to discriminate between Na^+ and other ions of similar size. The inactivation gate (green) closes (dotted lines) soon after the activation gate opens. **(c)** The voltage-sensing mechanism involves movement of helix 4 (blue) perpendicular to the plane of the membrane in response to a change in transmembrane potential. As shown at the top, the strong positive charge on helix 4 allows it to be pulled inward in response to the inside-negative membrane potential (V_m). Depolarization lessens this pull, and helix 4 relaxes by moving outward (bottom). This movement is communicated to the activation gate (orange), inducing conformational changes that open the channel in response to depolarization.

The nicotinic acetylcholine receptor has five subunits: single copies of subunits β, γ, and δ, and two identical α subunits each with an acetylcholine-binding site. All five subunits are related in sequence and tertiary structure, each having four transmembrane helical segments (M1 to M4) (Fig. 11–51a). The five subunits surround a central pore, which is lined with their M2 helices. The pore is about 20 Å wide in the parts of the channel that protrude on the cytoplasmic and extracellular surfaces, but narrows as it passes through the

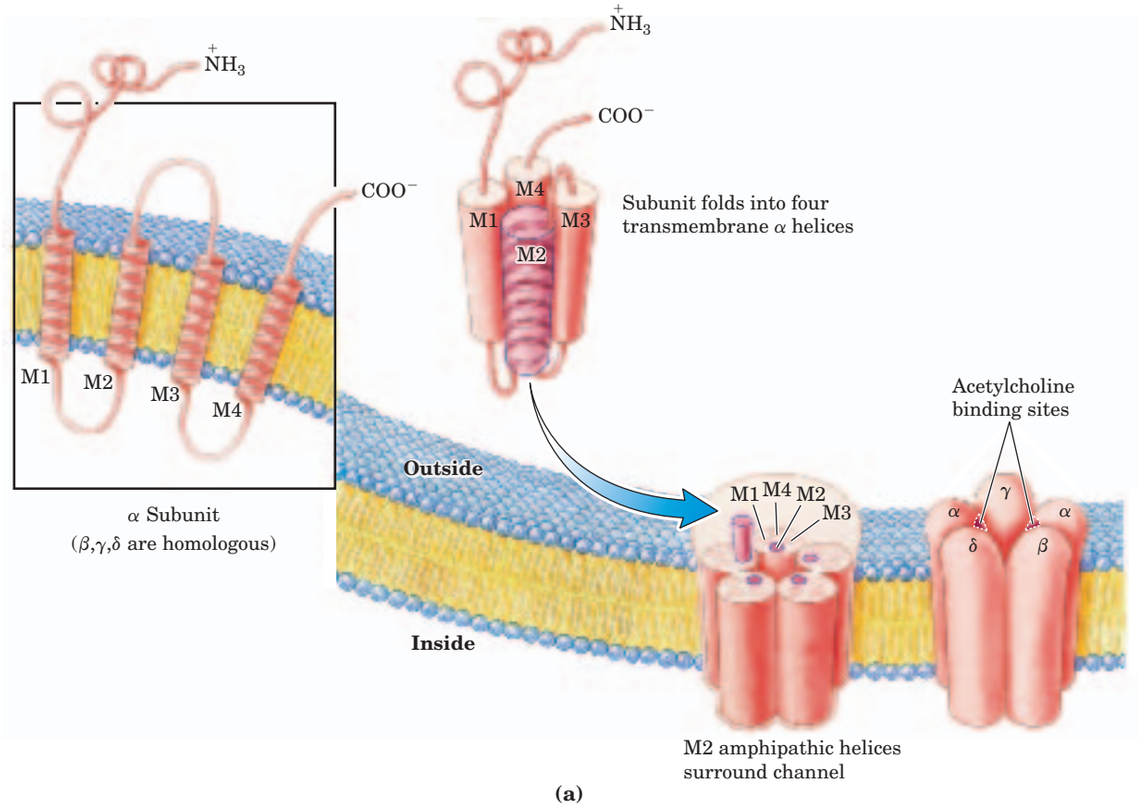

FIGURE 11–51 Structure of the acetylcholine receptor ion channel. (a) Each of the five subunits ($\alpha_2\beta\gamma\delta$) has four transmembrane helices, M1 to M4. The M2 helices are amphipathic; the others have mainly hydrophobic residues. The five subunits are arranged around a central transmembrane channel, which is lined with the polar sides of the M2 helices. At the top and bottom of the channel are rings of negatively charged amino acid residues. **(b)** This top view of a cross section through the center of the M2 helices shows five Leu side chains (one from each M2 helix) protruding into the channel, constricting it to a diameter too small to allow passage of ions such as Ca^{2+}, Na^+, and K^+. When both acetylcholine receptor sites (one on each α subunit) are occupied, a conformational change occurs. As the M2 helices twist slightly, the five Leu residues (yellow) rotate away from the channel and are replaced by smaller, polar residues (blue). This gating mechanism opens the channel, allowing the passage of Ca^{2+}, Na^+, or K^+.

lipid bilayer. Near the center of the bilayer is a ring of bulky hydrophobic side chains of Leu residues in the M2 helices, positioned so close together that they prevent ions from passing through the channel. Allosteric conformational changes induced by acetylcholine binding to the two α subunits include a slight twisting of the M2

TABLE 11–7 Transport Systems Described Elsewhere in This Text

Transport system and location	*Figure number*	*Role*
Adenine nucleotide antiporter of mitochondrial inner membrane	19–26	Imports substrate ADP for oxidative phosphorylation, and exports product ATP
Acyl-carnitine/carnitine transporter of mitochondrial inner membrane	17–6	Imports fatty acids into matrix for β oxidation
P_i-H^+ symporter of mitochondrial inner membrane	19–26	Supplies P_i for oxidative phosphorylation
Malate–α-ketoglutarate transporter of mitochondrial inner membrane	19–27	Shuttles reducing equivalents (as malate) from matrix to cytosol
Glutamate-aspartate transporter of mitochondrial inner membrane	19–27	Completes shuttling begun by malate–α-ketoglutarate shuttle
Citrate transporter of mitochondrial inner membrane	21–10	Provides cytosolic citrate as source of acetyl-CoA for lipid synthesis
Pyruvate transporter of mitochondrial inner membrane	21–10	Is part of mechanism for shuttling citrate from matrix to cytosol
Fatty acid transporter of myocyte plasma membrane	17–3	Imports fatty acids for fuel
Complex I, III, and IV proton transporters of mitochondrial inner membrane	19–15	Acts as energy-conserving mechanism in oxidative phosphorylation, converting electron flow into proton gradient
Thermogenin (uncoupler protein), a proton pore of mitochondrial inner membrane	19–30, 23–22	Allows dissipation of proton gradient in mitochondria as means of thermogenesis and/or disposal of excess fuel
Cytochrome *bf* complex, a proton transporter of chloroplast thylakoid	19–50, 19–54	Acts as proton pump, driven by electron flow through the Z scheme; source of proton gradient for photosynthetic ATP synthesis
Bacteriorhodopsin, a light-driven proton pump	19–59	Is light-driven source of proton gradient for ATP synthesis in halophilic bacterium
F_oF_1 ATPase/ATP synthase of mitochondrial inner membrane, chloroplast thylakoid, and bacterial plasma membrane	19–58	Interconverts energy of proton gradient and ATP during oxidative phosphorylation and photophosphorylation
P_i–triose phosphate antiporter of chloroplast inner membrane	20–15, 20–16	Exports photosynthetic product from stroma; imports P_i for ATP synthesis
Bacterial protein transporter	27–39	Exports secreted proteins through plasma membrane
Protein translocase of ER	27–33	Transports into ER proteins destined for plasma membrane, secretion, or organelles
Nuclear pore protein translocase	27–37	Shuttles proteins between nucleus and cytoplasm
LDL receptor in animal cell plasma membrane	21–42	Imports, by receptor-mediated endocytosis, lipid carrying particles
Glucose transporter of animal cell plasma membrane; regulated by insulin	12–8	Increases capacity of muscle and adipose tissue to take up excess glucose from blood
IP_3-gated Ca^{2+} channel of endoplasmic reticulum	12–19	Allows signaling via changes of cytosolic Ca^{2+} concentration
cGMP-gated Ca^{2+} channel of retinal rod and cone cells	12–32	Allows signaling via rhodopsin linked to cAMP phosphodiesterase in vertebrate eye
Voltage-gated Na^+ channel of neuron	12–5	Creates action potentials in neuronal signal transmission

helices (Fig. 11–51b), which draws these hydrophobic side chains away from the center of the channel, opening it to the passage of ions.

Based on similarities between the amino acid sequences of other ligand-gated ion channels and the acetylcholine receptor, the receptor channels that respond to the extracellular signals γ-aminobutyric acid (GABA), glycine, and serotonin have been classified in the acetylcholine receptor superfamily, and probably share three-dimensional structure and gating mechanisms. The $GABA_A$ and glycine receptors are anion channels specific for Cl^- or HCO_3^-, whereas the serotonin receptor, like the acetylcholine receptor, is cation-specific. The subunits of each of these channels, like those of the acetylcholine receptor, have four transmembrane helical segments and form oligomeric channels.

A second class of ligand-gated ion channels respond to *intracellular* ligands: 3′,5′-cyclic guanosine mononucleotide (cGMP) in the vertebrate eye, cGMP and cAMP in olfactory neurons, and ATP and inositol 1,4,5-trisphosphate (IP3) in many cell types. These channels are composed of multiple subunits, each with six transmembrane helical domains. We discuss the signaling functions of these ion channels in Chapter 12.

Table 11–7 shows a number of transporters not discussed in this chapter but encountered later in the book in the context of the paths in which they act.

Defective Ion Channels Can Have Adverse Physiological Consequences

The importance of ion channels to physiological processes is clear from the effects of mutations in specific ion-channel proteins (Table 11–8). Genetic defects in the voltage-gated Na^+ channel of the myocyte plasma membrane result in diseases in which muscles are periodically either paralyzed (as in hyperkalemic periodic paralysis) or stiff (as in paramyotonia congenita). As noted earlier, cystic fibrosis is the result of a mutation that changes one amino acid in the protein CFTR, a Cl^- ion channel; the defective process here is not neurotransmission but secretion by various exocrine gland cells whose activities are tied to Cl^- ion fluxes.

Many naturally occurring toxins act on ion channels, and the potency of these toxins further illustrates the importance of normal ion-channel function. Tetrodotoxin (produced by the puffer fish, *Sphaeroides rubripes*) and saxitoxin (produced by the marine dinoflagellate *Gonyaulax,* which causes "red tides") act by binding to the voltage-gated Na^+ channels of neurons and preventing normal action potentials. Puffer fish is an ingredient of the Japanese delicacy fugu, which may be prepared only by chefs specially trained to separate

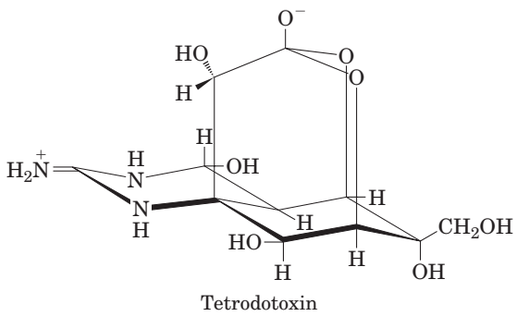

Tetrodotoxin

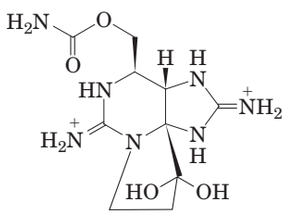

Saxitoxin

TABLE 11–8 Some Diseases Resulting from Ion Channel Defects

Ion channel	*Affected gene*	*Disease*
Na^+ (voltage-gated, skeletal muscle)	*SCN4A*	Hyperkalemic periodic paralysis (or paramyotonia congenita)
Na^+ (voltage-gated, neuronal)	*SCN1A*	Generalized epilepsy with febrile seizures
Na^+ (voltage-gated, cardiac muscle)	*SCN5A*	Long QT syndrome 3
Ca^{2+} (neuronal)	*CACNA1A*	Familial hemiplegic migraine
Ca^{2+} (voltage-gated, retina)	*CACNA1F*	Congenital stationary night blindness
Ca^{2+} (polycystin-1)	*PKD1*	Polycystic kidney disease
K^+ (neuronal)	*KCNQ4*	Dominant deafness
K^+ (voltage-gated, neuronal)	*KCNQ2*	Benign familial neonatal convulsions
Nonspecific cation (cGMP-gated, retinal)	*CNCG1*	Retinitis pigmentosa
Acetylcholine receptor (skeletal muscle)	*CHRNA1*	Congenital myasthenic syndrome
Cl^-	*CFTR*	Cystic fibrosis

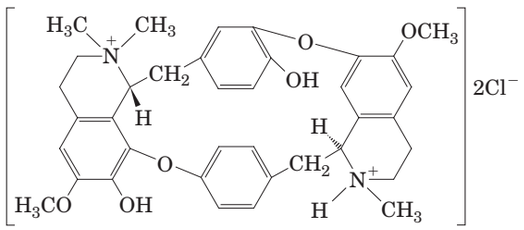

D-Tubocurarine chloride

succulent morsel from deadly poison. Eating shellfish that have fed on *Gonyaulax* can also be fatal; shellfish are not sensitive to saxitoxin, but they concentrate it in their muscles, which become highly poisonous to organisms higher up the food chain. The venom of the black mamba snake contains dendrotoxin, which interferes with voltage-gated K^+ channels. Tubocurarine, the active component of curare (used as an arrow poison in the Amazon), and two other toxins from snake venoms, cobrotoxin and bungarotoxin, block the acetylcholine receptor or prevent the opening of its ion channel. By blocking signals from nerves to muscles, all these toxins cause paralysis and possibly death. On the positive side, the extremely high affinity of bungarotoxin for the acetylcholine receptor ($K_d = 10^{-15}$ M) has proved useful experimentally: the radiolabeled toxin was used to quantify the receptor during its purification. ■

SUMMARY 11.3 Solute Transport across Membranes

- Movement of polar compounds and ions across biological membranes requires protein transporters. Some transporters simply facilitate passive diffusion across the membrane from the side with higher concentration to the side with lower. Others bring about active movement of solutes against an electrochemical gradient; such transport must be coupled to a source of metabolic energy.
- Carriers, like enzymes, show saturation and stereospecificity for their substrates. Transport via these systems may be passive or active. Primary active transport is driven by ATP or electron-transfer reactions; secondary active transport, by coupled flow of two solutes, one of which (often H^+ or Na^+) flows down its electrochemical gradient as the other is pulled up its gradient.
- The GLUT transporters, such as GLUT1 of erythrocytes, carry glucose into cells by facilitated diffusion. These transporters are uniporters, carrying only one substrate. Symporters permit simultaneous passage of two substances in the same direction; examples are the lactose transporter of *E. coli,* driven by the energy of a proton gradient (lactose-H^+ symport), and the glucose transporter of intestinal epithelial cells, driven by a Na^+ gradient (glucose-Na^+ symport). Antiporters mediate simultaneous passage of two substances in opposite directions; examples are the chloride-bicarbonate exchanger of erythrocytes and the ubiquitous Na^+K^+ ATPase.
- In animal cells, Na^+K^+ ATPase maintains the differences in cytosolic and extracellular concentrations of Na^+ and K^+, and the resulting Na^+ gradient is used as the energy source for a variety of secondary active transport processes.
- The Na^+K^+ ATPase of the plasma membrane and the Ca^{2+} transporters of the sarcoplasmic and endoplasmic reticulums (the SERCA pumps) are examples of P-type ATPases; they undergo reversible phosphorylation during their catalytic cycle and are inhibited by the phosphate analog vanadate. F-type ATPase proton pumps (ATP synthases) are central to energy-conserving mechanisms in mitochondria and chloroplasts. V-type ATPases produce gradients of protons across some intracellular membranes, including plant vacuolar membranes.
- ABC transporters carry a variety of substrates, including many drugs, out of cells, using ATP as energy source.
- Ionophores are lipid-soluble molecules that bind specific ions and carry them passively across membranes, dissipating the energy of electrochemical ion gradients.
- Water moves across membranes through aquaporins.
- Ion channels provide hydrophilic pores through which select ions can diffuse, moving down their electrical or chemical concentration gradients; they are characteristically unsaturable and have very high flux rates. Many ion channels are highly specific for one ion, and most are gated by either voltage or a ligand. In bacterial K^+ channels, a selectivity filter provides ligands with the right geometry to replace the water of hydration of a K^+ ion as it crosses the membrane. Some K^+ channels are voltage gated. The acetylcholine receptor/channel is gated by acetylcholine, which triggers subtle conformational changes that open and close the transmembrane path.

Key Terms

Terms in bold are defined in the glossary.

fluid mosaic model 371
micelle 372
bilayer 373
integral proteins 373
peripheral proteins 373
hydropathy index 377
β barrel 378
gel phase 380
liquid-disordered state 380
liquid-ordered state 380
flippases 382
FRAP 382
microdomains 383
rafts 384
caveolin 385
caveolae 385
fusion proteins 387
SNAREs 389
simple diffusion 389
membrane potential (V_m) 389
electrochemical gradient 391
electrochemical potential 391
facilitated diffusion 391
passive transport 391
transporters 391
carriers 392
channels 392
electroneutral 395
cotransport systems 395
antiport 397
symport 397
uniport 397
active transport 397
electrogenic 398
P-type ATPases 398
SERCA pump 400
F-type ATPases 401
ATP synthase 401
V-type ATPases 401
ABC transporters 402
multidrug transporter 402
ionophores 406
aquaporins (AQPs) 406
ion channel 408

Further Reading

Composition and Architecture of Membranes

Boon, J.M. & Smith, B.D. (2002) Chemical control of phospholipid distribution across bilayer membranes. *Med. Res. Rev.* **22,** 251–281.
Intermediate-level review of phospholipid asymmetry and factors that influence it.

Dowhan, W. (1997) Molecular basis for membrane phospholipids diversity: why are there so many lipids? *Annu. Rev. Biochem.* **66,** 199–232.

Ediden, M. (2002) Lipids on the frontier: a century of cell-membrane bilayers. *Nat. Rev. Mol. Cell Biol.* **4,** 414–418.
Short review of how the notion of a lipid bilayer membrane was developed and confirmed.

Haltia, T. & Freire, E. (1995) Forces and factors that contribute to the structural stability of membrane proteins. *Biochim. Biophys. Acta* **1241,** 295–322.
Good discussion of the secondary and tertiary structures of membrane proteins and the factors that stabilize them.

von Heijne, G. (1994) Membrane proteins: from sequence to structure. *Annu. Rev. Biophys. Biomol. Struct.* **23,** 167–192.
A review of the steps required to predict the structure of an integral protein from its sequence.

White, S.H., Ladokhin, A.S., Jayasinghe, S., & Hristova, K. (2001) How membranes shape protein structure. *J. Biol. Chem.* **276,** 32,395–32,398.
Brief, intermediate-level review of the forces that shape transmembrane helices.

Wimley, W.C. (2003) The versatile β barrel membrane protein. *Curr. Opin. Struct. Biol.* **13,** 1–8.
Intermediate-level review.

Membrane Dynamics

Brown, D.A. & London, E. (1998) Functions of lipid rafts in biological membranes. *Annu. Rev. Cell Dev. Biol.* **14,** 111–136.

Chen, Y.A. & Scheller, R.H. (2001) SNARE-mediated membrane fusion. *Nat. Rev. Mol. Cell Biol.* **2,** 98–106.
Intermediate-level review.

Edidin, M. (2003) The state of lipid rafts: from model membranes to cells. *Annu. Rev. Biophys. Biomol. Struct.* **32,** 257–283.
Advanced review.

Frye, L.D. & Ediden, M. (1970) The rapid intermixing of cell-surface antigens after formation of mouse-human heterokaryons. *J. Cell Sci.* **7,** 319–335.
The classic demonstration of membrane protein mobility.

Mayer, A. (2002) Membrane fusion in eukaryotic cells. *Annu. Rev. Cell Dev. Biol.* **18,** 289–314.
Advanced review of membrane fusion, with emphasis on the conserved general features.

Parton, R.G. (2003) Caveolae—from ultrastructure to molecular mechanisms. *Nat. Rev. Mol. Cell Biol.* **4,** 162–167.
A concise historical review of caveolae, caveolin, and rafts.

Sprong, H., van der Sluijs, P., & van Meer, G. (2001) How proteins move lipids and lipids move proteins. *Nat. Rev. Mol. Cell Biol.* **2,** 504–513.
Intermediate-level review.

van Deurs, B., Roepstorff, K., Hommelgaard, A.M., & Sandvig, K. (2003) Caveolae: anchored, multifunctional platforms in the lipid ocean. *Trends Cell Biol.* **13,** 92–100.

Vereb, G., Szöllósi, J., Matcó, J., Nagy, P., Farkas, T., Vigh, L., Mátyus, L., Waldmann, T.A., & Damjanovich, S. (2003) Dynamic, yet structured: the cell membrane three decades after the Singer-Nicolson model. *Proc. Natl. Acad. Sci. USA* **100,** 8053–8058.
Intermediate-level review of membrane structure and dynamics.

Transporters

Abramson, J., Smirnova, I., Kasho, V., Verner, G., Kaback, H.R., & Iwata, S. (2003) Structure and mechanism of the lactose permease of *Escherichia coli*. *Science* **301,** 610–615.

Fujiyoshi, Y., Mitsuoka, K., de Groot, B.L., Philippsen, A., Grubmüller, H., Agre, P., & Engel, A. (2002) Structure and function of water channels. *Curr. Opin. Struct. Biol.* **12,** 509–515.

Jorgensen, P.L., Håkansson, K.O., & Karlish, S.J.D. (2003) Structure and mechanism of Na,K-ATPase: functional sites and their interactions. *Annu. Rev. Physiol.* **65,** 817–849.

Kjellbom, P., Larsson, C., Johansson, I., Karlsson, M., & Johanson, U. (1999) Aquaporins and water homeostasis in plants. *Trends Plant Sci.* **4,** 308–314.
Intermediate-level review.

Mueckler, M. (1994) Facilitative glucose transporters. *Eur. J. Biochem.* **219,** 713–725.

Saier, M.H., Jr. (2000) A functional-phylogenetic classification system for transmembrane solute transporters. *Microbiol. Mol. Biol. Rev.* **64,** 354–411.

Schmitt, L. & Tampé, R. (2002) Structure and mechanism of ABC transporters. *Curr. Opin. Struct. Biol.* **12,** 754–760.

Sheppard, D.N. & Welsh, M.J. (1999) Structure and function of the CFTR chloride channel. *Physiol. Rev.* **79,** S23–S46.
This issue of the journal has 11 reviews on the CFTR chloride channel, covering its structure, activity, regulation, biosynthesis, and pathophysiology.

Stokes, D.L. & Green, N.M. (2003) Structure and function of the calcium pump. *Annu. Rev. Biophys. Biomol. Struct.* **32,** 445–468.
Advanced review.

Sui, H., Han, B.-G., Lee, J.K., Walian, P., & Jap, B.K. (2001) Structural basis of water-specific transport through the AQP1 water channel. *Nature* **414,** 872–878.
High-resolution solution of the aquaporin structure by x-ray crystallography.

Ion Channels

Changeux, J.P. (1993) Chemical signaling in the brain. *Sci. Am.* **269** (November), 58–62.
Discussion of structure and function of the acetylcholine receptor channel.

Doyle, D.A., Cabral, K.M., Pfuetzner, R.A., Kuo, A., Gulbis, J.M., Cohen, S.L., Chait, B.T., & MacKinnon, R. (1998) The structure of the potassium channel: molecular basis of K^+ conduction and selectivity. *Science* **280,** 69–77.
The first crystal structure of an ion channel is described.

Edelstein, S.J. & Changeux, J.P. (1998) Allosteric transitions of the acetylcholine receptor. *Adv. Prot. Chem.* **51,** 121–184.
Advanced discussion of the conformational changes induced by acetylcholine.

Hille, B. (2001) *Ion Channels of Excitable Membranes,* 3rd edn, Sinauer Associates, Sunderland, MA.
Intermediate-level text emphasizing the function of ion channels.

Jiang, Y., Lee, A., Chen, J., Ruta, V., Cadene, M., Chait, B.T., & MacKinnon, R. (2003) X-ray structure of a voltage-dependent K^+ channel. *Nature* **423,** 33–41.

Lee, A.G. & East, J.M. (2001) What the structure of a calcium pump tells us about its mechanism. *Biochem J.* **356,** 665–683.

Miyazawa, A., Fujiyoshi, Y., & Unwin, N. (2003) Structure and gating mechanism of the acetylcholine receptor pore. *Nature* **423,** 949–955.
Intermediate-level review.

Neher, E. & Sakmann, B. (1992) The patch clamp technique. *Sci. Am.* (March) **266,** 44–51.
Clear description of the electrophysiological methods used to measure the activity of single ion channels, by the Nobel Prize–winning developers of this technique.

Yellen, G. (2002) The voltage-gated potassium channels and their relatives. *Nature* **419,** 35–42.

Zhou, Y., Morias-Cabral, J.H., Kaufman, A., & MacKinnon, R. (2001) Chemistry of ion coordination and hydration revealed by a K^+ channel–Fab complex at 2.0 Å resolution. *Nature* **414,** 43–48.

Problems

1. Determining the Cross-Sectional Area of a Lipid Molecule When phospholipids are layered gently onto the surface of water, they orient at the air-water interface with their head groups in the water and their hydrophobic tails in the air. An experimental apparatus **(a)** has been devised that reduces the surface area available to a layer of lipids. By measuring the force necessary to push the lipids together, it is possible to determine when the molecules are packed tightly in a continuous monolayer; as that area is approached, the force needed to further reduce the surface area increases sharply **(b).** How would you use this apparatus to determine the average area occupied by a single lipid molecule in the monolayer?

(a)

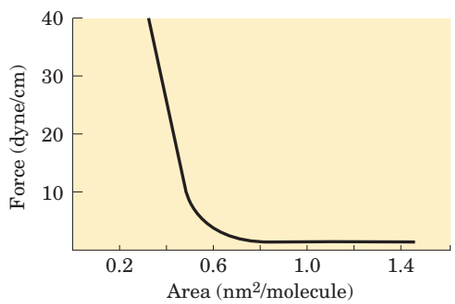

(b)

2. Evidence for a Lipid Bilayer In 1925, E. Gorter and F. Grendel used an apparatus like that described in Problem 1 to determine the surface area of a lipid monolayer formed by lipids extracted from erythrocytes of several animal species. They used a microscope to measure the dimensions of individual cells, from which they calculated the average surface area of one erythrocyte. They obtained the data shown in the

table. Were these investigators justified in concluding that "chromocytes [erythrocytes] are covered by a layer of fatty substances that is two molecules thick" (i.e., a lipid bilayer)?

Animal	*Volume of packed cells (mL)*	*Number of cells (per mm^3)*	*Total surface area of lipid monolayer from cells (m^2)*	*Total surface area of one cell (μm^2)*
Dog	40	8,000,000	62	98
Sheep	10	9,900,000	6.0	29.8
Human	1	4,740,000	0.92	99.4

Source: Data from Gorter, E. & Grendel, F. (1925) On bimolecular layers of lipoids on the chromocytes of the blood. *J. Exp. Med.* **41,** 439–443.

3. Number of Detergent Molecules per Micelle When a small amount of sodium dodecyl sulfate (SDS; $Na^+CH_3(CH_2)_{11}OSO_3^-$) is dissolved in water, the detergent ions enter the solution as monomeric species. As more detergent is added, a concentration is reached (the critical micelle concentration) at which the monomers associate to form micelles. The critical micelle concentration of SDS is 8.2 mM. The micelles have an average particle weight (the sum of the molecular weights of the constituent monomers) of 18,000. Calculate the number of detergent molecules in the average micelle.

4. Properties of Lipids and Lipid Bilayers Lipid bilayers formed between two aqueous phases have this important property: they form two-dimensional sheets, the edges of which close upon each other and undergo self-sealing to form liposomes.

(a) What properties of lipids are responsible for this property of bilayers? Explain.

(b) What are the consequences of this property for the structure of biological membranes?

5. Length of a Fatty Acid Molecule The carbon–carbon bond distance for single-bonded carbons such as those in a saturated fatty acyl chain is about 1.5 Å. Estimate the length of a single molecule of palmitate in its fully extended form. If two molecules of palmitate were placed end to end, how would their total length compare with the thickness of the lipid bilayer in a biological membrane?

6. Temperature Dependence of Lateral Diffusion The experiment described in Figure 11–17 was performed at 37 °C. If the experiment were carried out at 10 °C, what effect would you expect on the rate of diffusion? Why?

7. Synthesis of Gastric Juice: Energetics Gastric juice (pH 1.5) is produced by pumping HCl from blood plasma (pH 7.4) into the stomach. Calculate the amount of free energy required to concentrate the H^+ in 1 L of gastric juice at 37 °C. Under cellular conditions, how many moles of ATP must be hydrolyzed to provide this amount of free energy? The free-energy change for ATP hydrolysis under cellular conditions is about −58 kJ/mol (as explained in Chapter 13). Ignore the effects of the transmembrane electrical potential.

8. Energetics of the Na^+K^+ ATPase For a typical vertebrate cell with a transmembrane potential of −0.070 V (inside negative), what is the free-energy change for transporting 1 mol of Na^+ out of the cell and into the blood at 37 °C? Assume the concentration of Na^+ inside the cell is 12 mM, and that in blood plasma is 145 mM.

9. Action of Ouabain on Kidney Tissue Ouabain specifically inhibits the Na^+K^+ ATPase activity of animal tissues but is not known to inhibit any other enzyme. When ouabain is added to thin slices of living kidney tissue, it inhibits oxygen consumption by 66%. Why? What does this observation tell us about the use of respiratory energy by kidney tissue?

10. Energetics of Symport Suppose that you determined experimentally that a cellular transport system for glucose, driven by symport of Na^+, could accumulate glucose to concentrations 25 times greater than in the external medium, while the external [Na^+] was only 10 times greater than the intracellular [Na^+]. Would this violate the laws of thermodynamics? If not, how could you explain this observation?

11. Location of a Membrane Protein The following observations are made on an unknown membrane protein, X. It can be extracted from disrupted erythrocyte membranes into a concentrated salt solution, and it can be cleaved into fragments by proteolytic enzymes. Treatment of erythrocytes with proteolytic enzymes followed by disruption and extraction of membrane components yields intact X. However, treatment of erythrocyte "ghosts" (which consist of just plasma membranes, produced by disrupting the cells and washing out the hemoglobin) with proteolytic enzymes followed by disruption and extraction yields extensively fragmented X. What do these observations indicate about the location of X in the plasma membrane? Do the properties of X resemble those of an integral or peripheral membrane protein?

12. Membrane Self-sealing Cellular membranes are self-sealing—if they are punctured or disrupted mechanically, they quickly and automatically reseal. What properties of membranes are responsible for this important feature?

13. Lipid Melting Temperatures Membrane lipids in tissue samples obtained from different parts of the leg of a reindeer have different fatty acid compositions. Membrane lipids from tissue near the hooves contain a larger proportion of unsaturated fatty acids than those from tissue in the upper leg. What is the significance of this observation?

14. Flip-Flop Diffusion The inner leaflet (monolayer) of the human erythrocyte membrane consists predominantly of phosphatidylethanolamine and phosphatidylserine. The outer leaflet consists predominantly of phosphatidylcholine and sphingomyelin. Although the phospholipid components of the membrane can diffuse in the fluid bilayer, this sidedness is preserved at all times. How?

15. Membrane Permeability At pH 7, tryptophan crosses a lipid bilayer at about one-thousandth the rate of the closely related substance indole:

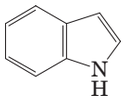

Suggest an explanation for this observation.

16. Water Flow through an Aquaporin Each human erythrocyte has about 2×10^5 AQP-1 monomers. If water molecules flow through the plasma membrane at a rate of 5×10^8 per AQP-1 tetramer per second, and the volume of an erythrocyte is 5×10^{-11} mL, how rapidly could an erythrocyte halve its volume as it encounters the high osmolarity (1 M) in the interstitial fluid of the renal medulla? Assume that the erythrocyte consists entirely of water.

17. Labeling the Lactose Transporter A bacterial lactose transporter, which is highly specific for its substrate lactose, contains a Cys residue that is essential to its transport activity. Covalent reaction of *N*-ethylmaleimide (NEM) with this Cys residue irreversibly inactivates the transporter. A high concentration of lactose in the medium prevents inactivation by NEM, presumably by sterically protecting the Cys residue, which is in or near the lactose-binding site. You know nothing else about the transporter protein. Suggest an experiment that might allow you to determine the M_r of the Cys-containing transporter polypeptide.

18. Predicting Membrane Protein Topology from Sequence You have cloned the gene for a human erythrocyte protein, which you suspect is a membrane protein. From the nucleotide sequence of the gene, you know the amino acid sequence. From this sequence alone, how would you evaluate the possibility that the protein is an integral protein? Suppose the protein proves to be an integral protein, either type I or type II. Suggest biochemical or chemical experiments that might allow you to determine which type it is.

19. Intestinal Uptake of Leucine You are studying the uptake of L-leucine by epithelial cells of the mouse intestine. Measurements of the rate of uptake of L-leucine and several of its analogs, with and without Na^+ in the assay buffer, yield the results given in the table. What can you conclude about the properties and mechanism of the leucine transporter? Would you expect L-leucine uptake to be inhibited by ouabain?

	Uptake in presence of Na^+		*Uptake in absence of Na^+*	
Substrate	V_{max}	K_t (mM)	V_{max}	K_t (mM)
L-Leucine	420	0.24	23	0.24
D-Leucine	310	4.7	5	4.7
L-Valine	225	0.31	19	0.31

20. Effect of an Ionophore on Active Transport Consider the leucine transporter described in Problem 19. Would V_{max} and/or K_t change if you added a Na^+ ionophore to the assay solution containing Na^+? Explain.

21. Surface Density of a Membrane Protein *E. coli* can be induced to make about 10,000 copies of the lactose transporter (M_r 31,000) per cell. Assume that *E. coli* is a cylinder 1 μm in diameter and 2 μm long. What fraction of the plasma membrane surface is occupied by the lactose transporter molecules? Explain how you arrived at this conclusion.

Biochemistry on the Internet

22. Membrane Protein Topology The receptor for the hormone epinephrine in animal cells is an integral membrane protein (M_r 64,000) that is believed to have seven membrane-spanning regions.

(a) Show that a protein of this size is capable of spanning the membrane seven times.

(b) Given the amino acid sequence of this protein, how would you predict which regions of the protein form the membrane-spanning helices?

(c) Go to the Protein Data Bank (www.rcsb.org/pdb). Use the PDB identifier 1DEP to retrieve the data page for a portion of the β-adrenergic receptor (one type of epinephrine receptor) from a turkey. Using Chime to explore the structure, predict where this portion of the receptor is located: within the membrane or at the membrane surface. Explain.

(d) Retrieve the data for a portion of another receptor, the acetylcholine receptor of neurons and myocytes, using the PDB identifier 1A11. As in (c), predict where this portion of the receptor is located and explain your answer.

If you have not used the PDB or Chemscape Chime, you can find instructions at www.whfreeman.com/lehninger.